FAST DETECTION AND MITIGATION OF CASCADING OUTAGES IN THE POWER SYSTEM

A Dissertation

by

CHENGZONG PANG

Submitted to the Office of Graduate Studies of
Texas A&M University
in partial fulfillment of the requirements for the degree of

DOCTOR OF PHILOSOPHY

December 2011

Major Subject: Electrical Engineering

Fast Detection and Mitigation of Cascading Outages in the Power System

FAST DETECTION AND MITIGATION OF CASCADING OUTAGES IN THE POWER SYSTEM

A Dissertation

by

CHENGZONG PANG

Submitted to the Office of Graduate Studies of
Texas A&M University
in partial fulfillment of the requirements for the degree of

DOCTOR OF PHILOSOPHY

Approved by:

Chair of Committee,	Mladen Kezunovic
Committee Members,	Chanan Singh
	Shankar P. Bhattacharyya
	William McCain Lively
Head of Department,	Costas Georghiades

December 2011

Major Subject: Electrical Engineering

ABSTRACT

Fast Detection and Mitigation of Cascading Outages in the Power System. (December 2011)

Chengzong Pang, B.S., North China Electric Power University, China

Chair of Advisory Committee: Dr. Mladen Kezunovic

This dissertation studies the causes and mechanism of power system cascading outages and proposes the improved interactive scheme between system-wide and local levels of monitoring and control to quickly detect, classify and mitigate the cascading outages in power system.

A novel method for evaluating the vulnerability of individual components as well as the whole power system, which is named as weighted vulnerability analysis, is developed. Betweenness centrality is used to measure the importance of each bus and transmission line in the modeled power system network, which is in turn used to determine the weights for the weighted vulnerability index. It features fast reaction time and achieves higher accuracy when dealing with the cascading outage detection, classification and mitigation over the traditional methods.

The overload problem due to power flow redistribution after one line tripped is

a critical factor contributing to the cascading outages. A parallel corridor searching method is proposed to quickly identify the most vulnerable components after tripping a transmission line. The power system topology model can be simplified into state graph after searching the domains for each generator, the commons for each bus, and links between the commons. The parallel corridor will be determined by searching the links and commons in system topology graph for the given state of power system operation.

During stressed operating state, either stable or unstable power swing may have impacts on distance relay judgment and lead to relay misoperation, which will result in the power system lines being tripped and as a consequence power system operating state becoming even more stressful. At the local level, an enhanced fault detection tool during power system swing is developed to reduce the chance of relay misoperation.

Comprehensive simulation studies have been implemented by using the IEEE 39-bus and 118-bus test systems. The results are promising because:

- The results from weighted vulnerability analysis could provide better system situational awareness and accurate information about the disturbance;
- The results form parallel corridor search method could identify the most vulnerable lines after power re-distribution, which will give operator time to take remedial actions;

- The results from new travelling wave and wavelet transform based fault detection could reduce the impact of relay misoperation.

DEDICATION

To my wife Xiaoyan Wang and my family for their love, patience and support.

ACKNOWLEDGEMENTS

I would like to express my sincere gratitude to my advisor Dr. Mladen Kezunovic for his support and guidance throughout my studies at Texas A&M University. His knowledge and experience contributed many of the inspiring ideas explored in this dissertation.

I gratefully thank my committee members Dr. Chanan Singh, Dr. Shankar P. Bhattacharyya, and Dr. William M. Lively for their time, comments and support.

Sincere acknowledgements are extended to my colleagues, Mr. Jinfeng Ren, Mr. Yufan Guan, Mr. Ce Zheng, Ms. Yimai Dong, Ms. Chenyan Guo, Ms. Papiya Dutta, Mr. Saeed Lotfifard, Ms. Biljana M. Cuka, and other group members for their corporation and assistance. It was a most enjoyable experience in my life working with them.

My research was mainly funded by financial resources from three projects. Two are funded by NSF I/UCRC Power System Engineering Research Center (PSERC): “Detection, Prevention and Mitigation Cascading Events-Prototype Implementations”, and “PHEVs as Dynamically Configurable Dispersed Energy Storage”; the third one is funded by NSF I/UCRC Center of Transportation and Electricity Convergence (CTEC): “The Impact of PHEVs/BEVs Charging on Utility Distribution System”. I would like to acknowledge the financial support from all the sponsors.

TABLE OF CONTENTS

Page

ABSTRACT iii

DEDICATION vi

ACKNOWLEDGEMENTS vii

TABLE OF CONTENTS viii

LIST OF FIGURES xii

LIST OF TABLES xv

1. INTRODUCTION 1

1.1 Problem Formulation 1
1.1.1 Frequency of Large Blackouts 2
1.1.2 Challenges of Cascading Analysis 5
1.2 Current Research Efforts 8
1.2.1 Cascading Outage Modeling and Simulation 8
1.2.2 Network Theory Approaches 9
1.2.3 Other Approaches 10
1.3 Proposed Research 11
1.3.1 Pre-disturbance Stage 14
1.3.2 Post-disturbance Stage 17
1.3.3 Post-disturbance Control 17
1.4 Organization of the Dissertation 18

2. BACKGROUND OF CASCADING OUTAGES IN POWER SYSTEM 19

2.1 Introduction 19
2.2 Problem of Cascading Outages 19
2.3 Major Blackouts in the World 20
2.3.1 North American Northeast Blackout in 2003 20
2.3.2 Europe Blackout in 2006 24
2.4 Lessons Learned from Cascading Outages 29
2.4.1 Causes of Cascading Outage 29

Page

2.4.2 Mechanism of Cascading Outages 30
2.5 Summary 32

3. POWER SYSTEM TOPOLOGICAL MODEL 33

3.1 Introduction 33
3.2 Power System Applications of Graph Theory 33
3.3 Power System as Directed Graph Network 35
3.3.1 Graph Model of Power System Elements 35
3.3.2 Directed Graph Model 37
3.4 Case Study 38
3.5 Summary 39

4. WEIGHTED VULNERABILITY ANALYSIS 40

4.1 Introduction 40
4.2 Review of Vulnerability Index [64] 40
4.2.1 Vulnerability Index for Generators 41
4.2.2 Vulnerability Index for Buses 42
4.2.3 Vulnerability Index for Branches 44
4.3 Weighted Vulnerability Analysis 46
4.3.1 Vertex Betweenness Centrality 47
4.3.2 Edge Betweenness Centrality 47
4.3.3 Betweenness Calculation Example 48
4.3.4 Weights Calculation 49
4.4 Case Study 51
4.4.1 Calculation of Betweenness Centrality 51
4.4.2 Weighted Vulnerability Analysis for Different Load Conditions 55
4.4.3 Weighted Vulnerability Analysis for N-1 Contingency 56
4.5 Summary 57

5. PARALLEL CORRIDOR SEARCH BASED ON GRAPH PARTITIONING 59

5.1 Introduction 59
5.2 Graph Partitioning based on Contributions 59
5.2.1 Domain of a Generator 60
5.2.2 Common of Buses 62
5.2.3 Links between Commons 63
5.3 Parallel Corridor Search Method 64
5.3.1 State Graph of Power System 64

Page

5.3.2 Parallel Corridor Search Method 65
5.4 Case Study 67
5.5 Summary 71

6. ENHANCED DISTANCE RELAY SCHEME USED FOR VULNERABLE PARTS IN POWER SYSTEM 73

6.1 Introduction 73
6.2 Distance Relay Behavior during Power Swing 74
6.2.1 Power Swing 74
6.2.2 Distance Relay under Power Swing 77
6.3 Principle of Enhanced Fault Detection Method 80
6.3.1 Traveling Wave Theory during Fault 82
6.3.2 Wavelet Transform Analysis 84
6.4 Implementation of Detection Method 88
6.4.1 Data Acquisition 90
6.4.2 Modal Transformation 90
6.4.3 Wavelet Transform Implementation 91
6.4.4 Fault Detection Criteria 95
6.5 Case Study 96
6.5.1 Simulation of Power Swing 96
6.5.2 Example Cases 97
6.6 Summary 102

7. CONCLUSIONS 104

7.1 Achievements and Contributions 104
7.2 Conclusions 106
7.3 Suggestion for Future Research 107

REFERENCES 109

APPENDIX A 127

APPENDIX B 130

APPENDIX C 144

Page

VITA.....151

LIST OF FIGURES

Page

Figure 1 North American Blackout Size Probability Distribution from NERC Distribution Analysis Working Group Data 4

Figure 2 The Relative Blackout Frequency to Blackout Risk from Large North America Blackouts in Various Size Categories 4

Figure 3 Flowchart of Proposed Method for Fast Detection and Mitigation of Cascading Outages 13

Figure 4 Commons for the 6-bus System 16

Figure 5 Timeline of 2003 Northeastern Blackout in Ohio 21

Figure 6 Rate of Line and Generator Trips during Cascading Outage 23

Figure 7 Exchange Programs and Physical Flows on Nov. 4 at 22:09 27

Figure 8 Schematic Map of UCTE Area Split into Three Areas 27

Figure 9 Frequency Recordings during the Blackout 28

Figure 10 A Graph with Five Vertices and Seven Edges 36

Figure 11 4-bus Power System and its Graph Model 39

Figure 12 A Graph with Five Vertices and Five Edges 49

Figure 13 IEEE 118-bus System Configuration 52

Page

Figure 14 Vertex Betweenness Distribution for IEEE 118-bus System 53

Figure 15 Edge Betweenness Distribution for IEEE 118-bus System..... 53

Figure 16 One Line Diagram 6-bus System with Power Flow..... 61

Figure 17 Commons for the 6-bus System 63

Figure 18 State Graph for the 6-bus System..... 65

Figure 19 IEEE 39-bus New England System Configuration 67

Figure 20 Commons and Links of IEEE 39-bus New England System..... 69

Figure 21 State Graph of IEEE 39-bus New England System 70

Figure 22 Voltage Simulation Example of Power Swing Observed by Relay..... 76

Figure 23 Z_c Trajectory in the $R-X$ Phase..... 79

Figure 24 Impedance Trajectory during Stable and Unstable Power Swing..... 80

Figure 25 Diagram for Single Phase Transmission Line..... 82

Figure 26 Diagram of MRA Decomposition into Two Scales..... 86

Figure 27 Daubechies-8 (Db8) Wavelet 89

Figure 28 Implementation Diagram of Symmetrical Fault Detection Method..... 89

Figure 29 Border Distortion Effect for Wavelet Analysis..... 93

Figure 30 Periodic-padding for Wavelet Analysis..... 93

Figure 31 Symmetric-padding for Wavelet Analysis..... 94

Page

Figure 32 One-line Diagram of IEEE EMTP Reference Model.....96

Figure 33 IEEE EMTP Reference Model in ATP 97

Figure 34 5-level Db8 Wavelet Transform Results.....98

Figure 35 3-phase Voltage Waveforms for a Symmetrical Fault during Power Swing99

Figure 36 Values of Criteria Factor k_e around the Fault Point 99

LIST OF TABLES

Page

Table 1 Summary of Cascading Outages and Related Consequences 6

Table 2 Weighted Vulnerability Index Values under Different Load Conditions 56

Table 3 Weighted Vulnerability Index Values for N-1 Contingency Analysis..... 57

Table 4 Domain of each Generator for IEEE 39-bus New England System 68

Table 5 Parallel Corridors Case Study 70

Table 6 Full AC Power Flow Results..... 72

Table 7 Simulation Case for Different Fault Locations for Symmetrical Fault under Power Swing 100

Table 8 Simulation Case for Different Fault Locations under Normal Condition... 101

Table 9 Simulation Case for Different Fault Locations under Power Swing 102

Table 10 Bus Data of IEEE 118-bus System 130

Table 11 PV Bus Data of IEEE-118 System..... 134

Table 12 Line Data of IEEE-118 System..... 136

Table 13 Generator Data of IEEE-118 System 142

Table 14 Exciter Data of IEEE-118 System..... 143

Table 15 Bus Data of IEEE 39-bus New England System 144

Table 16 PV Bus Data of IEEE 39-bus New England System 146

Page

Table 17 Line Data of IEEE 39-bus New England System.....147

Table 18 Generator Data of IEEE 39-bus New England System.....149

Table 19 Exciter Data of IEEE 39-bus New England System.....150

1. INTRODUCTION

1.1 Problem Formulation

Electric power system is one of the most complex man-made systems. With the development of flexible electricity markets operation under the deregulation rules, power system became more stressed and power network security and reliability criteria more complex. Power systems are exposed to many kinds of disturbances, which may come from animal contacts, human errors, equipment malfunction, natural disasters, intentional sabotage, etc., and some of these disturbances may cause major power service interruption [1]. Protective relays and other control actions may be invoked to steer the system away from severe consequences, and to limit the extent of the disturbance. This way, most disturbances can be mitigated without power service interruption. But in some specific circumstances the disturbances may not be mitigated and will cause major service interruption.

Here, we are interested in one of the most severe kind of system disturbances: *Cascading Failures*. Cascading failure is defined as "*a sequence of dependent failures of individual components that successively weaken the power system.*" [2] Cascading outage, especially the large-scale cascading outage, draws special attention since it can

---

This dissertation follows the style of *IEEE Transactions on Power Delivery*.

cause great economic loss to utility companies and other businesses and have devastating impact on people's life. For example, the Northwestern America Blackout in 1996 disconnected 30.39 GW of power to 7.5 million customers [3]; Northeastern System Blackout in 2003 led to the load loss of 61.8GW, which influenced more than 50 million people and spread through Northern Ohio, much of Michigan, Ontario, parts of Pennsylvania and Connecticut, and New York [1].

Considering the large number of individual components it involves, the wide range of time scales of the event dynamics, and the different mechanisms of how the components interact, the modeling and analysis of cascading outages is extremely complicated. Many researchers have put lots of efforts on analyzing and finding solutions to detect, classify, mitigate or prevent cascading outages. But till now, how to find the solution of fast detection and mitigation of the cascading outages still remains the industry challenge.

1.1.1 Frequency of Large Blackouts

A common perspective today is that large area blackouts are rarer than small size blackouts. It is true for sure. But, how much rarer are large area blackouts than the small ones? We might expect the probability distribution of blackout size, which includes power shed, energy unserved, customer disconnected, duration, and number of lines tripped [2], to fall off exponentially as the size of the blackout increases. After

squaring so many times when increasing the blackout size, the probability of the larger blackouts should vanished. However, Carreras *et al* [4] found that the probability distribution of the blackout sizes in North American does not decrease exponentially with the size of the blackouts, but rather has an approximate power law region with an exponent between -1 and -2. The impact of this power law is also proved in Literature [5] by the frequencies of blackouts in various size categories and their overall contributions to blackout risk in North America, In terms of the total amount of demand interrupted, the costs of cascading failures have enormous variance [5], which is shown in Figure 2. The same power law properties resulted from studies of the power system of China [6], Sweden [7], Norway [8], etc. Figure 1 shows the example on a log-log scale of the empirical probability distribution of the North American blackout size obtained from North American Electric Reliability Council (NERC) Disturbance Analysis Working Group data [9].

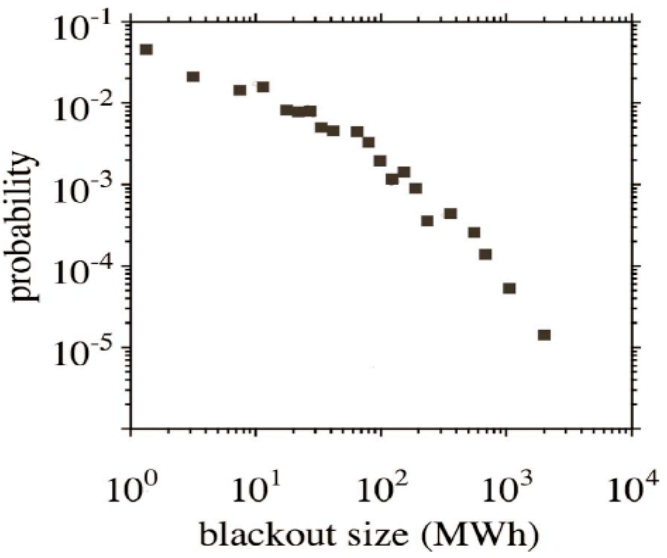

Figure 1 North American Blackout Size Probability Distribution from NERC Distribution Analysis Working Group Data

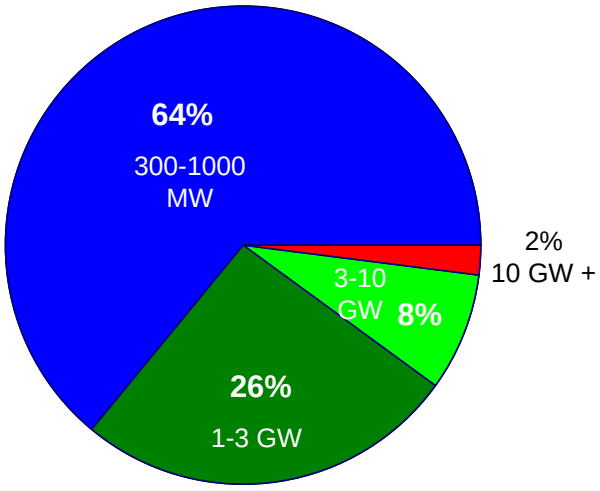

Figure 2 The Relative Blackout Frequency to Blackout Risk from Large North America Blackouts in Various Size Categories

The power law property suggests that large scale blackouts are much more likely than they are expected. This phenomenon can be explained by the dependency of failures in the blackout, or cascading failures. With the more failures occurring in the power system, the more stressed the power system becomes. The weakened power system makes the failures occur more likely, which will lead to the large scale blackout.

In summary, cascading outages cannot be eliminated completely and they occurrence is much more likely than the common exponential tails. To illustrate the severity of possible impacts, Table 1 shows the summary of some major consequences of the cascading outages throughout the world in the past several decades. [1], [10]-[13]

1.1.2 Challenges of Cascading Analysis

In the United States, the monitoring of cascading outages has been addressed by NERC as voluntary effort in the beginning. But now the monitoring and reporting has been changed to the mandatory effort by addressing it in the standards, which include TOP-004-2, TPL-001-0, TPL-002-0a, TPL-003-0a, TPL-004-0, etc. [14]. Since the large-area blackouts cannot be eliminated, and their occurrences always come with catastrophic social and economical impacts, it is very urgent and important to find a solution for fast detection and mitigation of cascading outages in power system.

Table 1 Summary of Cascading Outages and Related Consequences

	Location	*Data*	*Lost of MW*	*Affected People*	*Collapse Time*	*Restoration Time*
1	US-Northeastern	Nov. 9, 1965	20000	30 million	13mins	13 hrs
2	New York	July 13, 1977	6000	9 million	1 hr	26 hrs
3	France	Dec. 19, 1978	29000		26mins	5 hrs
4	Sweden	Dec. 27, 1983	> 7000	4,5 million	53 secs	About 5 hrs
5	Tokyo (Japan)	July 23, 1987	8200	2.8 million	20 mins	About 75 mins
6	US-Western	July 2, 1996	11850	2 million	36 secs	a few mins to several hrs
7	US-Western	Aug. 10, 1996	30500	7.5 million	>6 mins	A few mins to 9 hrs
8	Brazil	Mar. 11, 1999	25000	75 million	30 secs	30 mins to 4 hrs
9	US- Northeastern	Aug. 14, 2003	61800	50 million	> 1hr	Up to 4 days
10	Denmark/Sweden	Sept. 23, 2003	6550	4.85 million	7 mins	Average 2 to 4.3 hrs
11	Italy	Sept. 28, 2003	27700	57 million	27 mins	2.5 to 19.5 hrs
12	Moscow/Russia	May 24, 2005	2500	4 million	> 6hr	
13	US-EI	Aug. 4, 2007	4261		6 mins	
14	Brazil	Nov. 10, 2009	18000	60 million		>3 hr
15	US-San Diego	Sept. 8, 2011	6982	2.7 million	11 mins	1.5 to 12 hrs
16	South Korea	Sept. 15, 2011	240	2.1 million	2 hr	> 3hr
17	Chile	Sept. 25, 2011		9 million		> 2hr

After an extensive study of the major blackouts in the history, it appears that relaying problems and inadequate understanding of unfolding events are two major contributing factors to inability of predicting or preventing cascading events. This is discussed in the reports for the August 1996 US West Coast System Blackout [3] and August 2003 US Northeast System Blackout [1]. Protective relays can quickly identify and isolate faulted area in a power system to maintain the power system security and reliability. However, when the relays trip one faulted transmission line in the stressed power system, the power flow on this line will be transferred to the other transmission lines. Those lines may be overloaded and new faults may develop and then cascading trips may be induced by the backup relays even if there are no new faults. The existing traditional protection only utilizes the local data and the ultimate goals are to eliminate the fault as soon as possible. The impact of power flow transferring within the system cannot be considered ahead of the time. Thus the capability of relays to deal with any unforeseen or unfolding events is drastically reduced. Hence new tools for power system operators to enhance power system security and reliability under such circumstances are needed. The tools to evaluate the impact after any disturbance happened in the system and to provide the suggested emergency control actions when relaying operates unexpectedly are not available.

1.2 Current Research Efforts

Many methods have been proposed so far aiming at understanding and finding ways for detecting, preventing, and mitigating the cascading events. IEEE Computer Analytical Methods Subcommittee (CAMS) had a Task Force on Understanding, Predication, Mitigation and Restoration of Cascading Failures, which describes the state of art of cascading risk assessment tools by means of an updated view prepared by experts representing utilities, universities, research institutes and consulting companies [2], [5], [15]. An overview of existing major methods of cascading outages analysis is summarized as following:

1.2.1 Cascading Outage Modeling and Simulation

Considering that the cascading phenomena are very complicated because of the diversity of failures and interactions, it is not possible to accomplish an exhaustive computation of all possible combinations of failures in power system. Thus a very detailed model of all the failures and their interactions is infeasible. Different researchers have made some compromises in modeling and simulating the cascading outages. Based on the Self-organized Criticality (SOC) theory, three different models have been proposed: Oak Ridge-Pserc-Alaska (OPA) model, CASCADE model, and Branch Process model. OPA model [16]-[18] tries to explain the propagating of cascading outages in long-term view of slow and fast dynamics behavior. CASCADE

model [20] is an analytically tractable probabilistic model of cascading outages that captures the weakening of the system as the cascade proceeds. It tries to explain the probability relations between the blackout size and the initial disturbance of power system. The Branching Process model [21]-[23] is an approximation of CASCADE models that quantifies the propagation of cascading failures with parameter and simplifies the mathematical modeling for the purpose of estimating the distribution of the final blackout size. The three models neglect many of the cascading processes in blackouts and the timing of the events. A protection system reliability model, which proposes an integrated scheme to study power system vulnerability considering protection system failures leading to the cascading outages has been introduced in [24][25]. This scheme can assess the system vulnerability based on Bus Isolation Probability (BIP), Loss of Load Probability (LOLP), Expected Power Loss (EPL), Probability of Stability (POS), and Integrated System Vulnerability (ISV). By using Monte Carlo simulation approach, this scheme simulates system behavior of cascading outages. Other models, such as the Manchester model [26], hidden failures model of the protection system [27], stochastic model [28], etc. have also been proposed.

1.2.2 Network Theory Approaches

Motivated by the propagation of failures and congestion in the Internet, some researchers have studied the statistical properties of the power system network by

neglecting power flows. Watts has proved that the topology of a typical power system network is a small-world network [29]. Hines and Blumsack [30] suggest that the power systems have a scale free structure by accounting for the electrical distances. Lesieutre , et al. [31] refined the concept of topological graph concepts in order to be more consistent with power system generation and load patterns. Motter, et al. [32]**Error! Reference source not found.** try to formulate the problem of cascading attack and work on cascading phase transitions by complex networks theory.

1.2.3 Other Approaches

Dynamic event tree analysis [33] combines the probability and event tree technique for prediction and mitigation of cascading events. It is still very difficult to generate comprehensive event trees due to the complexity and large number of components of the power system. For the wide area back up protection expert system [34], it may be easy to apply it in the radial system, but it is not easy to do the same in a large and mashed transmission network. Pattern recognition method has been discussed in [35] by identifying and capturing the typical basic patterns of cascading events, and then combining them into cascading sequences. However, it is very complicated to understand the typical pattern for the large power system. Self-healing system [36] could determine the actions it should take and offers the capability of adaptive reconfiguration, such as load shedding.

1.3 Proposed Research

In summary, detecting and preventing cascading outages is crucial to maintaining the power system reliability and security. Many methods have been proposed for risk assessment of cascading outages, which could be used to benefit for power system planning. But study of methods to detect and mitigate the cascading outages still requires much research efforts. Developing a generalized tool for power system operator's decision support for corrective control after the initialing contingency occurs is still desirable.

Texas A&M University researchers have developed a series of new methods and new tools to help detect, prevent and mitigate the outages, which include steady state control scheme, transient stability control scheme, and interactive system-wide and local scheme [37]. Based on those developed methods and tools, this dissertation improves the interactive scheme solution for the fast detection and mitigation of cascading outages in power system.

At system-wide level, weighted vulnerability analysis method and parallel corridor searching method are proposed. The weighted vulnerability analysis method is developed to evaluate vulnerability of the whole power system as well as individual elements, not only from the view of electrical properties but also from the view of topology network. The parallel corridor searching method is presented to quickly

identify the most vulnerable components after tripping any transmission line to solve the overloading problem due to power flow redistribution. The proposed method is based on topological partitioning used in graph theory. The vulnerability evaluation and vulnerable components identification tool could make the system operator better understand the unfolding events and take remedial actions under extreme conditions.

At local level, an enhanced fault detection method during power swing is proposed to reduce the risk of relay misoperation. Since power swing, either stable or unstable, may have impacts on distance relay judgment and lead to relay misoperation, which will result in the system becoming more stressful. It may cause catastrophic outcomes especially when the power system is an emergency state. The enhanced fault detection method will increase system security when installing it on those vulnerable elements located by using the weighted vulnerability analysis and parallel corridor searching method.

Figure 3 shows the framework of the proposed method, which covers three stages. The key algorithms of the proposed solution will be discussed in details in the following sections.

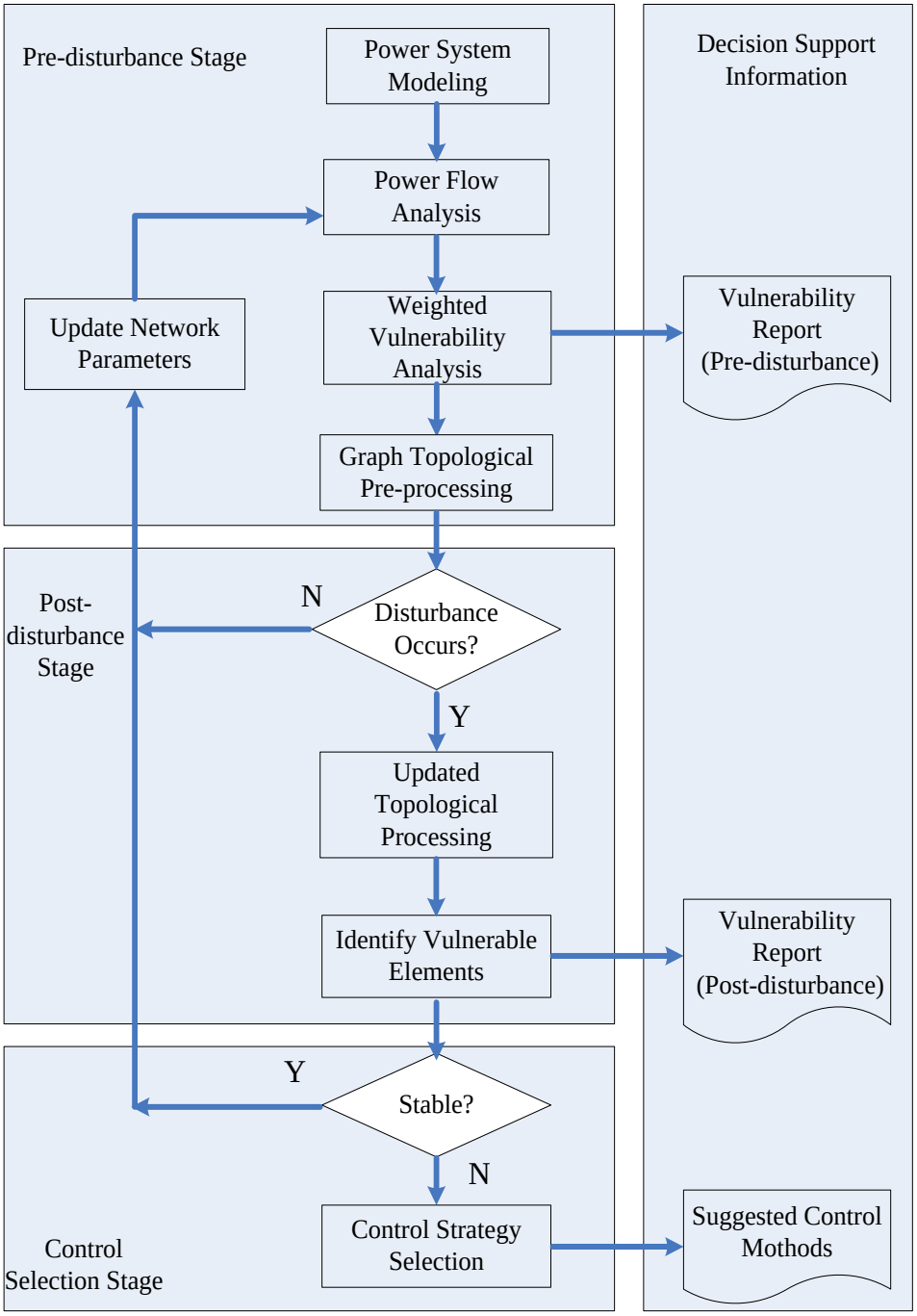

Figure 3 Flowchart of Proposed Method for Fast Detection and Mitigation of Cascading Outages

1.3.1 Pre-disturbance Stage

In this stage, the power system is in normal condition. After getting the base power flow results from state estimation, two main analysis tasks need to be accomplished.

Weighted Vulnerability Analysis: Song has proposed the concepts of Vulnerability Index (VI) and Margin Index (MI) [37] for the main elements in power system: generators, buses, and branches. The system-wide vulnerability and security of individual elements can be evaluated by the different VI and MI values computed for various system conditions. But those VIs and MIs only considered the electrical properties of power system. When performing the steady state analysis to find the vulnerability of system elements, the weights for all VIs and MIs are assigned with value of one as default value or based on historical experience of system operator. The weight values present the importance of each VI and MI in system-wide or individual vulnerability. How to determine the weight values still remains a challenge. In this dissertation, a method to calculate the weight values for each VI and MI which is based on the concepts of vertex and edge betweenness centralities is proposed. With those calculated weights, the new weighted vulnerability analysis can be implemented based on Weighted Vulnerability Index (WVI). The improved WVI values provide a combined consideration of both electrical characteristics of power system and topology

parameters in the graph representation of the electrical network. This way, the vulnerable system elements could be identified and the whole system conditions could be evaluated. Section 4 will discuss the detailed procedures.

Topological Pre-processing: The power system can be modeled as a graph network and analyzed to solve practical problems. When modeling power system, the generators, bus bars and loads can be identified as the graph nodes and the connecting transmission lines can be modeled as the edges. It any steady state, a power system would be a directed graph network because of the directions of power flow.

After the topological model is created, the domain of each generator, the common of buses and links between commons will be determined, which is called topological pre-processing. The concepts of generator domain and bus common were proposed by Kirschen, et al. to determine which generators are supplying a particular load, how much use each generator is making of a transmission line, and what is each generator's contribution to the system losses [38]. The domain of a generator is defined as the set of buses which are reached by power produced by this generator. A common is defined as a set of contiguous buses supplied by the same generators. Unconnected sets of buses supplied by the same generators are treated as separate commons. A bus belongs to one and only on common. Figure 4 shows an example of commons for 6-bus system. It has three commons under the given power flow result: Common 1

includes Bus 1 and 2, which are supplied by generator A only; Common 2 includes Bus 3, 4, and 5, which are supplied by both generator A and B; Common 3 only includes Bus 6, which is supplied by generator A, B, and C. These concepts are used here for fast searching vulnerable parts due to power flow redistribution in power system during cascading outages. Typical four steps will be taken: creating power system topological model, searching the domain for each generator and common for each bus, building state graph by partitioning the original topological model into different zones with homogenous characteristics, and identifying the links in the state graph. The detailed procedures will be discussed in Section 5.

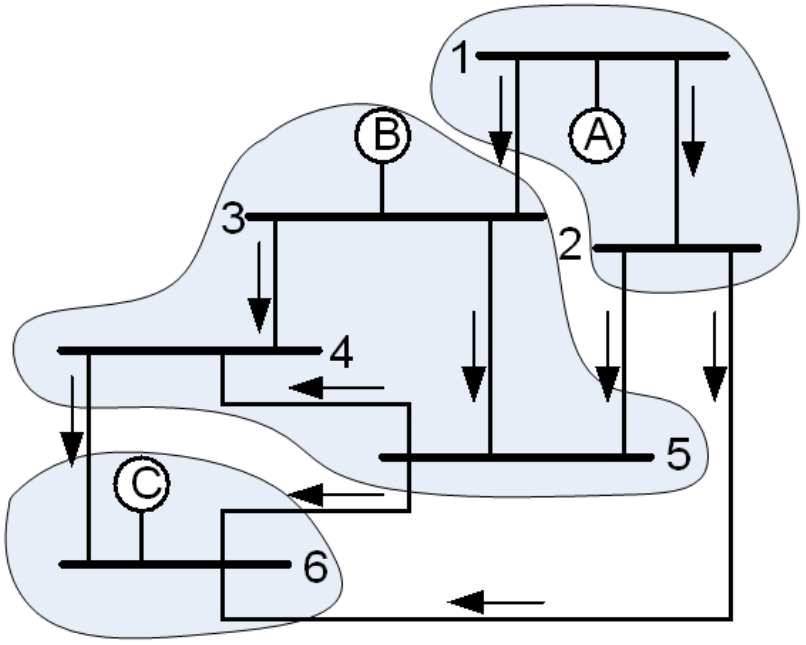

Figure 4 Commons for the 6-bus System

1.3.2 Post-disturbance Stage

If some disturbance happens, such as transmission line tripping due to faults, the topology of the power system network will change. The updated topological processing will be performed based on the available pre-processing results, which could be accomplished very fast. The power system may still be in stable but more stressed condition. The power flow on the tripped transmission line will be transferred to the other lines and may cause overload problem and the occurrence of power swing, which may cause relay misoperation. The most vulnerable elements suffering from the disturbance greatly could be identified by searching the links related with faulted lines in the generated state graph, which may take most of the power flow from the tripped line. An effective method to detect the fault during power swing is proposed to increase relay dependability. The detailed description will be provided in Section 6.

1.3.3 Post-disturbance Control

After the key vulnerable elements have been identified, the associated remedial control actions need to be taken to solve the overload and/or low voltage problems. For the given power system, there are many available network control methods, such as line switching, Thyristor Controlled Series Capacitors (TCSC) control, Static Var Compensation (SVC) control, shunt capacitor or reactor switching, etc [39]-[43]. A control scheme, which will be used as the primary control selection method for this

stage has been proved effective in solving the line overload, congestion, bus high or low voltage problems [44],. The control scheme is based on methods of network contribution factor (NCF), generator distribution factor (GDF), load distribution factor (LDF), and selected minimum load shedding (SMLS). The optimal control actions will be taken to enhance system security level. The detailed description about these control methods can be found in [37] and [44].

1.4 Organization of the Dissertation

The dissertation is organized as follows. The background of cascading outages in power system is provided in Section 2. Section 3 describes the power system applications of graph theory and the topological model. The proposed weighted vulnerability analysis method is presented in Section 4. Section 5 describes the parallel corridor searching method based on graph partitioning. Section 6 introduced the enhanced distance relay scheme for vulnerable parts in power system. The conclusions and contribution of the dissertation are discussed in Section 7. References and Appendices are attached in the end.

2. BACKGROUND OF CASCADING OUTAGES IN POWER SYSTEM

2.1 Introduction

Power systems are exposed to all kinds of disturbances. Among the disturbances, cascading outage, especially the large-scale cascading outage, may cause great economic damage to the power system and devastating impact on people's life. In this section, the background of cascading outages in power system will be discussed. Section 2.2 explains the problem of cascading outages. Section 2.3 reviews the major blackouts in the world. The key lessons learned from those major blackouts are presented in section 2.4. Section 2.5 gives the summary.

2.2 Problem of Cascading Outages

Power system security and stability are the top priority when operating the electric power system. Power systems are exposed to all kinds of disturbances, which may come from bad weather, human errors, equipment malfunction, natural disasters, etc., and some of these disturbances may cause power service interruption. This situation is getting even worse under new market rules introduced by deregulation causing more stressed operation.

As one of those disturbances, cascading failure is defined as "*a sequence of dependent failures of individual components that successively weaken the power*

system." [2]. Cascading outage, especially the large-scale cascading outage, draws special attention since it can cause great economic loss in revenue for the power system owners and devastating impact on people's life, such as North America northeastern system blackout in 2003 [1], Europe blackout in 2006 [45], and Brazil blackout in 2009 [46], etc.

2.3 Major Blackouts in the World

2.3.1 North American Northeast Blackout in 2003

The 2003 Northeast Blackout was summarized in the final report by North American Electric Reliability Council (NERC) [1].

This blackout happened on August 14, 2003, which was a typical hot summer day. System loads in the eastern Great Lakes had exceeded the day-ahead forecasts but still were below the historical record level. FirstEnergy was importing power into the Cleveland area to meet the demand. With the increase of load and some local unit outages, voltage in this area began sagging. Midwest Independent System Operator (MISO) encountered software problem with their system analysis and monitoring tools beginning from 12:15. Figure 5 summarizes the timeline of major events in the origin of the blackout in Ohio for different phases [1].

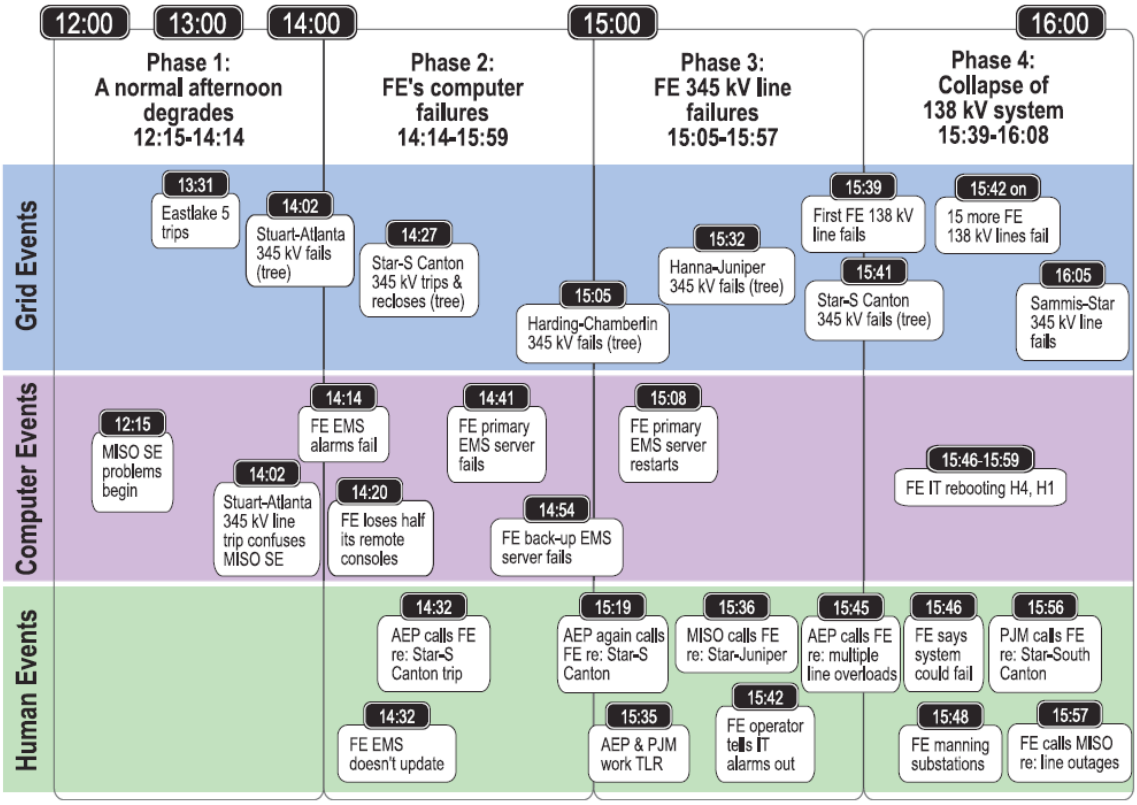

Figure 5 Timeline of 2003 Northeastern Blackout in Ohio

The Eastlake 5 unit near Cleveland tripped at 13:31 due to short of enough reactive output to support the voltage. This trip removed about 500 MW active power and similar amount of reactive power generation from the area, further increasing the imports to serve the load and the voltage situation. It cannot be concluded that this trip is the event that caused the blackout, since the power system is planned to withstand such contingencies. Any probable single event leading to a loss of power system elements should not endanger the security of interconnected operation. The remaining

network elements should be able to accommodate the additional load or change of generation, voltage deviation or transient stability regime caused by the initial failure. But unfortunately the alarm and event logging software in the FirstEnergy Energy Management System (EMS) failed after 14:14. The system operators were unaware of those failures. One 345 kV transmission line, Chamberlin-Harding, which connects the Cleveland area to generation in the Ohio River Valley to the southeast tripped at 15:05,. This line tripped due to a ground fault caused by conductors sagging into a 42 foot tall tree growing in the line's right of way. The second 345 kV line, Hanna-Juniper, tripped after about half an hour later. Loss of these two lines caring power into Cleveland caused flows from the south to squeeze onto other more indirect paths. At 15:41, the third 345 kV line to the southeast of Cleveland, Star-South Canton, also tripped and locked out. At this point, only one 345 kV line, Sammis-Star and several 138 kV lines remained in service to maintain the connection of the Cleveland area to the Ohio Valley. From 15:39 to 15:59, the 138-kV system began to collapse due to overloads and lines tripping.

At 16:05, the last 345 kV line, Sammis-Star, tripped, which is considered as the cascade trigger. The trip of Sammis-Star initiated a rapid cascade that would have been virtually impossible to stop by human intervention. Two more 345 kV lines in northwest Ohio, Muskingum-Ohio Central-Galion and East Lima-Fostoria Central,

tripped around 16:09, which completed the separation of northern Ohio from central Ohio and forced the loop power flow further north into Michigan. Figure 6 shows the rate of line and generator trips during the cascading outage [1]. The events in the cascade started relatively slowly during the initial stage of the blackout, but picked up the speed after 16:08:59 EDT. From 16:09 to 16:10, large number of generators were lost and system collapsed.

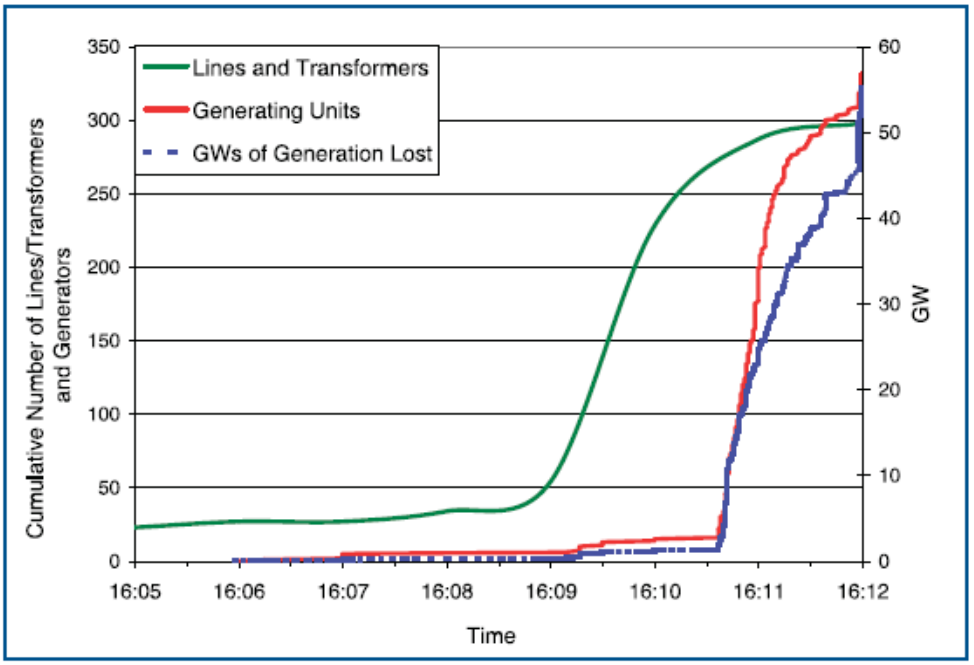

Figure 6 Rate of Line and Generator Trips during Cascading Outage

The post-mortem investigation had identified the typical causes of this blackout

were the lack of understanding of the transmission system and inadequate real-time diagnostic support from the reliability coordinators. The northeastern system was in extreme condition due to lack of reactive power. Although the tripping of the first few transmission lines was due to inadequate tree trimming, overload is the major contributor to the subsequent cascading trips of transmission lines. If system operator have had better situational awareness and took remedial actions through load shedding, it might have prevented the cascading outage.

2.3.2 Europe Blackout in 2006

The 2006 Europe major disturbance of November 4, 2006 was summarized in the final report by Union for the Co-ordination of Transmission of Electricity (UCTE) [45].

November 4th was a weekend. As usual, when demand is lower than during the working days, several transmission network elements were not in operation due to scheduled maintenance and construction work. In the meantime, the specific topology in the 380 kV substation of Borken in E.ON Netz, a local control center, changed due to construction work. Two busbars in the substation were split in two parts each, which made the power flow from East to West in this region impossible. Additionally, as the normal configuration, the 380 kV Landesbergen substation in E.ON Netz was operated with two separated busbars in order to reduce the short-circuit current which would

exceed the limit of the switchgear in case Robert Frank 4 power plant is in operation.

An exchange program represents the total scheduled energy interchange between two control areas or between control blocks. Figure 7 shows both exchange programs resulted from trading activities (red) and physical flows (blue) as recorded on November 4 at 22:09 [45]. It shows the physical flows significantly differ from the exchange programs, which is pretty normal in a highly meshed network. There is high flow from Germany to The Netherlands and to Poland due to the high wind generation in Germany.

There was also a planning for the Conneforde-Diele outage, which is a 380 KV transmission line with double circuits. Before the opening, RWE Transmission System Operators (TSO) has made the power flow calculation and an N-1 analysis with the outage of the Conneforde-Diele line. The results confirmed the grid would be highly loaded but still secure.

At 21:38, E.ON Netz switched off first circuit of the 380 kV line Conneforde-Diele. And one minute later, the second circuit was switched off. After the switching operation, E.ON Netz received several warning messages about the high power flow on the lines Elsen-Twistetal and Elsen-Bechterdissen. At 21:41, RWE TSO informed E.ON Netz about the safety limit value of 1795 A on the line Landesbergen-Wehrendorf (an interconnection line between E.ON Netz and RWE

TSO). At this point of time the current on this line has not reached its given limit (1795 A), and the internal RWE TSO network still met the N-1 criterion. The protection setting on both sides of Landesbergen-Wehrendorf line were different: 3000 A on the E.ON side and 2100 A on the RWE side. The dispatchers were not aware of the settings in the protection system, which make the dispatchers not take into account the correct values of their evolution of the situation later. The load on the Landesbergen-Wehrendorf line increased by 100 MW between 22:05 and 22:07, and exceeded the warning value of 1795 A for RWE TSO. E.ON Netz made an empirical assessment of corrective switching measures without any load flow calculations for checking N-1 criterion after receiving the urgent intervention to restore safe grid operation from RWE TSO at 22:08. In the end, the line was tripped by the distance relays in the Wehrendorf side due to overloading. This tripping led to cascading line tripping throughout the UCTE area. Eventually, the UCTE system was split at 22:10 into three subsystems as shown in Figure 8 [45]. The area 1 and 3 remained asynchronously connected through the DC link between Italy and Greece during the whole event. Figure 9 shows the frequency recordings retrieved by Wide Area Measurement Systems (WAMS) before, during and after the split-up in the three areas. The manual switching in the Landesbergen substation is considered as the trigger event for the frequency oscillations leading to different lines tripping.

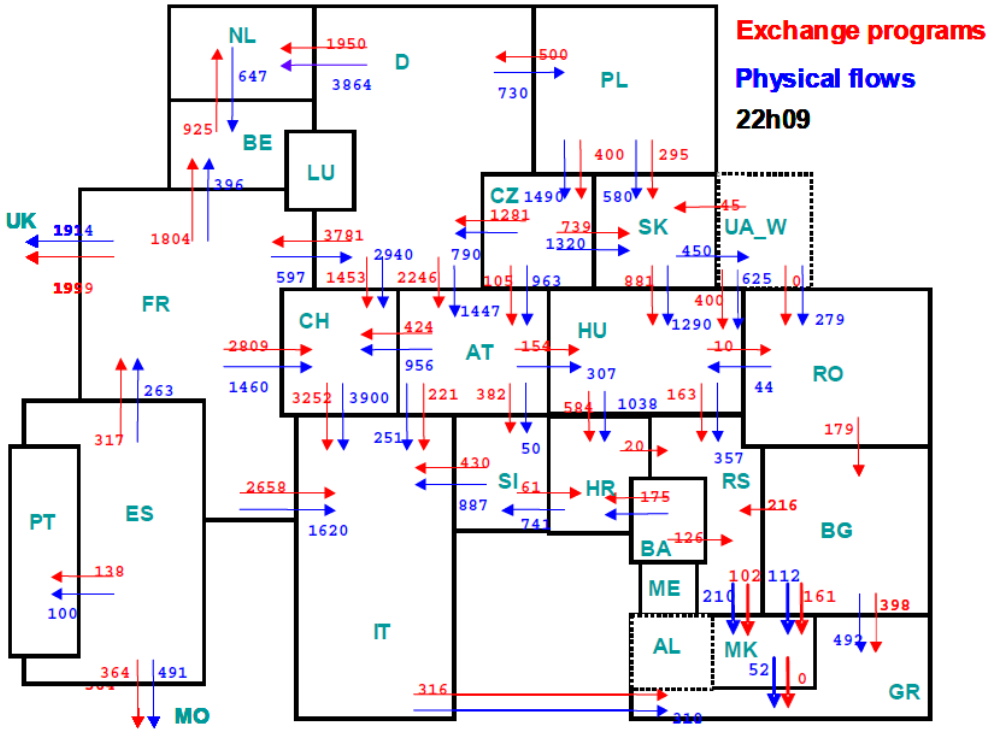

Figure 7 Exchange Programs and Physical Flows on Nov. 4 at 22:09

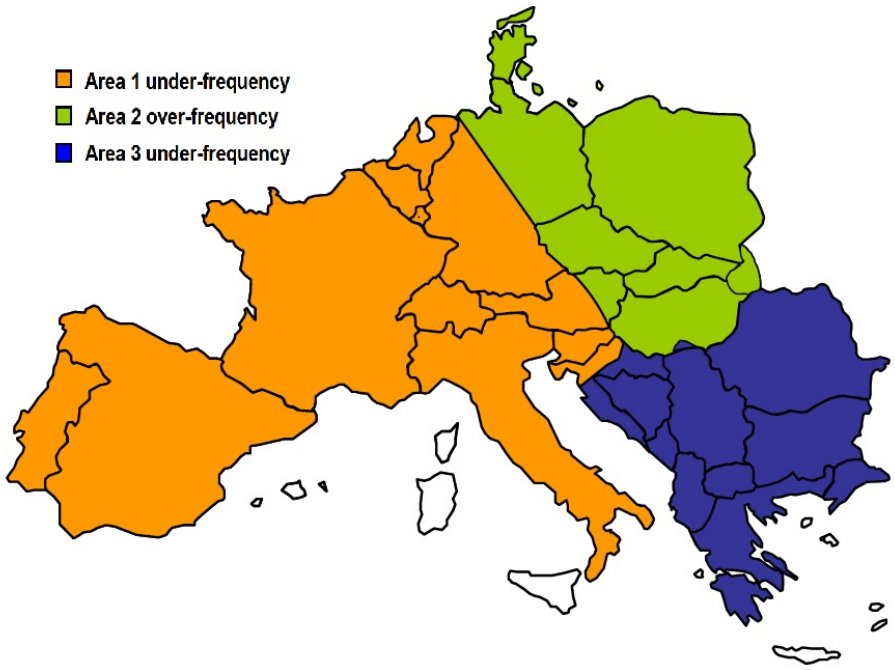

Figure 8 Schematic Map of UCTE Area Split into Three Areas

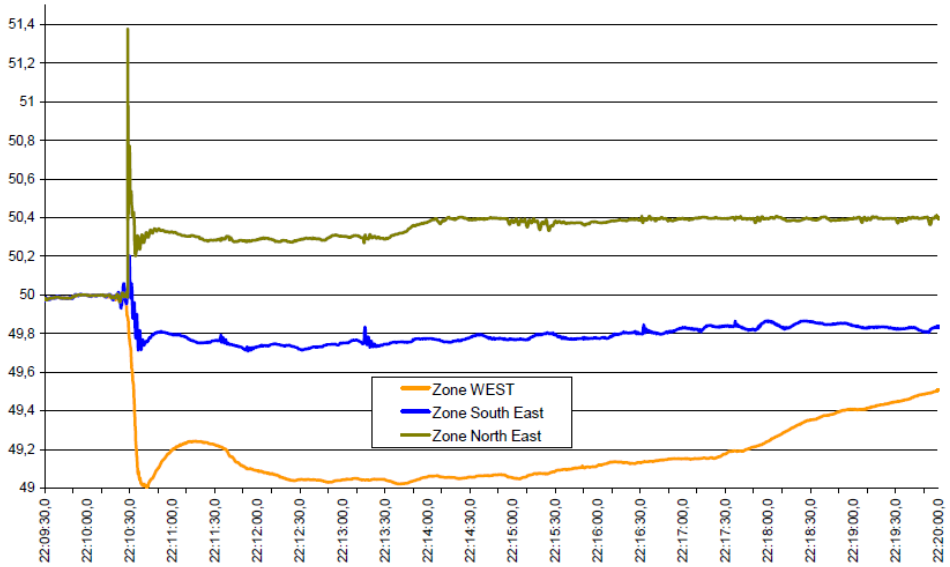

Figure 9 Frequency Recordings during the Blackout

The 2006 UCTE blackout led to power supply disruptions for more than 15 million European households. The immediate action taken by all TSOs according to the UCTE security standards prevented this disturbance to turn into a Europe-wide blackout. However, this event ranks among the most severe and largest disturbances in Europe. It took 38 minutes after the splitting to complete the full resynchronization of the UCTE system and almost 2 hours to e-establish a normal situation in all European countries.

The main cause of this blackout was non-compliance with the N-1 criterion. Transmission line overloading occurred right after the scheduled Conneforde-Diele 380 KV transmission line outage, which triggered the cascading trips. Similar to 2003

Northeastern Blackout, insufficient coordination and communication among the TSOs/ISOs was also an important contributing factor.

2.4 Lessons Learned from Cascading Outages

2.4.1 Causes of Cascading Outage

The cascading outage is a sequence of events in which an initial disturbance triggers a sequence of one or more dependent component outages. As mentioned above, many factors can contribute to the cascading outages. IEEE Computer Analytical Methods Subcommittee (CAMS) has formed a Task Force on Understanding, Prediction, Mitigation and Restorations of Cascading Failures to promote development of new methods, technologies and tools. The Task Force has summarized the immediate causes of cascading trips during blackouts, which include: [5]

- Overloaded transmission lines that subsequently contact vegetation
- Overcurrent/undervoltage conditions triggering distance relay actions
- Hidden failures in protection devices, which are exposed by a change in operating state
- Voltage collapse
- Insufficient reactive power resources
- Stalled motors triggered by low voltages or off-nominal frequency
- Generator rotor dynamic instability

- Small signal instability
- Over (or under) excitation in generators
- Over (or under) speed in generators
- Operator or maintenance personnel error
- Computer or software errors and failures
- Errors in operational procedures

Each large blackout typically combines several of these interactions into dependent failures. One common aspect of these interactions is that the interactions tend to be stronger when the power system is more stressed or loaded. Due to the complex factors causing cascading outage, to detect, prevent and mitigate cascading outages is still one of the most difficult and challenging tasks for power system researchers and engineers.

2.4.2 Mechanism of Cascading Outages

Cascading outages are always complex and many factors influence cascading outages. Chen has divided the blackouts into four typical stages of cascading sequences when the outages propagate [47]:

- Initiating contingency;
- Steady-state progression;
- Transient progression;

- Uncontrolled islanding and blackout.

In this dissertation, the four propagating stages can be simplified into two stages as temporal view:

- Steady state progress stage
- Transient progress stage.

Steady state progression is the slow succession comparing to the fast succession of transient progression. The initiating contingency is part of the steady state progress. The transient progress stage is a fast transient process resulting in cascading blackouts and finally the collapse of the entire system. Uncontrolled islanding and blackout occur in this stage.

During the steady-state progression stage, the system becomes stressed with heavy loading on system components, such as transmission lines, generators, and transformers. Successive events occur, and the time intervals between the trips of components are fairly long. For example, the sequence tripping for transmission line overload or generator over-excitation caused by one line tripping may follow after several minutes or even hours. These long time intervals may be long enough for the system operators to take corrective actions needed to mitigate the unfolding events or undesired trend. Developing a generalized tool or set of tools for power system operator’s decision support for corrective control after the initialing contingency

occurs is not only desirable but also feasible.

2.5 Summary

Although the risk of large area cascading outages occurring is low, the consequences of cascading outages may bring catastrophic social and economic impacts. By reviewing the major blackouts in the world, the background of cascading outages have been introduced. It is obvious that many factors can cause cascading outages. Most of cascading outages have two stages: steady-state progression and transient progression. Steady state progress stage is an important period, since the system operators may have enough time to evaluate the system condition, identify some vulnerable contingencies, take some control to increase the security level and prevent the possible cascading blackouts.

3. POWER SYSTEM TOPOLOGICAL MODEL

3.1 Introduction

Electric power system is one of the most complex man-made systems. With the advances in complex network theory, the power system can be modeled as a graph network and analyzed to solve practical problems. In this section, the power system topological model will be discussed. Section 3.2 reviews the applications of graph theory in power system. The method of modeling power system as directed graph network is presented in Section 3.3. Case study and summary are given in Section 3.4 and 3.5 respectively.

3.2 Power System Applications of Graph Theory

Graph theory is an important branch of mathematics concerned about how networks can be encoded and how their properties may be measured [48]. It provides a feasible way to simplify the complex problems into a set of linked nodes. Because of its wide applicability, graph theory is one of the fast-growing areas of modern mathematics. Graph theory has been widely introduced into the research of many areas, such as mathematics, computer programming and networking, business administration, sociology, economics, communications, etc.[48]-[55].

Electric power system is an integrated huge synchronous machine system

composed by thousands of generators, transformers, transmission lines, substations, and loads, with the interfaces to numerous measurement, communication, and control units. The power system can be modeled as a graph network and analyzed to solve practical problems.

Lee, et al. proposed a transportation method for economic dispatch application based on graph theory [56]. Watts showed that the topology of a typical power system network is a small-world network [57]. Hines and Blumsack [58] derived a measure of electrical centrality for power system networks, which describes the structure of the network as a function of its electrical topology rather than its physical topology. Leisieutre, et al. [59] refined the topological graph concepts in order to be more consistent with power system generation and load patterns by offering an approximate solution through relaxation of the integer problem and suggesting refinement using stochastic methods. Motter and Lai [32] tried to formulate the problem of cascading attack and worked on cascading phase transitions by complex networks theory. They demonstrated that the heterogeneity of power system networks makes them particularly vulnerable to attacks in that a large-scale cascade may be triggered by disabling a single key event, which brings serious concerns on the security of such systems. Korres and Katsikas presented a hybrid topological-numerical approach for observability analysis in power system state estimation by partitioning the network in

observable areas based on graph theory [60]. Liu, et al. introduced the attack graph and multiple criteria decision-making (MCDM) to deal with the difficulties of security assessment: the security analysis of power control process and the security degree of each control step [61]. Dustegor, et al. presented model-based fault detection and location methodology based on structural analysis, which utilizes the analytical redundancy inherent in the system structure and provided a strategy for systematic and automatic generation of residuals [62]. In this dissertation, graph theory will be used to identify the vulnerable elements in the power system.

3.3 Power System as Directed Graph Network

3.3.1 Graph Model of Power System Elements

Suppose $G = (V, E)$ is a graph network with v nodes (vertices) and e links (edges). V is the set of vertices, and E is the set of connecting edges, which is showing the relations between those vertices. The graph will be getting more complex with the increasing number of vertices and edges. Two important matrices are widely used to study graphs: adjacency matrix and incidence matrix.

The adjacency matrix $A = \{a_{ij}\}$ implies the connectivity of the vertices, which is defined by:

$$a_{ij} = \begin{cases} 1 & \text{if there is an edge between } v_i \text{ and } v_j \\ 0 & \textit{otherwise} \end{cases} \quad (1)$$

The incidence matrix $A' = \{a'_{ij}\}$ implies the connectivity of the vertex to edge,

which is defined by:

$$a_{ij}^{'} = \begin{cases} 1 & \text{if vertex } v_i \text{ connected to edge } e_j \\ 0 & \textit{otherwise} \end{cases} \qquad (2)$$

For example, for a graph with five vertices and seven edges shown in Figure 10, the adjacency matrix A and incidence matrix $A^{'}$ can be obtained based on Equation (1) and (2), respectively.

$$A = \begin{bmatrix} 0 & 1 & 1 & 0 & 0 \\ 1 & 0 & 1 & 1 & 1 \\ 1 & 1 & 0 & 0 & 1 \\ 0 & 1 & 0 & 0 & 1 \\ 0 & 1 & 1 & 1 & 0 \end{bmatrix} \qquad A^{'} = \begin{bmatrix} 1 & 1 & 0 & 0 & 0 & 0 & 0 \\ 1 & 0 & 1 & 1 & 1 & 0 & 0 \\ 0 & 1 & 1 & 0 & 0 & 0 & 1 \\ 0 & 0 & 0 & 1 & 0 & 1 & 0 \\ 0 & 0 & 0 & 0 & 1 & 1 & 1 \end{bmatrix}$$

If the graph is undirected graph as shown in Figure 10, the adjacency matrix is symmetric.

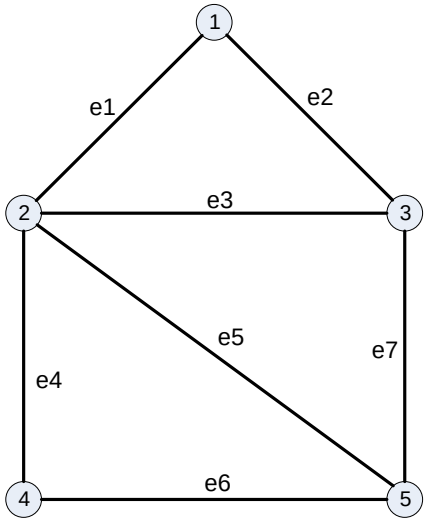

Figure 10 A Graph with Five Vertices and Seven Edges

Since the power system is an integrated synchronous system, in which the substations are connected to each other by transmission lines, it is very easy to get the topological model of power system represented as a graph. When modeling power system using graphs, the generators, bus bars and loads can be identified as the graph nodes and the connecting transmission lines can be modeled as the edges. Thus the undirected graph model of the power system is easily obtained.

3.3.2 Directed Graph Model

In power engineering, the power flow study is always an important tool involving numerical analysis applied to a power system. It has been studied that in any steady state, a power system would be a directed graph network [63], because the directions of power flow in the modeled network can be measured in any given steady state. Hence, the power system should be modeled as the directed graph. For the directed graph, the definitions of adjacency matrix and incidence matrix are different than those in undirected graph.

The directed acyclic graph is defined as a directed graph with no directed cycles, which is formed by a collection of vertices and directed edges, each edge connecting one vertex to another, such that there is no way to start at some vertex v and follow a sequence of edges that eventually loops back to v again [63].

For a directed graph G, the adjacency matrix $A = \{a_{ij}\}$ implies the connectivity

of the vertices, which is defined by:

$$a_{ij} = \begin{cases} 1 & \text{if there is a directed edge from } v_i \text{ to } v_j \\ 0 & \textit{otherwise} \end{cases} \quad (3)$$

For a directed graph G, the incidence matrix $A' = \{a'_{ij}\}$ implies the connectivity of the vertex to edge, which is defined by:

$$a'_{ij} = \begin{cases} 1 & \text{if vertex } v_i \text{ is sending end of edge } e_j \\ -1 & \text{if vertex } v_i \text{ is receiving end of edge } e_j \\ 0 & \text{if vertex } v_i \text{ and vertex } v_i \text{ is not connected by edge } e_j \end{cases} \quad (4)$$

3.4 Case Study

Figure 11 shows a simple example of 4-bus system connected by five transmission lines. The directed graph model of this 4-bus system is also shown in Figure 11. The adjacency matrix A and incidence matrix A' can be obtained based on Equation (3) and (4), respectively.

$$A = \begin{bmatrix} 0 & 1 & 1 & 1 \\ 0 & 0 & 0 & 1 \\ 0 & 0 & 0 & 1 \\ 0 & 0 & 0 & 0 \end{bmatrix} \qquad A' = \begin{bmatrix} 1 & 1 & 1 & 0 & 0 \\ 0 & 1 & 0 & 0 & 1 \\ 1 & 0 & 0 & 1 & 0 \\ 0 & 0 & 1 & 1 & 1 \end{bmatrix}$$

The adjacency matrix of the directed graph is asymmetric due to the directions of the power flow on transmission lines.

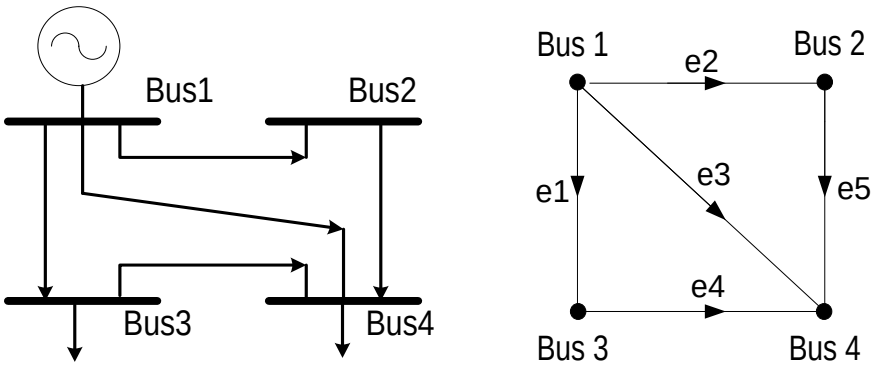

Figure 11 4-bus Power System and its Graph Model

3.5 Summary

This section reviewed the basic concepts of graph theory and the typical applications of graph theory in power system. The power system can be modeled as directed graph network based on the power flow results. With the help of linear algebra, the adjacency matrix and incidence matrix are formulated in order to study the modeled topological network of the power system.

4. WEIGHTED VULNERABILITY ANALYSIS*

4.1 Introduction

As described in section 2, most cascading outages have two stages: steady state and transient state. Steady state is a period of slowly evolving successive events, during which the cascading outages may be prevented if system operator understand the accurate system conditions and takes remedial actions. This dissertation proposes an improved approach, weighted vulnerability analysis method to evaluate the vulnerability of the individual element and the whole system. The weights for each vulnerability index are based on vertex and edge betweenness centrality. Those weight values provide a combined consideration of both electrical characteristics in power systems and topology parameters in graph representation of the power network.

The traditional vulnerability index and margin index are reviewed in section 4.2. Section 4.3 discusses how to determine the weighting factor for the proposed weighted vulnerability analysis method. Section 4.4 provides the case study and summary is given in section 4.5

4.2 Review of Vulnerability Index [64]

---

* Part of the material in this section is reprinted from "Static Security Analysis based on Weighted Vulnerability Index" by Chengzong Pang and Mladen Kezunovic, *Presented in IEEE Power and Energy Society General Meeting*, Detroit, MI, USA, July 2011, ©2011 IEEE.

Vulnerability index and margin index are proposed by Dr. Song to represent comprehensive and quantitative vulnerability and security information of the individual part and whole system [37], [64]. Since there are no weighs in the definitions of MIs, we only give the review of the concept of vulnerability index. For the detailed discusses on vulnerability index and margin index, please refer to the literature [37] and [64].

At the generator level, vulnerability indices for real power output, reactive power output and generation loss and margin indices for real and reactive power outputs were considered. At the bus level, vulnerability indices for bus voltage performance, loadability and load loss and margin indices for bus voltage performance and loadability were presented. Islanding and isolated buses due to the line outages were considered in the load loss part. At the transmission line level, vulnerability indices for line real power, reactive power, line charging, line bus voltage angle difference, line distance relay performance, and line-off influence were discussed. Given a system with “m” generators, “n” buses, “p” lines and “q” loads, the comprehensive Vulnerability Index (VI) sets are defined as below:

4.2.1 Vulnerability Index for Generators

$$VI_{Pg,i} = \frac{W_{Pg,i}}{2N}\left(\frac{Pg_i}{Pg_{i,\max}}\right)^{2N} \tag{5}$$

$$VI_{Qg,i} = \frac{W_{Qg,i}}{2N}\left(\frac{Qg_i}{Qg_{i,\max}}\right)^{2N} \quad (6)$$

$$VI_{gen\_loss,i} = W_{gen\_loss,i} k_i \quad (7)$$

$$VI_{gen} = \sum_{i=1}^{m} (VI_{Pg,i} + VI_{Qg,i} + VI_{gen\_loss,i}) \quad (8)$$

where

$VI_{Pg,i}$: *VI* of individual generator real power output

$VI_{Qg,i}$: *VI* of individual generator reactive power output

$VI_{gen\_loss,i}$: *VI* of individual generator loss

VI_{gen}: total *VI* of all generators

$W_{Pg,i}$: weight of individual generator real power output

$W_{Qg,i}$: weight of individual generator reactive power output

$W_{gen\_loss,i}$: weight of individual generator loss influence

Pg_i, Qg_i: individual generator real, reactive power output

$Pg_{i,\max}$: maximum real power output of generator

$Qg_{i,\max}$: maximum reactive power output of generator when Qg_i is positive; minimum reactive power output of generator when Qg_i is negative

k_i: 1 when generator is off, 0 when generator is on

N: 1 in general

4.2.2 Vulnerability Index for Buses

$$VI_{V,i} = \frac{W_{V,i}}{2N}\left(\frac{V_i - V_i^{sche}}{\Delta V_{i,\lim}}\right)^{2N} \quad (9)$$

$$VI_{Loadab,i} = \frac{W_{Loadab,i}}{2N}(r_{Loadab,i})^{2N} \quad (10)$$

$$VI_{load\_loss,i} = W_{load\_loss,i} r_i \quad (11)$$

$$VI_{bus} = \sum_{i=1}^{n}(VI_{V,i} + VI_{Loadab,i} + VI_{load\_loss,i}) \quad (12)$$

where

$VI_{V,i}$: *VI* of individual bus voltage magnitude

$VI_{Loadab,i}$: *VI* of individual load bus loadbility

$VI_{load\_loss,i}$: *VI* of individual load bus load loss

VI_{bus} : total *VI* of all buses

$W_{V,i}$: weight of individual bus voltage influence

$W_{Loadab,i}$: weight of individual bus loadability

$W_{load\_loss,i}$: weight of individual bus load loss influence

V_i : bus voltage magnitude

V_i^{sche} : scheduled bus voltage magnitude

$\Delta V_{i,\lim}$: voltage variance limit

$r_{Loadab,i}$: bus loadability, which is defined as $r_{Loadab,i} = \frac{Z_{th,i}}{Z_{L0,i}}$

$Z_{th,i}$: Thevenin equivalent system impedance

$Z_{L0,i}$: equivalent load impedance at steady state

r_i : load loss ratio, 0~1, 0: no loss; 1: completely loss

N : 1 in general

4.2.3 Vulnerability Index for Branches

$$VI_{Pf,i} = \frac{W_{Pf,i}}{2N}\left(\frac{Pf_i}{S_{i,\max}}\right)^{2N} \tag{13}$$

$$VI_{Qf,i} = \frac{W_{Qf,i}}{2N}\left(\frac{Qf_i}{S_{i,\max}}\right)^{2N} \tag{14}$$

$$VI_{Qc,i} = \frac{W_{Qc,i}}{2N}\left(\frac{Qc_i}{Q_{\Sigma}}\right)^{2N} \tag{15}$$

$$VI_{line\_ang,i} = \frac{W_{line\_ang,i}}{2N}\left(\frac{La_i}{La_{i,\max}}\right)^{2N} \tag{16}$$

$$VI_{\mathrm{Re}lay,i} = \frac{W_{\mathrm{Re}lay,i}}{2N}\left((1/d_{sr,i})^{2N} + (1/d_{rs,i})^{2N}\right) \tag{17}$$

$$VI_{line\_off,i} = W_{line\_off,i}k_i \tag{18}$$

$$VI_{line} = \sum_{i=1}^{p}\left(VI_{Pf,i} + VI_{Qf,i} + VI_{Qc,i} + VI_{line\_ang,i} + VI_{\mathrm{Re}lay,i} + VI_{line\_off,i}\right) \tag{19}$$

where

$VI_{Pf,i}$: *VI* of individual line real power

$VI_{Qf,i}$: *VI* of individual line reactive power

$VI_{Qc,i}$: *VI* of individual line charging

$VI_{line\_ang,i}$: *VI* of individual bus voltage angle difference at each line

$VI_{\mathrm{Re}lay,i}$: *VI* of individual line distance relay

$VI_{line\_off,i}$: *VI* of individual line outage influence

VI_{line} : total *VI* of all lines

$W_{Pf,i}$: weight of individual line real power influence

$W_{Qf,i}$: weight of individual line reactive power influence

$W_{Qc,i}$: weight of individual line charging influence

$W_{line\_ang,i}$: weight of individual line bus angle difference

$W_{Relay,i}$: weight of individual line distance relay

$W_{line\_off,i}$: weight of individual line off influence

Pf_i , Qf_i , Sf_i : line real, reactive and apparent power

$S_{i,\max}$: individual line transmission limit, which can be either thermal limit or transfer limit due to security constraints

Qc_i : individual line charging

Q_Σ : total reactive power output of all generators, or total reactive power of the whole system

La_i : individual bus voltage angle difference at each line

$La_{i,\max}$: bus voltage angle difference limit at each line

$d_{sr,i}$: magnitude of normalized apparent impedance seen by distance relay from the sending end to receiving end of that line

$d_{rs,i}$: magnitude of normalized apparent impedance seen by distance relay from the receiving end to sending end of that line

k_i : 1 when line is off, 0 when line is on

The aggregate system vulnerability index can be presented by

$$VI = VI_{gen} + VI_{bus} + VI_{line} \tag{20}$$

The larger the *VI* value, the more vulnerable the system condition. By calculating the different VI and MI values, the security for system-wide and individual elements could be obtained.

4.3 Weighted Vulnerability Analysis

In the traditional vulnerability index approach, the weights in VIs are set as one or chosen by system operators based on their experience. Like any other network, there are some buses and branches in the power system which are more critical than the others due to their locations, properties, and functions. They have more influences on the system security and hence should have larger weights than the others. It is not an easy task to identify the critical elements in power system based only on the operation experiences.

The centrality indices have been introduced as an essential tool for the analysis of different networks [65][66]. For example, these centrality indices were designed to rank the actors according to their position in the network and interpreted as the prominence of actors embedded in a social structure [67]. It was an effective way to measure the critical degree of different elements in the network. In this section, a weighted vulnerability index for power system vulnerability analysis is proposed, which will apply graph-theoretic concept of betweenness centrality to power grid

topology. As discussed in section 3, the directed graph is formed with vertices representing busses and the edges representing transmission lines. The weights for each vulnerability index will be calculated based on the values of betweenness centralities for each bus and branch in power system. This way the weighted vulnerability index method is an effective tool to consider both the inherent electrical properties of power system and the network topological properties.

4.3.1 Vertex Betweenness Centrality

The concept of betweenness centrality was first defined by Freeman [68], where he defined a number of measures of centrality to find out how influential a person or group in a social network is. Betweenness centrality is one of these measures.

For the given graph $G=(V,E)$, the vertex betweenness centrality $BC(v)$ of a vertex $v \in V$ is the sum over all pairs of vertices $u, w \in V$, of the fraction of shortest paths between u and w that pass through vertex v, which is shown as:

$$BC(v)=\sum_{\substack{u,w\in V \\ u\neq w\neq v}} \frac{\sigma_{uw}(v)}{\sigma_{uw}} \tag{21}$$

where $\sigma_{uw}(v)$ denotes the total number of shortest path between vertex u and w that pass through v, and σ_{uw} denotes the total number of shortest paths between u and w.

4.3.2 Edge Betweenness Centrality

The edge betweenness centrality $BC(e)$ of a edge $e \in E$ is the sum over all

pairs of vertices $u, w \in V$, of the fraction of shortest paths between u and w that pass through edge e, which is shown as:

$$BC(e) = \sum_{\substack{u,w \in V \\ u \neq w}} \frac{\sigma_{uw}(e)}{\sigma_{uw}} \tag{22}$$

where $\sigma_{uw}(e)$ denotes the total number of shortest path between vertex u and w that pass through e, and σ_{uw} denotes the total number of shortest paths between u and w.

4.3.3 Betweenness Calculation Example

Take the example of a graph with five vertices and five edges shown in Figure 12. The vertex betweenness centrality of node b is calculated as:

$$\begin{aligned} BC(b) &= \sum_{\substack{u,w \in V \\ u \neq w \neq v}} \frac{\sigma_{uw}(b)}{\sigma_{uw}} \\ &= (\sigma_{ac}(b)/\sigma_{ac}) + (\sigma_{ad}9b)/\sigma_{ad}) + (\sigma_{ae}(b)/\sigma_{ae}) \\ &= 1+1+1=3 \end{aligned}$$

Similarly, the edge betweenness centrality of edge ab is calculated as:

$$\begin{aligned} BC(ab) &= \sum_{\substack{u,w \in V \\ u \neq w}} \frac{\sigma_{uw}(ab)}{\sigma_{uw}} \\ &= (\sigma_{ab}(\mathrm{b})/\sigma_{ab}) + (\sigma_{ac}(\mathrm{b})/\sigma_{ac}) + (\sigma_{ad}(\mathrm{b})/\sigma_{ad}) + (\sigma_{ae}(\mathrm{b})/\sigma_{ae}) \\ &= 1+1+1+1=4 \end{aligned}$$

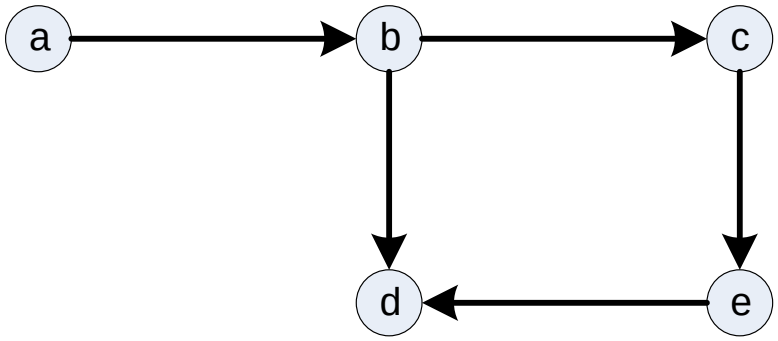

Figure 12 A Graph with Five Vertices and Five Edges

4.3.4 Weights Calculation

As already mentioned, the vertex and edge betweenness centrality are the standard measures for the influence of a vertex or an edge over the rest of the system. The vertices and edges with higher betweenness centralities indicate that they have relatively higher importance than the other elements within the graph network. By applying the betweenness centralities of buses and transmission lines to the power system topology model, the high-impact buses and transmission lines would be identified, which could be used to calculate the weights for the weighted vulnerability index approach proposed in this dissertation.

When modeling power system into a topology model, the generators and buses are identified as nodes and the transmission lines are modeled as the edges. So the weights for VIs of generators and buses will be calculated based on vertex betweenness

centrality; the weights for VIs of branches will be calculated based on edge betweenness centrality.

Considering whether the value of betweenness centrality is becoming large with the increasing number of buses in the power system, the normalized vertex and edge betweenness centralities are used to the real world implementation. The normalized vertex and edge betweenness centralities are defined as:

$$BC\_Norm(v) = \frac{BC(v)}{(n-1)(n-2)} \tag{23}$$

$$BC\_Norm(e) = \frac{BC(e)}{(n-1)(n-2)} \tag{24}$$

where n is the total number of nodes in the power system.

The detailed procedures of the proposed method to calculate the weights are:

- Run power flow analysis to get the direction of power flow on each transmission line;
- Model the power system as a directed graph according to the graph principles;
- For each pair of vertices (u, w), compute all shortest paths between them;
- For each pair of vertices (u, w), determine the fraction of shortest paths that pass through the vertex in question;
- Sum this fraction over all pairs of vertices (u, w) to get the betweenness

centrality for the vertex in question;

- Propagate the calculation to all the vertices and edges to get the betweenness centralities of whole network;
- Normalize the values of betweenness centralities;
- Add the normalized betweenness centrality values to the original weights for each VIs of generators, buses, and branches.

4.4 Case Study

The IEEE 118-bus test system is used to demonstrate the performance of proposed approach. Figure 13 shows the IEEE 118-bus system configuration. The detailed system configuration, base power flow data and machine data can be found in Appendix B [69]-[71].

4.4.1 Calculation of Betweenness Centrality

After obtaining the power flow results either from power system analysis or from state estimation, the basic directed graph-based model of power system is obtained with the directions of power flow on each transmission line. The vertex and edge betweenness centrality is computed according to the adjacency matrix of the power system. The distributions of vertex and edge betweenness centrality with descending sort are shown in Figure 14 and Figure 15, respectively.

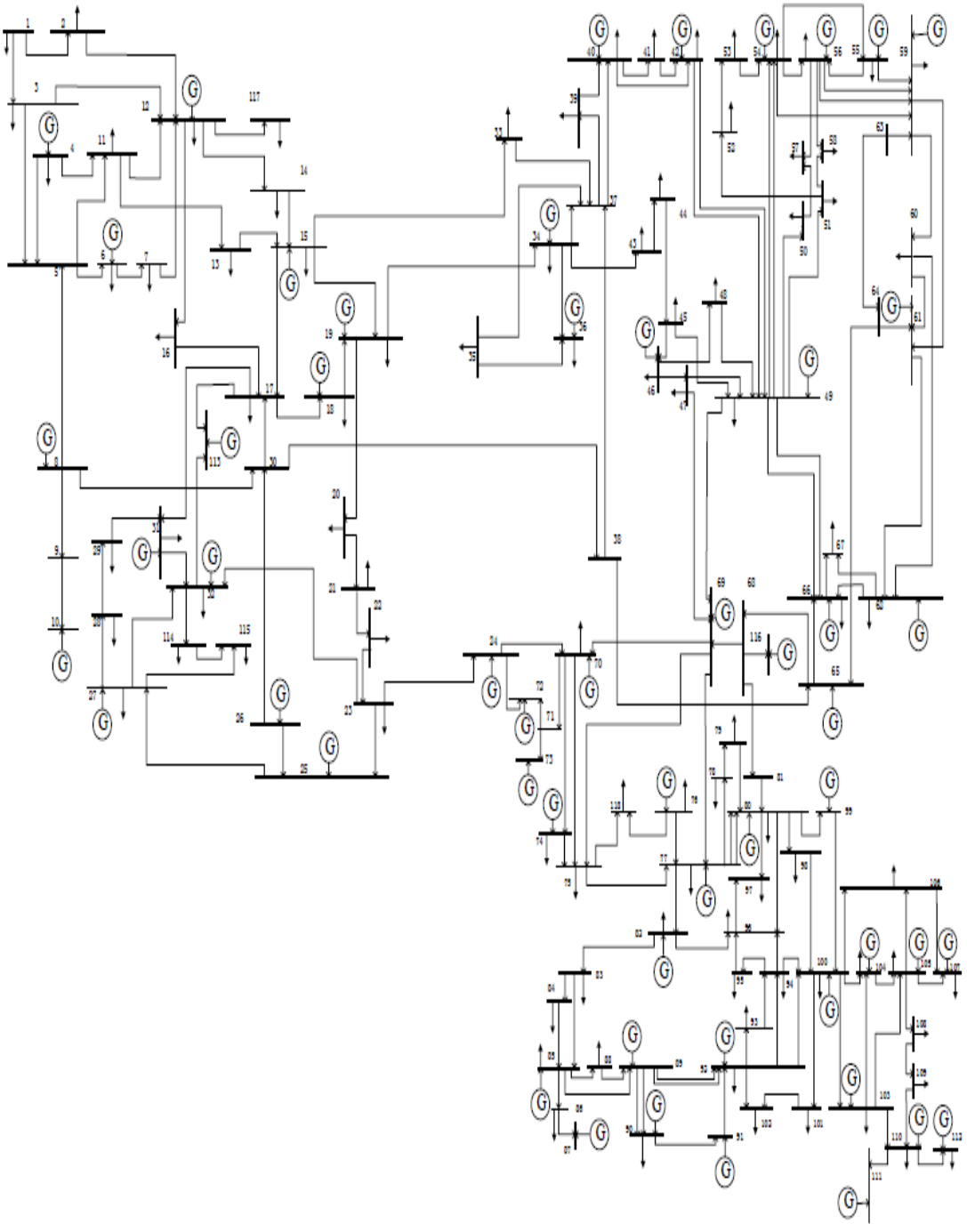

Figure 13 IEEE 118-bus System Configuration

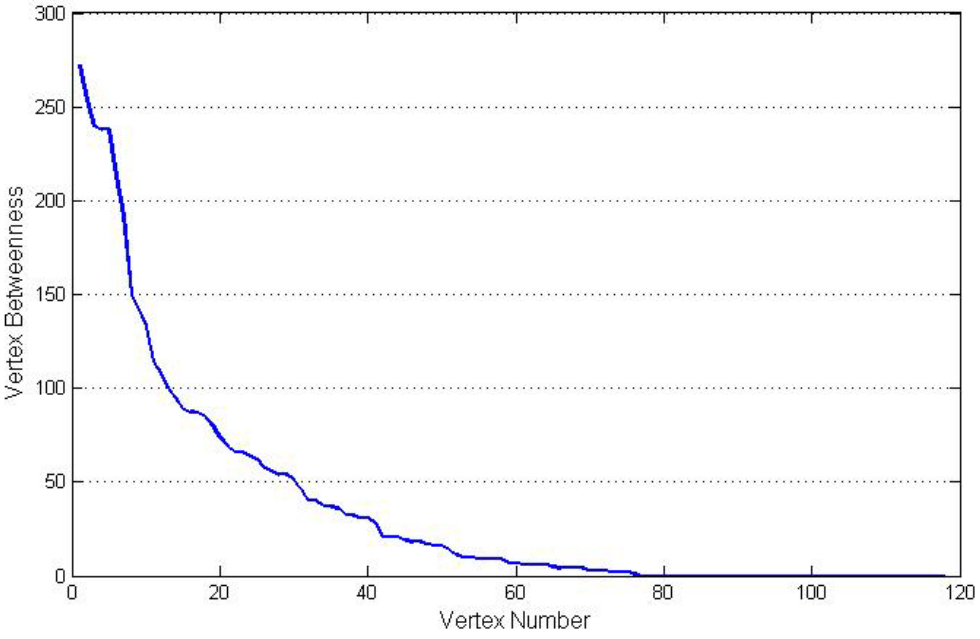

Figure 14 Vertex Betweenness Distribution for IEEE 118-bus System

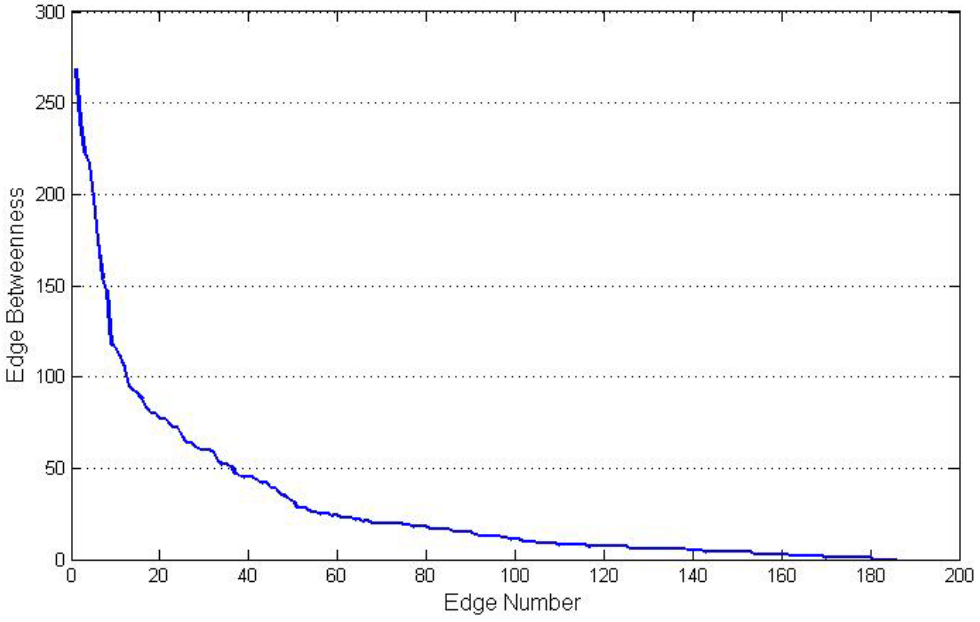

Figure 15 Edge Betweenness Distribution for IEEE 118-bus System

Figure 14 and Figure 15 show that there are a small number of vertices and edges that have high betweenness centrality values, which means they have high-impacts to the power system grid. The real world power system holds the same properties found in a small set of buses and transmission lines, which carry significantly higher importance compared to the remaining parts of the system. For example, Bus 77 has the highest value of vertex betweenness centrality. It has a very important topological position in the network.

Regarding topological features, betweenness centralities of buses and transmission lines are good measurements of the influence of selected buses and transmission lines over the rest of the system. Regarding electrical features, the vulnerability indices can provide precise vulnerability measure for individual system element and the whole system performance. Certainly, it is possible that some important nodes or branches may have lower value of betweenness centrality. However, the vulnerability index calculation is capable of detecting all the vulnerable elements. For example, Bus 89 will be very important node if it had a great amount of generation attached to it. The value of its betweenness centrality is not large considering its topological role in this network. However, from Equation (5), large generator means high value of $Pg_{i,\max}$. So any major loss of generation in this node will affect the value of $VI_{Pg,i}$ and $VI_{Qg,i}$ of this generator. This node has low-value betweenness centrality

bus still can be picked out as vulnerable element due to its abnormal condition.

4.4.2 Weighted Vulnerability Analysis for Different Load Conditions

For the IEEE 118-bus test system, we compare the weighted vulnerability index values for three difference cases:

- Case A: base load;
- Case B: 1.1 times the base load ;
- Case C: 1.2 times the base load.

The real and reactive power outputs for generators increase with the same corresponding ratio to balance the increasing load. When defining the case study, the following assumptions are taken:

- The branch transfer limit is 3.0 p.u.;
- Voltage variance is 0.075 p.u.;
- Bus voltage angle difference limit for transmission line is set as 40 degrees.

Table 2 shows the results of weighted vulnerability index values for the three cases under different load conditions. Besides the system total vulnerability index (VI_{total}), Table I also shows the results of some individual vulnerability indices.

From the results of Table 2, we can see that the whole power system is getting more vulnerable when the load is increasing. To balance the load, generators provide more real and reactive power. The power flow and bus voltage angle differences at

transmission lines are also increasing. The case studies show that weighted vulnerability analysis is a good way to assess the system security under different load conditions.

Table 2 Weighted Vulnerability Index Values under Different Load Conditions

	VI_{total}	VI_{Loadab}	VI_{Pg}	VI_{Qg}	VI_{Pf}	VI_{line_ang}
Case A	30.1043	4.8454	3.6525	5.3471	7.2893	0.9987
Case B	37.8324	5.8354	4.4506	8.7768	8.8612	1.2367
Case C	50.7279	6.9125	5.3365	16.8603	10.5993	1.5059

4.4.3 Weighted Vulnerability Analysis for N-1 Contingency

For the same IEEE 118-bus system, N-1 static contingency analysis is performed to evaluate our proposed weighted vulnerability analysis approach. For the simple demonstration, we only apply line outages for this case study. From the topological analysis, we can find that there are some branches whose tripping will result in islanding, such as the branches B9-10 which connect generator G1. In our case study, we only rank the non-islanding contingencies. Table 3 shows the results of the weighted vulnerability index values for top five vulnerable line outages. The results of

same individual vulnerability index in Table 2 are also given in Table 3. From the results we can see that the top two vulnerable line outages are the branches connected with bus 81, which holds the very important topological position based on the rank of vertex betweenness centrality.

Table 3 Weighted Vulnerability Index Values for N-1 Contingency Analysis

Line Outage Number	VI_{total}	VI_{Loadab}	VI_{Pg}	VI_{Qg}	VI_{Pf}	VI_{line_ang}
L126 (B68-81)	53.6543	4.9733	3.8320	24.9428	8.4276	1.5278
L127 (B81-80)	53.5619	4.9829	3.8320	24.9225	8.4276	1.5278
L51 (B38-37)	48.7722	5.0594	3.6968	21.4290	7.8072	1.2866
L50 (B34-37)	40.4250	4.9092	3.6555	14.6525	7.3430	1.0031
L116 (B69-75)	39.9103	5.0902	3.6627	13.5047	7.4511	1.0719

4.5 Summary

This section proposes the weighted vulnerability analysis to identify the most vulnerable components when evaluating system-wide security situation under different conditions. Vertex and edge betweenness centrality have been proven to be a good measure of the importance of a bus or transmission line in the power system over the

rest of the network. There is a small portion of buses and lines that have high-impacts on the power system. The proposed weighted vulnerability index method could provide a comprehensive representation of power system vulnerability information, which would consider both the topological properties and electrical properties of power system. Case studies demonstrate that proposed method can be used in power system static security analysis, which helps system operators to evaluate the system operating condition and find most vulnerable elements.

5. PARALLEL CORRIDOR SEARCH BASED ON GRAPH PARTITIONING

5.1 Introduction

During cascading outage, tripping a highly loaded transmission line will cause a larger transient and a larger steady-state redistribution of power flow, which may cause power swing occurring and leading to relay misoperation. Moreover, the impact on the operating margins of other components is larger if the power system is more stressed. In this section, a fast parallel corridor detection method is proposed to identify the most severe transmission lines after power flow redistribution when one line was tripped. The proposed method is based on graph partitioning. Section 5.2 introduces the graph partitioning based on contributions. The proposed parallel corridor search method is presented in Section 5.3. Case study and summary are given in Section 5.4 and 5.5, respectively.

5.2 Graph Partitioning based on Contributions

The Power system topological model introduced in Section 3 can be partitioned into different zones with homogenous characteristics, which is called state graph. The graph partitioning is done by searching the domain of each generator, the common of buses and links between commons. The concepts of generator domain and bus common were proposed by Kirschen, et al. [38] to determine which generators are

supplying a particular load, how much use each generator is making of a transmission line, and what is each generator's contribution to the system losses. These concepts are used here for fast search for parallel corridor after line tripping during cascading outages. The introduction about the concepts of domain of a generator, common of buses, and links is given as follows [38]:

5.2.1 Domain of a Generator

The domain of a generator is defined as the set of buses which are reached by power produced by this generator. Based on the direction of power flow on each transmission line, if it is possible to find a path through the network from the studied generator to the bus, the power from the studied generator can reach this bus.

Take an example of a 6-bus test system, which is shown in Figure 16. Under the given directions of power flow, the domain of generator A includes all the buses: Bus 1-6; the domain of generator B includes Bus 3, 4, 5, and 6; the domain of generator C only includes Bus 6 since no power can be delivered to other buses. It is normal that there is a significant overlap among the domains of different generators.

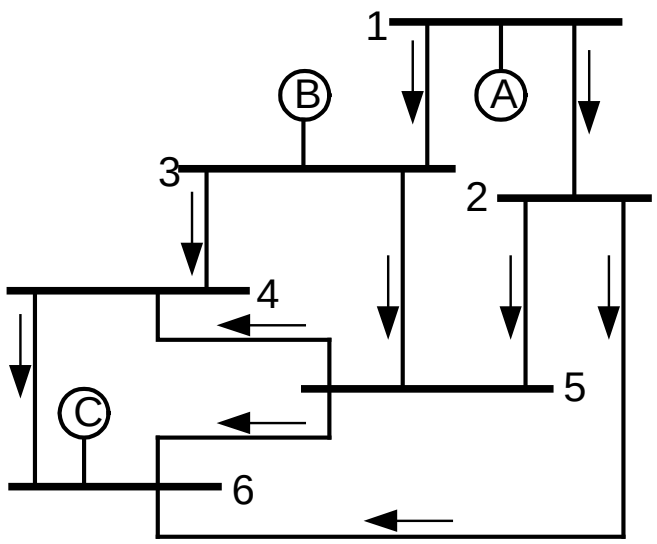

Figure 16 One Line Diagram 6-bus System with Power Flow

For large system, the fast search algorithm to determine the domain for each generator was proposed in [38]:

Place the bus where the generator is connected on the open list

While there are busses on the open list do:

Remove the first bus from the open list

Add this bus to the domain of the generator

Loop over all the branches connected to this bus;

If the power on this branch flows away from this bus and if the bus at opposite end of the branch is not yet part of the domain, then:

Add the opposite buses to the list of open buses.

End if

End loop

End while

5.2.2 Common of Buses

A common is defined as a set of contiguous buses supplied by the same generators. Unconnected sets of buses supplied by the same generators are treated as separate commons. A bus belongs to one and only on common. The rank of a common is defined as the number of generators supplying power to the busses comprising this common. It can never be lower than one or higher than the number of generators in the system.

Take the same example of 6-bus system, it has three commons as shown in Figure 17: Common 1 includes Bus 1 and 2, which are supplied by generator A only; Common 2 includes Bus 3, 4, and 5, which are supplied by both generator A and B; Common 3 only includes Bus 6, which is supplied by generator A, B, and C.

Similarly, the fast searching algorithm was proposed in [38] to determine the common of buses for large power system:

Determine the domain of each generator

Record with each bus the generators which supply this bus

Loop over all the buses

If this bus is not yet part of a common, then:

Create a new common based on the generators supplying this bus

Recursively propagate this common to all the buses connected to this bus

End if

End loop

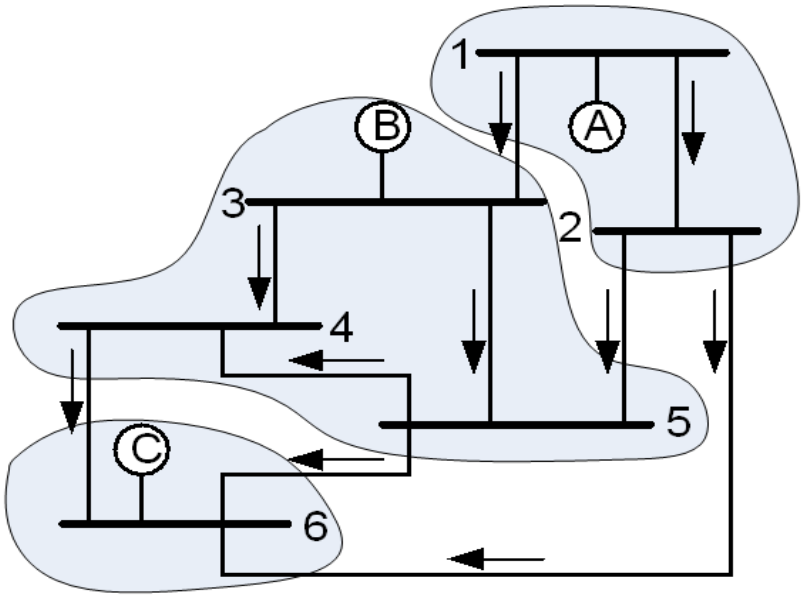

Figure 17 Commons for the 6-bus System

5.2.3 Links between Commons

After determining the domain of each generator and common of buses, each

branch either connects two busses which are part of the same common (internal to the common) or connects two buses which are part of different commons (external to the common). The concept of link is defined as one or more external branches connecting the same commons. Links have two properties:

- The actual flows in all the branches of a link are all in the same direction.
- The actual flow in a link is always from a common with lower rank to a common with higher rank.

For the same 6-bus system shown in Figure 16, there are three links in this system: Link 1 includes Branch 1-3 and 2-5, which connects Common 1 and 2; Link 2 includes Branch 4-6 and 5-6, which connects Common 2 and 3; Link 3 only includes Branch 2-6, which connects Common 1 and 3.

5.3 Parallel Corridor Search Method

5.3.1 State Graph of Power System

Under the given power flow directions, the procedures of determining the domain of each generator, the common of buses and links between commons, will produce unique sets of domains, commons, and links. If the commons are represented as nodes and the links as branches, the power system topological network will be simplified into a state graph, which is a directed and acyclic graph. The link can only

go from a common supplied by fewer generators to a common supplied by more generators [38].

For the same 6-bus system shown in Figure 16, the directed acyclic state graph is shown in Figure 18.

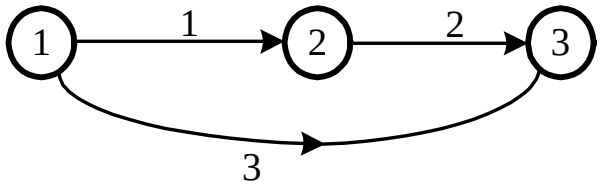

Figure 18 State Graph for the 6-bus System

5.3.2 Parallel Corridor Search Method

From the state graph shown in Figure 18, some commons generate power and function as source, like Common 1; some commons absorb power and function as load, like Common 3; some commons transmit power from one common to the other common, like Common 2. It is possible that the source common also encompasses load buses or the load common also includes generator buses. To view the situation as whole, each common has the homogenous characteristic.

The proposed fast search method for parallel corridor can only work when the

tripped transmission line is external to the commons, which means it belongs to one link in the state graph. For those transmission lines internal to a common, the weighted vulnerability analysis method proposed in Section 4 will be used.

The detailed procedures of the proposed method to find the parallel corridors are:

- Identify the link that the tripped transmission line belongs to;
- Identify the source common and load common that the identified link connected, which are called key commons;
- Search other links which are connected to the same source common and/or load common in the state graph of the power system, which are called key links;
- Identify the transmission lines comprised in those key links and commons.

The set of these transmission lines is defined as the parallel corridor related to the tripped branch. The search procedures could be done without running any power flow analysis. They are only running topological search based on adjacent matrix.

For example, in the 6-bus system shown in Figure 16, if branch 4-6 is tripped due to overload, the parallel corridor from the key links is the set of branch 2-6 and branch 5-6, based on the state graph shown in Figure 18.

5.4 Case Study

The standard IEEE 39-bus New England system [72] is used for case study. Figure 19 shows the IEEE 39-bus system configuration. The detailed system data, base power flow data and machine data can be found in Appendix C.

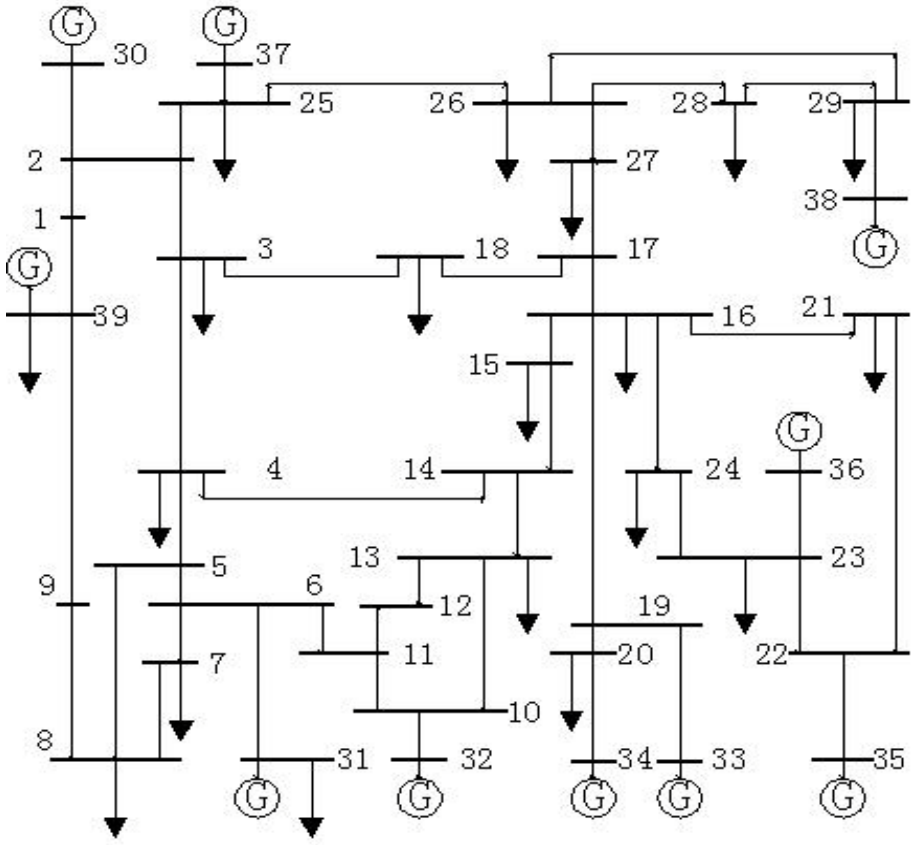

Figure 19 IEEE 39-bus New England System Configuration

For the typical normal operation mode, Table 4 shows the domain of different

generators. $Bi\,(i=1,2,3\ldots39)$ represents Bus i. Figure 20 shows the commons of buses and the related links. Figure 21 shows the generated state graph. The parallel corridor for tripped branch can be found by searching those links between commons.

Table 4 Domain of each Generator for IEEE 39-bus New England System

Generator	***Domain of Generator***
G30	B1, B2, B3, B4, B8, B9, B30, B39
G31	B4, B5, B6, B7, B8, B31
G32	B4, B5, B6, B7, B8, B10, B11, B12, B13, B14, B15, B32
G33	B3, B4, B15, B16, B17, B18, B19, B20, B27, B33
G34	B20, B34
G35	B3, B4, B15, B16, B17, B18, B21, B22, B23, B24, B27, B35
G36	B3, B4, B15, B16, B17, B18, B23, B24, B27, B36
G37	B1, B2, B3, B4, B8, B9, B25, B26, B27, B37, B39
G38	B26, B27, B28, B29, B38
G39	B8, B9, B39

Based on the state graph shown in Figure 21, the parallel corridors due to tripping any line in the links could be determined. Table 5 shows result for three case studies with tripping branch L3 (B3-2), L8 (B14-4), and L20 (16-15), respectively. As the result, the parallel corridors from key links and commons are provided in this table.

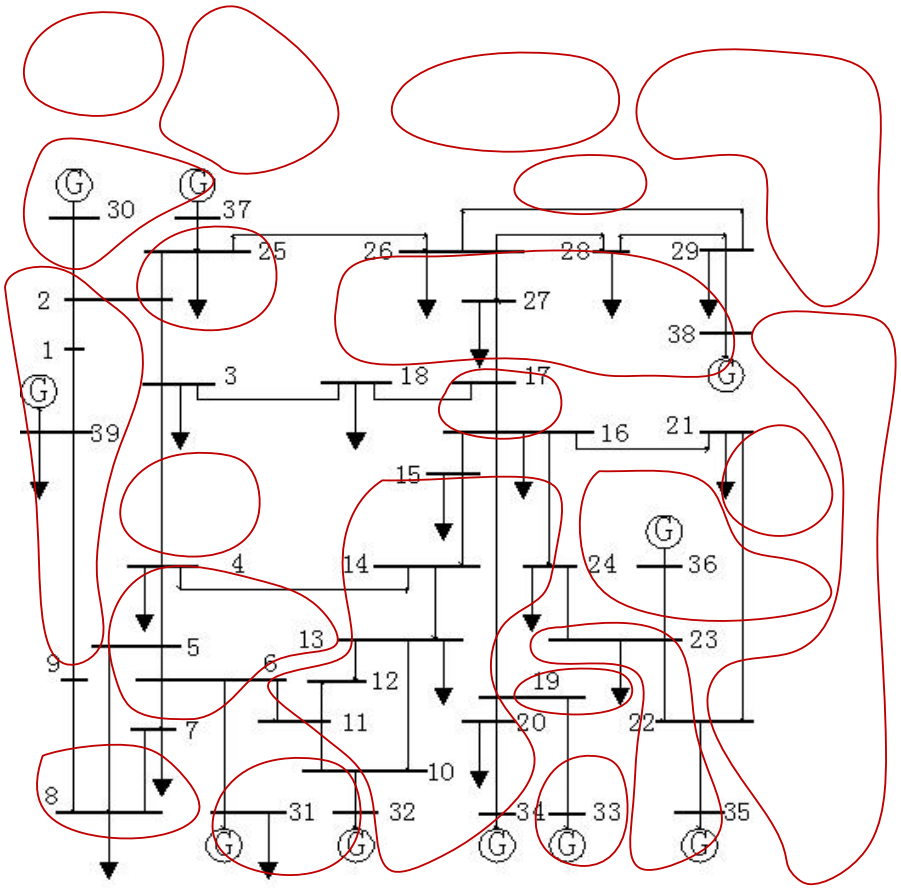

Figure 20 Commons and Links of IEEE 39-bus New England System

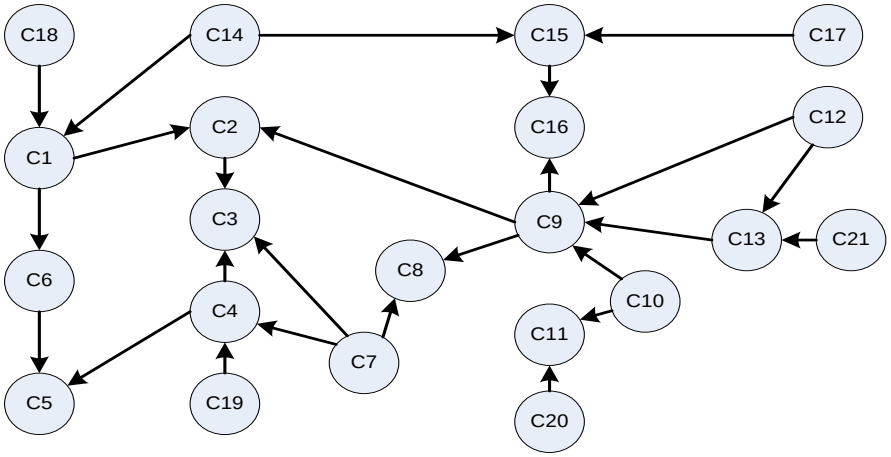

Figure 21 State Graph of IEEE 39-bus New England System

Table 5 Parallel Corridors Case Study

Faulted Line	***Key Links***	***Key Commons***	***Lines from Key Links***	***Lines from Key Commons***
L3 (B3-2)	C2-3, C2-9, C1-6, C1-14, C1-18	C1, C2	L2(B39-1), L4(B25-2), L5(B4-3), L6(B18-3), L44(B2-30)	L1(B2-1)
L8 (B14-4)	C2-3, C3-4, C4-7, C7-8	C3, C7	L5(B4-3), L7(B5-4), L12(B11-6), L19(B15-14)	L16(B11-10), L17(B13-10), L18(B14-13), L35(B12-11), L36(B12-13), L38(B10-32)
L20 (B16-15)	C7-8, C2-9, C9-10, C9-13, C9-12, C9-16	C8, C9	L6(B18-3), L19(B15-14), L22(B19-16), L23(B21-16), L24(B24-16), L26(B27-17)	L21(B17-16), L25(B18-17)

Taking the case example of tripping branch L8 (B14-4), the power flow on this transmission line will be distributed to other branches. Parallel corridors search method provides the list of most vulnerable lines due to this event as shown in Table 5. In order to verify the results, the full AC power flow analysis is used to check the numerical results of power flow re-distribution. Table 6 shows the active power flow results for the parallel corridors due to tripping branch L8 (B14-4). The detailed parameters for running the power flow can be found in Appendix C.

From Table 6, we can conclude that the identified parallel corridors suffer most of the power flow re-distribution. Branch L38 (B10-32) is a generator bus, and the flow on this line did not change much due to the generator output limit.

5.5 Summary

This section proposed a parallel corridor search method to quickly identify the most vulnerable components after tripping any transmission line. The proposed method is based on topological partitioning in graph theory. The power system topology model can be simplified into state graph after searching the domains for each generator, commons for each bus, and links between commons. The parallel corridor will be found by searching the key links connected to the same source common and/or load common and the key commons in the state graph of the power system. The whole search process is executed without any power flow calculation, which makes the

proposed method have the property of increased speed.

Table 6 Full AC Power Flow Results

Line	***Pre-fault Power Flow (p.u.)***	***Post-fault Power Flow (p.u.)***	***Percentage of Change***
L5(B4-3)	-0.749835623	-1.67608256	123.53%
L7(B5-4)	1.630748973	3.331610673	104.30%
L12(B11-6)	3.440732315	5.138402971	49.34%
L16(B11-10)	-3.46930441	-5.025156839	44.85%
L17(B13-10)	-3.026452464	-1.469305015	-51.45%
L18(B14-13)	-2.957199385	-1.254787113	-57.57%
L19(B15-14)	-0.325868494	-1.252683894	284.41%
L35(B12-11)	-0.021880128	0.12775897	683.90%
L36(B12-13)	-0.063437532	-0.21312768	235.97%
L38(B10-32)	-6.499999421	-6.499999161	0.00%

6. ENHANCED DISTANCE RELAY SCHEME USED FOR VULNERABLE PARTS IN POWER SYSTEM*

6.1 Introduction

Power system is beginning to reach its security limit when losing major parts resulting in a serious of problems. The large fluctuation of power, which is known as power swing, is one of the most significant consequences. It may impact the behavior of distance relays and jeopardize the system security level. The vulnerable components in power system during cascading outage could be identified by using weighted vulnerability analysis proposed in Section 4, and parallel corridor search method proposed in Section 5. Those vulnerable branches operate in stressed conditions and their relay operations should be paid attention to. This section proposes enhanced fault detection method during power swing to improve the security of distance relay. Section 6.2 reviews the distance relay behavior during power swing. The principle of proposed fast distance relay scheme for fault detection during power swing is discussed in detail in Section 6.3. Section 6.4 discusses the implementation of detection method. Case study given in Section 6.5 and Section 6.6 provides the summary.

---

* Part of the material in this section is reprinted from “Fast Distance Relay Scheme for Detecting Symmetrical Fault during Power Swing” by Chengzong Pang and Mladen Kezunovic, *Power Delivery, IEEE Transactions on*, vol.25, no.4, pp.2205-2212, Oct. 2010, doi: 10.1109/TPWRD.2010.2050341, ©2010 IEEE., with permission from IEEE.

6.2 Distance Relay Behavior during Power Swing

6.2.1 Power Swing

Power system security and stability are becoming even more challenging and important characteristics due to the increasing complexity of power system operations. Since transmission lines are the vital links that enable delivering of electrical power to the end users, improved dependability and security of transmission line relays is required. According to the historical data [73], relay misoperation contributes to 70 percent of the major disturbances in the United States. Finding effective means to monitor and improve distance relay operations is very important for understanding and mitigating relay misoperations on high voltage transmission lines.

Power swing is a phenomenon of large fluctuations of power between two areas of a power system. It is referred as the variation of power flow. Figure 22 shows the simulation example of voltage waveform from power swing observed at relay location. Power swing often occurs with the instability of synchronous generators. Transmission line faults, line switching, loss of generator, and loss of heavy load will result in sudden changes to electrical power. In this case, the mechanical power input to generators remains relatively constant. These system disturbances cause oscillations in machine rotor angles and can result in severe power flow swings. Depending on the severity of the disturbance and the actions of power system controls, the power swing

can be categorized into stable power swing and unstable power swing. In stable power swing, the system may remain stable and return to a new equilibrium state experiencing. Unstable power swing could cause large separation of generator rotor angles, large swings of power flows, large fluctuations of voltages and currents, and eventual loss of synchronism between groups of generators [74].

The occurrence of power swings is very difficult to predict since they are quite unexpected [75]-[78]. When power swing takes place, the apparent impedance measured by a distance relay may move away from the normal load area and into one or more of the distance relay operating characteristics. This may cause unintended trips [79]-[81]. For example, the Northeast Blackout in 2003 was caused by distance relays operation in zone 3 under the overload and power swing condition, which stressed the system and made it collapse at the end [1].

To ensure the security of operation, most modern distance relays detect and block the operation during the power swing [82]. If a fault occurs during the power swing, the distance relay should be able to detect the fault and operate correctly. In that case it is necessary to unblock the relay during power swing. The procedure is easy to implement for unsymmetrical faults, since the negative and zero sequence components do not exist during power swing, which can be used as fault detection criterion. However, it is much more difficult to identify symmetrical fault during stable power

swing, which may delay the operation of relay [83].

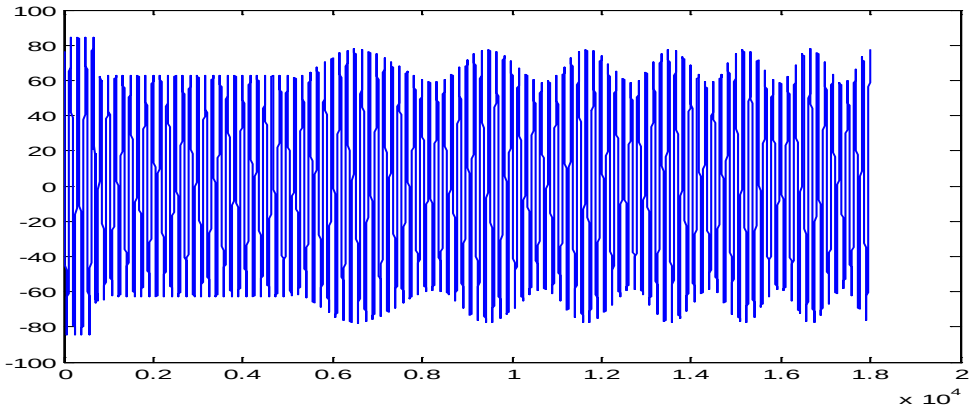

Figure 22 Voltage Simulation Example of Power Swing Observed by Relay

To solve this problem, many schemes using different methods have been proposed. Mechraoui and Thomas presented fault detection method based on load angle differences identification [77]. They did not consider the symmetrical fault in their case studies. Benmouyal *et al* presented a fault detector based on tracking the power swing center voltage (SCV) [84]. Choosing the appropriate thresholds is still very difficult to implement. Su *et al* introduced an improved method for a fast detector [85]. Their scheme still needs two cycles to finish the fault detection, which is not good enough when applied in Extremely High Voltage (EHV) system. Brahma introduced the use of wavelet transform (WT) to detect the symmetrical fault quickly and reliably

[86], but the sampling rate of 40.96 kHz is needed to satisfy all the cases studied.

6.2.2 Distance Relay under Power Swing

The responses of the power system to different disturbances depend on both the initial operating state of the system and the severity of the disturbances [87]. The steady state power system operates at an equilibrium, which maintains the balance between the generated and consumed power. When system disturbances happen, such as various faults, transmission line switching, sudden loss of load, loss of generators, loss of excitation, etc., the mechanical power input to the generators remains constant for a short time under those sudden changes in power system. This will cause the oscillations in machine rotor angles and result in power flow swings [75], [88]. Power swing is a variation in power flow which occurs when generator rotor angles are advancing or retracting relative to each other. It is possible for one generator, or group of generators that terminal voltage angles (or phases) go past 180 degrees with respect to the rest of the connected power system, which is known as pole slipping. The power swing is considered stable if pole slipping does not happen and system remains stable and returns to a new equilibrium state [89]. However, large power swings, no matter whether they are stable or unstable, will cause large fluctuations of voltages and currents, which may leads to relay misoperations and finally result in loss of synchronism between groups of generators.

Distance relays play an important role in assuring stability of power systems by eliminating faults on transmission lines leading to instability. The distance relays are proven to be influenced by power swing [75], [83]-[85].When and only when the faults occur within the desired zone, distance relay should isolate the faults. It should not trip the line during power swing caused by the disturbances outside the protected line. That is the reason why power swing blocking function is intergraded in most of modern distance relays, so that the relays shall be blocked while power swing without faults is occurring.

Either stable or unstable power swing will have impacts on distance relay judgment. The detailed reasoning and an example of two machine system are given in [90].

If there is no fault on the considered transmission line, the impedance seen by distance relay at bus is [91]:

$$Z_c = \frac{\dot{V}_m}{\dot{I}_{mn}} = \frac{\dot{V}_m}{\left(\dot{V}_m - \dot{V}_n\right)/ Z_L} = Z_L \left(\frac{1}{1 - \left|\frac{V_n}{V_m}\right| \angle \theta_{nm}} \right) \tag{25}$$

From the above equation, the apparent impedance Z_c seen by relay is determined by two variables: the magnitude ratio (V_n / V_m) and the angle difference ($\theta_{nm} = \theta_n - \theta_m$) of the bus voltages at the two ends. Since the bus voltages will oscillate during power swing, Z_c will also vary accordingly. The plots of Z_c trajectories in the

$R-X$ plane with respect to voltage magnitude ratios and angle differences is shown in Figure 23 [91], under the condition of $Z_L = 1\angle 80^\circ$. If the power swing causes the angle difference large enough, the impedance seen by relay will reach the zone settings and relay will misoperate. An example of actual impedance trajectories during a stable power swing and an unstable power swing is shown in Figure 24.

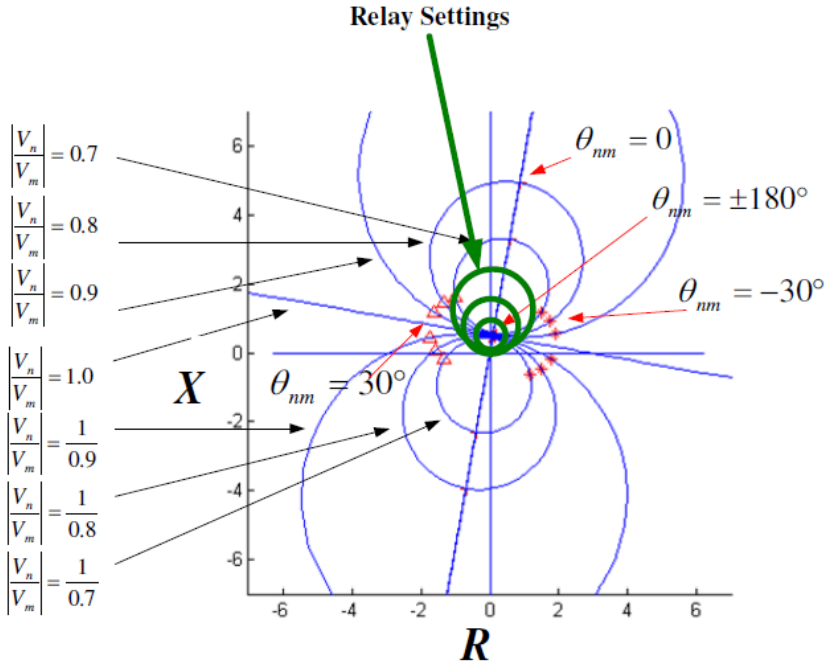

Figure 23 Z_c Trajectory in the $R-X$ Phase

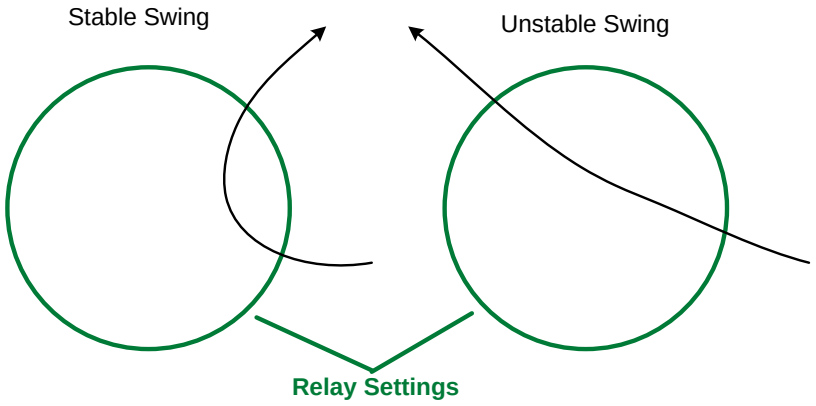

Figure 24 Impedance Trajectory during Stable and Unstable Power Swing

During power swing, if certain values of the magnitude ratio and angle difference are satisfied, the impedance seen by relay will reach the zone settings and relay misoperation will happen. Traditional method for power swing blocking is to measure the rate of change of impedance through the zones of relay [92]. The speed of impedance moving during power swing is slower than during fault condition. This is the basic theory of how a relay may be able to distinguish the power swing from fault. However, as Brahma mentioned in [86], if a symmetrical fault occurs during a power swing, it is not possible to detect it based on the mentioned principle because both power swing and symmetrical fault are both balanced phenomena, which may result in the relay not being able to "see" the fault and clear it.

6.3 Principle of Enhanced Fault Detection Method

The system frequency during power swing only varies over the range around

the nominal frequency, which can be as high as 4-7 Hz [84]. The occurrence of fault, on the contrary, will generate transient signals in the waveforms of currents and voltages. The type and degree of existences of transient signals are largely determined by the fault location, fault duration, incidence angle, fault resistance, and system pre-fault conditions. Based on the difference in frequency component behavior, it is feasible to detect the symmetrical fault during power swing by extracting the high frequency components from the voltage and current waveform.

Ultra-high-speed (UHS) protection schemes based on the traveling wave detection techniques have been introduced [93]-[96]. Some are limited by their weakness in reliability and feasibility. With the development of signal processing tools, the improved UHS protection schemes such as Mathematical Morphology (MM) based method [97], WT based method [98], [99] have been proposed. Although traveling wave protection scheme may not substitute the traditional protection methods right now, it provides a feasible method for fault detection with fast response and immunity to power swing and other influences.

Wavelets are one of the relatively new mathematical tools for signal processing [100]. Wavelet based signal processing technique is an effective tool for power system transient analysis and power system relaying. The applications of wavelet transform in power system have been reported for fault detection, fault classification, power system

disturbance modeling and identification, power quality analysis, etc.[74], [90], [100]-[102]. This section presents a fast detection method for symmetrical faults by using wavelet analysis to extract the high frequency components from the fault-induced voltage and current traveling waves propagating along transmission line.

6.3.1 Traveling Wave Theory during Fault

When a fault occurs in power system, the voltage and current signals could be decomposed into two parts: the pre-fault steady-state component and the fault injected component, or often called superimposed component. The superimposed component can be expressed in terms of traveling waves, including forward travelling wave and backward travelling wave. Figure 25 shows a single line diagram of a transmission system.

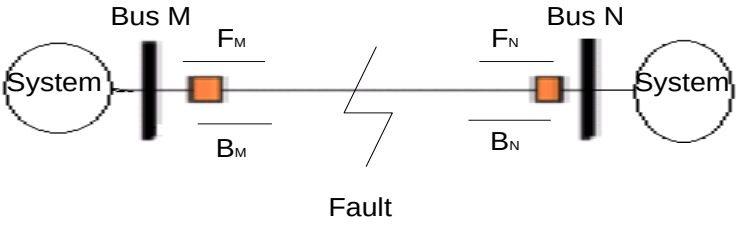

Figure 25 Diagram for Single Phase Transmission Line

When fault occurs, the traveling wave will propagate along the line. The wave propagation can be obtained by solving the partial differential equations, which are expressed as [99]:

$$u(x,t) = u^{+}(x - vt) + u^{-}(x + vt) \tag{26}$$

$$i(x,t) = \frac{1}{Z_0}\left(u^{+}(x - vt) - u^{-}(x + vt)\right) \tag{27}$$

where v is the surge velocity, $v = \frac{1}{\sqrt{L_0 C_0}}$, Z_0 is line surge impedance, $Z_0 = \sqrt{\frac{L_0}{C_0}}$, L_0 and C_0 are the inductance and capacitance per unit length, x represents the distance that a surge travels away from the fault point. u^{+} and u^{-} are the forward and backward travelling wave, respectively, which can be derived from equation (26) and (27) as:

$$u^{+} = \frac{1}{2}(\Delta u + Z_0 \Delta i) \tag{28}$$

$$u^{-} = \frac{1}{2}(\Delta u - Z_0 \Delta i) \tag{29}$$

where Δu, Δi are the fault injected voltage and current, respectively. They can be obtained by subtracting the steady-state components from the post fault signals [103], and the steady-state components are those voltage and current waveforms one cycle before the fault. Thus the forward and backward travelling waves can be calculated easily and fast.

6.3.2 Wavelet Transform Analysis

Wavelet transform (WT) is a relatively new and efficient signal processing tool, which was introduced first at the beginning of the 1980s [104]. The application of wavelet-based techniques has been widely spread in the field of mathematics, physics and engineering because of its capability of time and frequency domain analysis, which is its unique characteristic. The fundamental theory and mathematics of the wavelet transform was extensively studied and can be found in literature [104]-[108].

The definition of continuous wavelet transform (CWT) for a given signal $x(t)$ with respect to a mother wavelet $\psi(t)$ (t) is:

$$CWT(a,b) = \frac{2}{\sqrt{a}} \int_{-\infty}^{\infty} x(t) \psi\left(\frac{t-b}{a}\right) dt \tag{30}$$

where a is scaling (dilation) factor and b is the shifting (translation) factor.

The application of continuous wavelet transform in engineering requires the feasibility evaluation. Similarly to discrete Fourier transform, a discrete wavelet transform (DWT) is proposed by adapting the discrete forms of t, a, and b in equation (28), which can be written as:

$$DWT(m,n) = \frac{2}{\sqrt{a_0{}^m}} \sum_k x(k) \psi\left(\frac{k - nb_0 a_0^m}{a_0^m}\right) \tag{31}$$

where m, n, and k are integer variables related to the number of samples in the input signal. The scaling and shifting factors changed to the functions of m, n, and

k .

The performance of Wavelet transform highly depends on the selection of the mother wavelet. All mother wavelets have the common characteristics: the mother wavelet should be attenuating and oscillating [104]. To perform Wavelet transform, many approaches for the mother wavelet can be selected, such as Daubechies (Db), Symlets, Coiflets, Biorthogonas, etc [107]. The different mother wavelets will affect the performance of Wavelet-based methods. Selecting the appropriate mother wavelet is very important to implementing the wavelet analysis.

Power swing is mostly the phenomena of low frequency oscillation. The fault voltage or current contains high frequency transient signals. The multi-resolution analysis (MRA) will be a best tool for decomposing the signal at the expected levels [106], by which the faulted-derived signals can be represented in terms of wavelets and scaling functions. Thus, we can easily extract the desired information from the input signals into different frequency bands related to the same time period.

Considering an acquired digitized time signal $y(t)$, the approximation coefficient (scaling coefficients) $c_j(n)$ and wavelet coefficient (detail coefficients) $d_j(n)$ after the decomposition at j scales can be computed as [100]:

$$c_j(n) = \sum_k h(k-2n) c_{j-1}(k) \tag{32}$$

$$d_j(n) = \sum_k g(k-2n) c_{j-1}(k) \tag{33}$$

where $j = 1, 2, ..., J$. J is the total number of resolution levels (The maximum value of J is determined by the number of sampling points), $h(n)$ and $g(n)$ are the low-pass and high-pass filter respectively. Figure 26 shows the procedure of two-scale decomposition using by MRA.

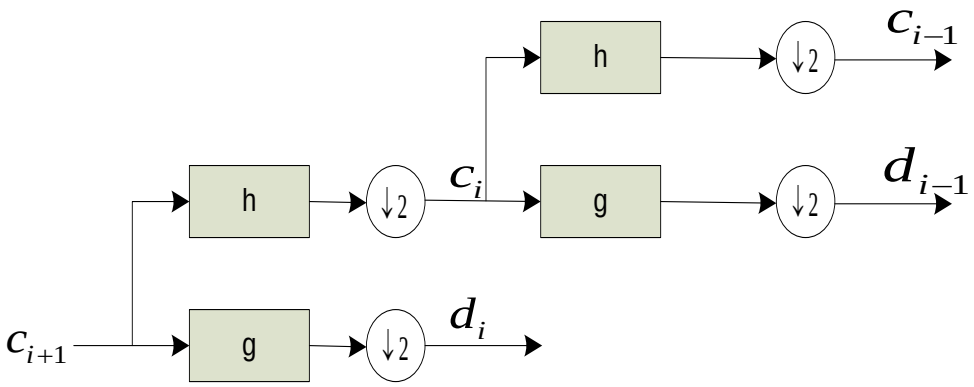

Figure 26 Diagram of MRA Decomposition into Two Scales

In order to represent the high frequency component in its quantity, the wavelet energy spectrum is used to calculate the transient energy in different frequency band. From Parseval's Theorem, the energy of the analyzed signal can be represented by the energy in each expansion components and their wavelet coefficients if the used scaling function and wavelets form an orthogonal basis, which can be shown as [100]:

$$\int |f(t)|^2 dt = \sum_{k \in Z} |c_{J,k}|^2 + \sum_{j=1}^{J} E_j \tag{34}$$

where $E_j = \sum_{k \in Z} \left| d_{j,k} \right|^2$ is the norm value or the energy of the signal component at j level after wavelet transform.

Multi-resolution analysis is a hierarchical and fast solution. It can be implemented by a set of successive filter banks as shown above. An import issue remains for the wavelet analysis: choice of a suitable wavelet. A particular type of wavelet should be selected depending on the application purpose of wavelet analysis. The main concerns when selecting the appropriate wavelet are:

- It should be one of the orthogonal wavelets.
- It should be easy to implemented and with acceptable performance.

When wavelet analysis is used to detect transient disturbances, the mother wavelet shape should be close to the shape of the detected disturbance in order to reach the higher efficiency. However, the proposed method in this section wants to extract the energy distribution at each frequency band in the detected signals. Thus an orthogonal wavelet should be adopted to satisfy energy conservation of the Parseval's Theorem. Among those mother wavelets, Daubechies wavelet family is one of the most suitable orthogonal wavelets in multi-resolution analysis due to their powerful performance, which has been widely used in different fields [108]. Other orthogonal wavelets may also have the ability to function as well as Daubechies wavelets. But Daubechies wavelets are very easy to implement by using the fast wavelet transform

with remarkable performance [107].

Different Daubechies wavelets have different filter lengths, which determined the performances of Daubechies wavelet family. The longer the length of the wavelet the higher the computation burden of the filter. The smoother the wavelet waveform in the time domain the better the localization capability in the frequency domain. Reference [109] discussed the comparison results in fault diagnosis using Daubechies-4 (Db4), Daubechies-8 (Db8), and Daubechies-20 (Db20) wavelets, which shows that the wavelet with longer filter length is superior to the shorter ones. However, the computation burden is also an important factor to be considered when choosing the wavelets to implement the fast detecting scheme.

Based on these considerations, multi-resolution analysis based on Daubechies-8 (Db8) wavelet shown in Figure 27 is selected for the investigations in this section. Db8 wavelet is compactly represented in time, and this is good for the short and fast transient analysis due to its better localization performance in frequency [104]. It is relatively easy to localize and detect the fault part under power swing by extracting features of transients in the wavelet domain.

6.4 Implementation of Detection Method

The diagram of proposed symmetrical fault detection method based on travelling wave technique and wavelet transform is conceptually shown in Figure 28.

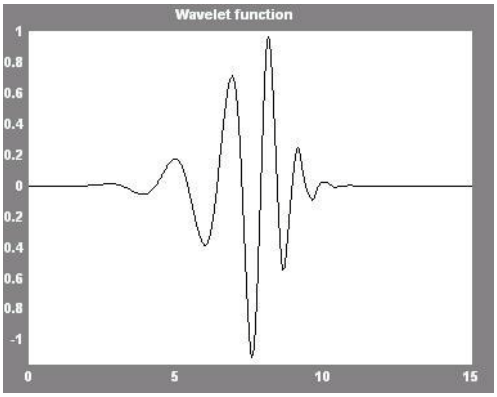

Figure 27 Daubechies-8 (Db8) Wavelet

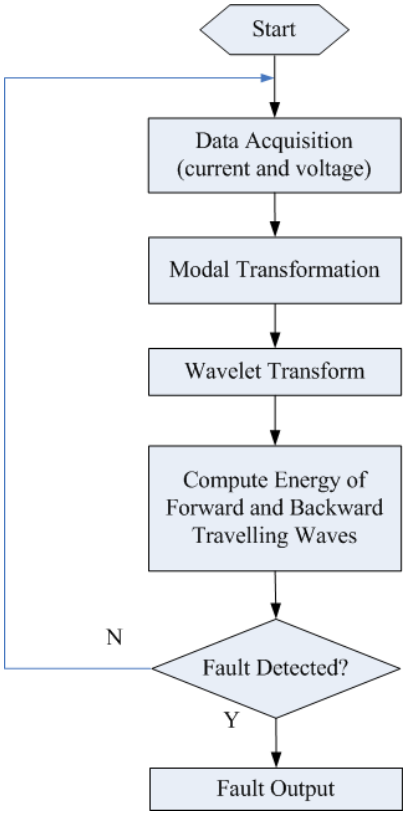

Figure 28 Implementation Diagram of Symmetrical Fault Detection Method

6.4.1 Data Acquisition

The proposed symmetrical fault detection during power swing requires data acquisition for all three phase voltages and currents. Those data can be obtained directly from measurement units of advanced digital relays. Most wavelet transform based methods require high sampling rate. The detection method proposed in this section can be used in a wide range of sampling rates. Considering advanced digital relays using sampling rate of 10 kHz, the same sampling rate is selected in this study, which can satisfy the requirements of wavelet transform proposed in this scheme with good results. In order to avoid aliasing due to the fault transients and low sampling rate, an analog antialiasing filter needs to be employed before the sampling of the input waveforms coming from instrument transformers. There are many known solutions available for implementing the antialiasing filters, hence no further discussion is given.

6.4.2 Modal Transformation

In three phase power transmission line, the electromagnetic coupling exists among three phases. Thus when a fault occurs in one phase, transient currents will be induced in the other phases due to the mutual coupling. The induced currents may distort the travelling waves on each phase, and it’s difficult to solve the coupled equations describing wave propagation. Therefore, the modal transformation to

uncouple the dependent phase components into three independent propagation modes is adopted in the proposed scheme. Clarke transformation is selected for three phase voltage and current, which shows as:

$$u_{0,\alpha,\beta} = T^{-1} u_{a,b,c} \tag{35}$$

$$i_{0,\alpha,\beta} = T^{-1} i_{a,b,c} \tag{36}$$

where T^{-1} is called Clarke transformation matrix:

$$T^{-1} = \frac{1}{3}\begin{bmatrix} 1 & 1 & 1 \\ 2 & -1 & -1 \\ 0 & \sqrt{3} & -\sqrt{3} \end{bmatrix}$$

After Clarke transformation, three phase variables will be converted into earth mode 0, and two aerial modes: α and β. 0 mode is prone to frequency dispersion and is not appropriate to be used since our goal is to extract the high frequency components. Since a symmetrical fault is considered, choosing between the mode α or β is not a critical decision. Here the aerial mode α is selected to be used with the voltage and current signals.

6.4.3 Wavelet Transform Implementation

As mentioned before, the frequency of the system varies over a range around the nominal frequency during power swing. The fault will result in transient components of the voltages and currents, which may typically be DC or higher harmonics. In order to implement the proposed method, the levels of wavelet transform

and the choice of key level for analysis are carefully studied. For a given signal, multi-resolution analysis based on Daubechies-8 (Db8) wavelet is performed. Different level components are the analysis results for different frequency bands, which can offer different information about given signals. Selection of sampling rate affects the frequency band for the wavelet transform. Based on the sampling rate of 10 kHz and Nyquist theorem, the wavelet level d1 will cover 2.5 kHz – 5 kHz. Our study shows that the d1 component from the wavelet transform is able to capture the energy of the transients for all kinds of faults, which includes symmetrical fault, and it is sensitive to the fault occurrence irrespective of the occurrence of power swing condition. However, the high frequency transient component will disperse up to 100 kHz, so higher sampling rate will be helpful to improve the detection reliability.

When implementing the wavelet analysis, one cycle window data is calculated by wavelet transform. The moving speed of shifting data window can be set based on the requirements of system protection scheme. The proposed fault detection method could be running at point-by-point shifting, which is feasible with the aids of high-speed DSPs.

Since the data for wavelet analysis is windowed discrete signal, the results after wavelet transform will have border distortion, which is shown in Figure 29. Although many extended signal methods have been used in FFT, WT and etc., such as

zero-padding, symmetric-padding, smooth padding, periodic-padding, none of them could eliminate the border distortion effects completely. For example, Figure 30 and Figure 31 show the results after WT with periodic-padding and symmetric-padding, respectively, in which border distortion still exists although it has been improved by those signal extending methods.

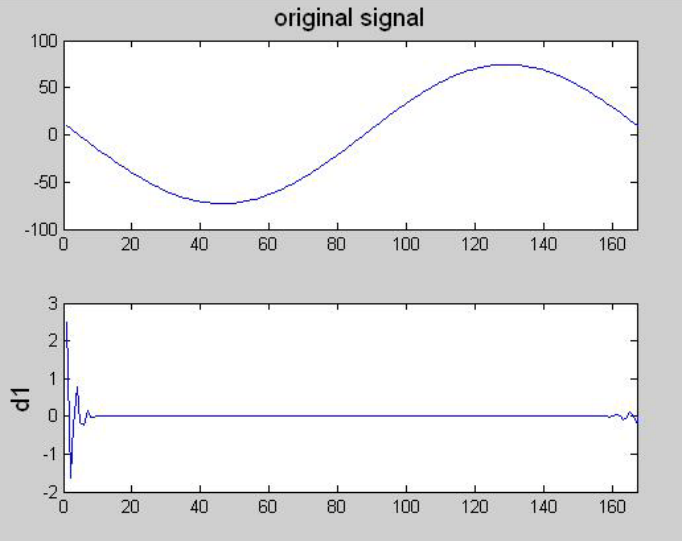

Figure 29 Border Distortion Effect for Wavelet Analysis

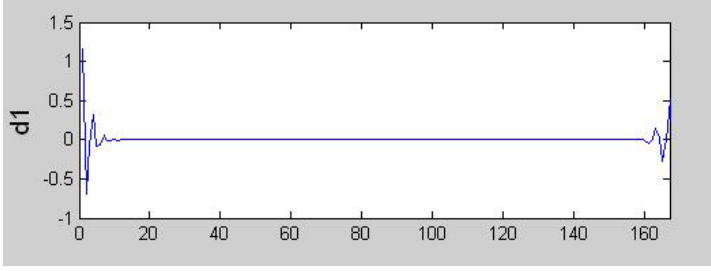

Figure 30 Periodic-padding for Wavelet Analysis

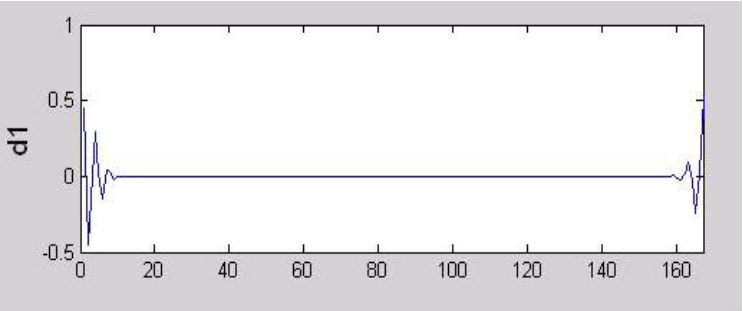

Figure 31 Symmetric-padding for Wavelet Analysis

The detection scheme proposed in this section adopts a compromised method: discarding the first and last 10 coefficients in the d1 component after the wavelet transform. It will cause 1 ms time delay for the fault detection based on the sampling rate of 10 kHz. The proposed method is still fast enough to detect the symmetrical fault. The only factor to consider when introducing a detection lag is the time needed for calculations. The calculation burden is mainly coming from performing modal transform, wavelet transform, and wavelet energy spectrum. This is less than the calculation burden of newly transient-based ultra-high-speed directional protection relays that use the same wavelet transforms. It is estimated that they use less than 6000 multiplication and 5500 addition operations, which can be completed within 1.5ms [99].The method proposed in this section is able to finish the fault detection within 2.5 ms after fault occurs based on the sampling rate of 10 kHz. This detection scheme may be made more rapid with faster DSPs and higher sampling rate. For example, the time

delay for discarding the 10 points will be 0.1 ms based on the sampling rate of 100 kHz.

6.4.4 Fault Detection Criteria

The criterion for the symmetrical fault detection is defined as:

$$k_e = \frac{E_f}{E_b} \tag{37}$$

where E_f and E_b are the energy of the d1 wavelet component for the forward and backward travelling waves u^+ and u^- respectively. According to the principles discussed above, E_f and E_b only exist after fault occurs, and are not only limited to symmetrical faults. Because of the reflection effects at bus boundary, E_f is bigger than E_b after the reflection at the boundary. Thus the fault detection criteria will be defined as: if $k_e \geq k_{e0}$, the symmetrical fault occurs. When it is used in practice, in order to avoid the possible situation of dividing by zero, the values of E_f and E_b are being monitored. If any of them is close to zero (for example, less than 10^{-5}), value of k_e is set to zero. The threshold value of k_{e0} is determined by the bus reflection coefficient. Here k_{e0} is set to be 1.15 after large number of simulation trials. More test cases are discussed in Section 6.5.

6.5 Case Study

6.5.1 Simulation of Power Swing

In this section, the power system model for case study is based on the EMTP reference model for transmission line relay testing, which is introduced by the IEEE PES Power System Relaying Committee (PSRC) WG D10 [110]. This model is described as a “standard” system model, which can be used to generate uniform relay test scenarios. In order to generate the needed conditions, Alternative Transient Program (ATP) is used to simulate the power swing [111]. The one-line diagram of the studied system and its ATP model are shown in Figure 32 and Figure 33 respectively.

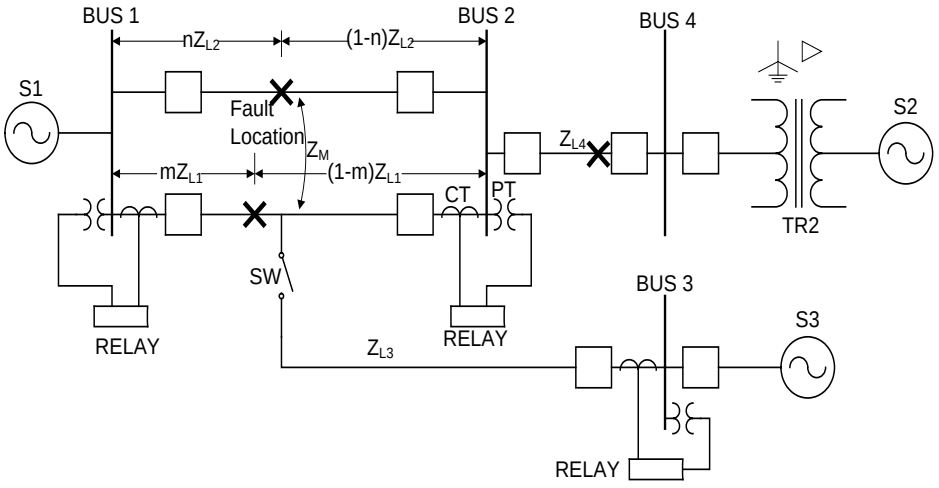

Figure 32 One-line Diagram of IEEE EMTP Reference Model

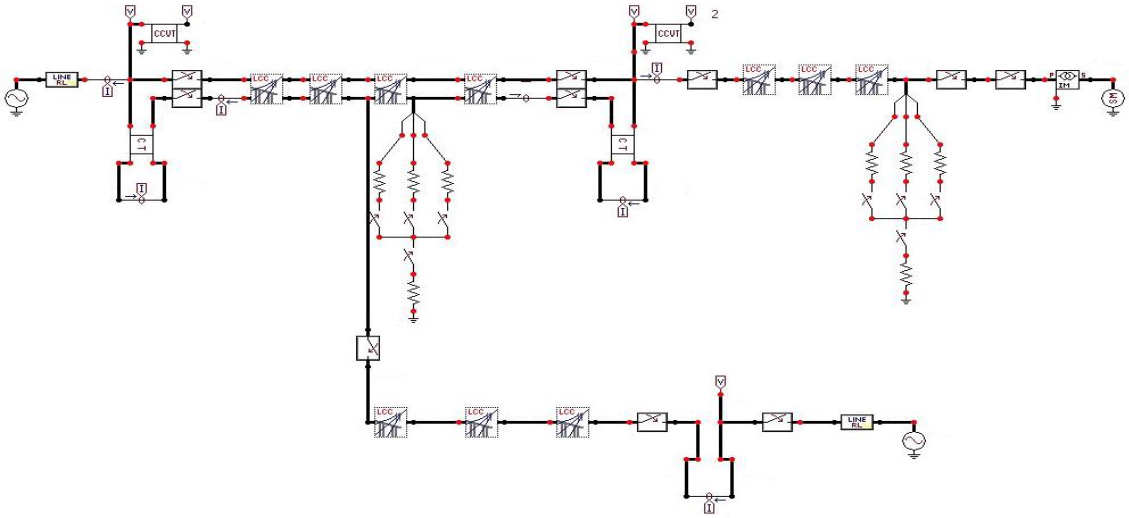

Figure 33 IEEE EMTP Reference Model in ATP

6.5.2 Example Cases

In this part, some case scenarios to test the performance of the proposed fault detection method during power swing are illustrated.

Figure 34 shows typical power swing voltage waveform generated by the model discussed above with the 5-level multi-resolution wavelet analysis based on Db8. d1- d5 are the high frequency components at different wavelet level, respectively. It is obvious that wavelet d1 component is “quiet” during power swing.

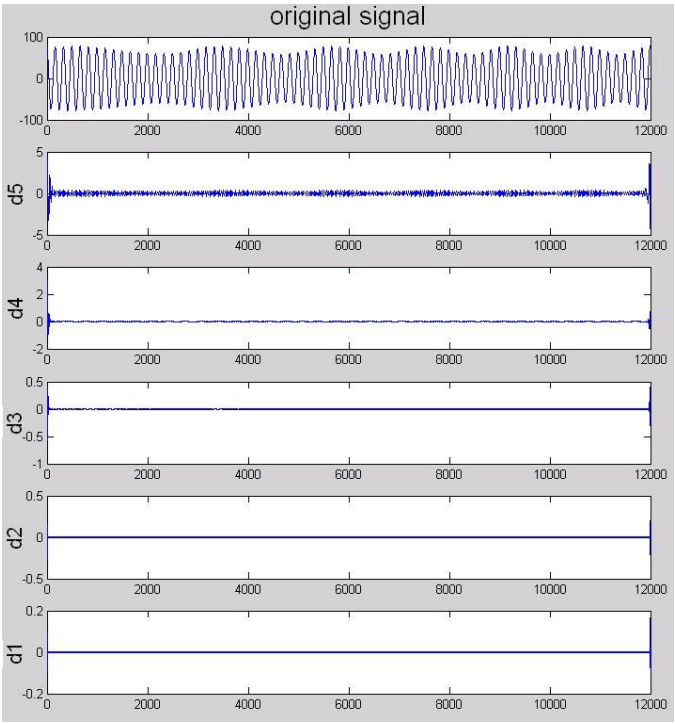

Figure 34 5-level Db8 Wavelet Transform Results

Figure 35 shows the three phase voltage of a symmetrical fault during power swing. The values of criteria factor k_e around the fault point are shown in Figure 36. In this case, there is at least one point that $k_e \geq k_{e0}$, which means a fault occurred during power swing.

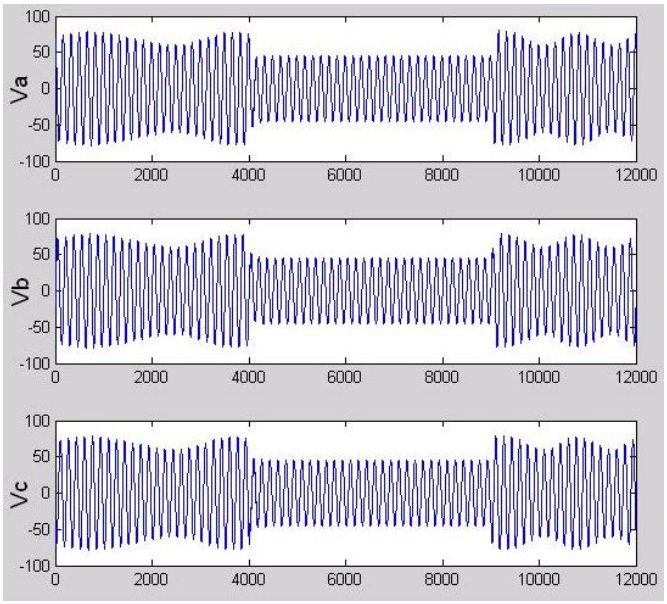

Figure 35 3-phase Voltage Waveforms for a Symmetrical Fault during Power Swing

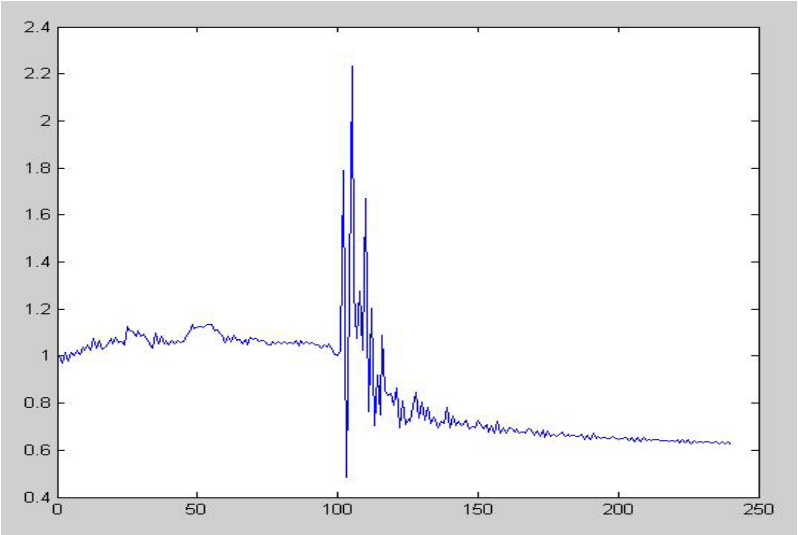

Figure 36 Values of Criteria Factor k_e around the Fault Point

In order to validate that the proposed scheme is transparent to fault locations, a variety of scenarios under different locations has been conducted. Table 7 shows some typical simulation results for the three phase symmetrical fault under power swing.

Table 7 Simulation Case for Different Fault Locations for Symmetrical Fault under Power Swing

Case	***Fault Distance (mile)***	***Maximum Value of*** k_e
1	0	1.2100
2	4.5	1.2958
3	13	1.3353
4	19.5	1.2717
5	42	2.2330

The proposed scheme is also immune to the variety of fault types and locations, under both power swing and normal conditions. In order to validate the effectiveness of this scheme, the cases of one single-phase-to-ground fault (Fault AG) and one double-phase fault (Fault AB) are studied and results are equally good without loss of

generality. Table 8 shows the case of simulated results for different fault locations of Fault AG and Fault AB when power swing is absent and Table 9 shows the results for different locations when the power swing is present. All the results show the proposed scheme is effective under such conditions as well.

Table 8 Simulation Case for Different Fault Locations under Normal Condition

Case	***Fault Distance (mile)***	***Maximum Value of*** k_e	
		Fault AG	***Fault AB***
1	0	1.2777	1.2765
2	4.5	1.3142	1.2952
3	13	1.3435	1.3566
4	19.5	1.2705	1.2700
5	42	2.2246	2.0778

Table 9 Simulation Case for Different Fault Locations under Power Swing

Case	*Fault Distance (mile)*	*Maximum Value of* k_e	
		Fault AG	*Fault AB*
1	0	1.2454	1.2200
2	4.5	1.3141	1.2951
3	13	1.3440	1.3589
4	19.5	1.2703	1.2720
5	42	2.2097	2.2511

6.6 Summary

This section presents a novel and fast fault detection scheme to be used to improve dependability of a distance relay during power swing aiming at avoiding possible relay misoperations during power swing conditions. It extracts the travelling waves from transient signals induced by faults and calculates the energy of high frequency components extracted using the wavelet transform. The proposed scheme is very fast. It could detect the fault within 3 ms after the symmetrical fault occurs during power swing, which could be beneficial for system protection, especially in EHV system. The sampling rate for data acquisition can be as low as 10 kHz, which fits the

requirements of most modern microprocessor based distance relays. Higher sampling rate could offer better results. The implementation of the proposed scheme is straight forward since the theoretical research results may easily be transferred into practical application.

7. CONCLUSIONS

This section has the discussion of the contributions and conclusions about what the contributions can be used for, and the future work directions as well.

7.1 Achievements and Contributions

Although the risk of large area cascading outages occurring is low, the consequences of cascading outages may have catastrophic social and economic impacts. Many researchers and engineers have put dedicated efforts to understanding the cascading outages and finding a feasible way to detect, prevent and mitigate them. This dissertation studied several major cascading blackouts in the world aiming at better understanding the mechanism of cascading outages, and presents an approach for fast detection and mitigation of cascading outages in power system. This approach could be integrated into the existing EMS functionality at the control center as the decision-making support tool for the system operators to better understand the unfolding events. The main contributions of this dissertation are summarized as follows:

- *Investigate the mechanism of cascading outages*.

  This dissertation explored several major cascading blackouts in the world. By investigating the mechanism of cascading outages, it can be concluded that most cascading outages have two stages: steady-state progression and transient

progression stages. Steady state progress stage may give system operators enough time to evaluate the system condition, identify some vulnerable contingencies, take some control to increase the security level and prevent the possible cascading blackouts.

- *Develop the weighted vulnerability analysis method*.

  Weighted vulnerability analysis method based on topology processing is proposed. It could provide a comprehensive evaluation for individual components as well as system-wide security situation under different conditions. The weights calculated from the vertex and edge betweenness centrality can present the importance of each bus and transmission line in the modeled power system topological network. The proposed weighted vulnerability analysis method can achieve higher accuracy since it considers both the topological properties and electrical properties of power systems.

- *Develop a method for fast search for parallel corridor after disturbance*.

  Parallel corridor search method based on the simplified state graph after searching the domains for each generator, commons for each bus, and links between commons is proposed. It could quickly identify the most vulnerable components due to the large power flow redistribution by tripping a highly loaded transmission line and providing the precious time for the system

operator to take remedial actions if needed.

- *Propose a fast fault detection method for improvement of distance relay operation during power swing*.

  Tripping a highly loaded transmission line may cause power swing occurring and leading to relay misoperation during cascading outages. A novel and fast fault detection scheme is proposed for distance relay during power swing. It could detect the fault with increased speed, which could be beneficial for system protection, especially in EHV system. The sampling rate for data acquisition can be as low as 10 kHz, which can be used in the existing microprocessor based distance relays. The implementation of the proposed scheme could reduce the risk of relay misoperations and improve relay dependability.

7.2 Conclusions

The purpose of this dissertation is to find some effective methods to help detect, prevent and mitigate power system cascading outages since the research in this area is still far from mature to better understand cascading outages. The contributions of this dissertation may benefit both theoretical research and practical applications in detection, prevention and mitigation of power system cascading outages. The following contributions can be obtained:

- Weighted vulnerability analysis could provide better system situational awareness and accurate information about the disturbance since it considered both electrical and topological properties.
- Parallel corridor search method could identify the most vulnerable lines after power re-distribution, which will give operator time to take remedial actions.
- New travelling wave and wavelet transform based fault detection could reduce the impact of relay misoperation.

7.3 Suggestion for Future Research

The research and study in this dissertation can be continued in the future. Extensive research and analysis tools are required for transient progress stage during cascading outage. The existing method is not fast and accurate enough to accomplish the transient analysis.

The system-wide vulnerability analysis method is based on the outputs from state estimation. When implementing the proposed system-wide tools, the topology error processing should be considered when building the topological model of power system, and parameter error processing should be studied.

For the local fault detection scheme during power swing, an adaptive method for determining the threshold value for the fault detection criterion should be developed, which could provide more accurate results.

All the proposed methods are programmed in Matlab. They need to be converted to high efficient programming code using different programming language when the field test is applied in the future.

REFERENCES

[1] U.S.-Canada Power System Outage Task Force, “Final report on the August 14, 2003 blackout in the United States and Canada: Causes and recommendations,” April 5, 2004, [Online] Available: http://www.nerc.com

[2] IEEE PES CAMS Task Force on Understanding, Prediction, Mitigation and Restoration of Cascading Failures, “Initial review of methods for cascading failure analysis in electric power transmission systems,” IEEE Power and Energy Society General Meeting, Pittsburgh, PA, USA, July 2008.

[3] NERC (North American Electric Reliability Council), 1996 system disturbances, Princeton Forrestal Village, Aug. 2002. [Online] Available: http://www.nerc.com

[4] B. A. Carreras, D. E. Newman, I. Dobson, and A. B. Poole, “Evidence for self-organized criticality in a time series of electric power blackouts,” *IEEE Trans. on Circuits and System*, vol. 51, no. 9, pp. 1733-1740, 2004.

[5] IEEE PES CAMS Task Force on Understanding, Prediction, Mitigation and Restoration of Cascading Failures, “Risk assessment of cascading outages: Part I – Overview of methodologies,” IEEE Power and Energy Society General Meeting, Detroit, MI, USA, July 2011.

[6] X. Weng, Y. Hong, A. Xue, and S. Mei, “Failure analysis on China power grid based on power law,” *Journal of Control Theory and Applications*, vol. 4, no. 3, pp. 235-238, August 2006.

[7] A. J. Holmgren, S. Molin, “Using disturbance data to assess vulnerability of electric power delivery systems,” *Journal of Infrastructure Systems*, vol. 12, no. 4, pp. 243 – 251, December 2006.

[8] J.H. Bakke, A. Hansen, and J. Kertesz, “Failures and avalanches in complex networks,” *Europhysics Letters*, vol. 76, no. 4, pp. 717-723, 2006.

[9] I. Dobson, “Where is the edge for cascading failure?: challenges and opportunities for quantifying blackout risk,” IEEE Power and Energy Society General Meeting, Tampa, FL, USA, June 2007.

[10] PSerc Projcet S29 Final Report - Part I, “Detection, prevention and mitigation of cascading events,” PSerc Publication 08-18. [Online] Available: http://www.pserc.org

[11] PSerc Projcet S26 Final Report, “Risk of Cascading Outages,” PSerc Publication 08-04. [Online] Available: http://www.pserc.org

[12] K. Sun; Z. Han, "Analysis and comparison on several kinds of models of cascading failure in power system," Transmission and Distribution Conference and Exhibition: Asia and Pacific, 2005 IEEE/PES, pp.1-7, 2005.

[13] P. Hines, J. Apt, and S. Talukdar, “Large blackouts in North America: Historical trends and policy implications,” *Energy Policy*, vol. 37, pp.5249–5259, 2009.

[14] NERC, Transmission Operations (TOP) Standards, 2006 – 2010, [Online] Available: http://www.nerc.com

[15] IEEE PES CAMS Task Force on Understanding, Prediction, Mitigation and Restoration of Cascading Failures, "Vulnerability assessment for cascading failures in electric power systems," IEEE Power and Energy Society Power Systems Conference and Exposition 2009, March 2009, Seattle, WA

[16] B. A. Carreras, V. E. Lynch, I. Dobson, and D. E. Newman, “Complex dynamics of blackouts in power transmission systems,” *Chaos*, vol.14, pp. 643–652, 2004.

[17] I. Dobson, B. A. Carreras, V. E. Lynch, and D. E. Newman, “An initial model for complex dynamics in electric power system blackouts,” 34th Hawaii International Conference on System Sciences, Maui, Hawaii, January 2001.

[18] B. A. Carreras, V. E. Lynch, M. L. Sachtjen, I. Dobson, and D. E. Newman, “Modeling blackout dynamics in power transmission networks with simple structure,” 34th Hawaii International Conference on System Sciences, Maui, Hawaii, January 2001.

[19] I. Dobson, B.A. Carreras, “Number and propagation of line outages in cascading events in electric power transmission systems,” 48th Annual Allerton Conference on Communication, Control and Computing, Monticello, IL USA, September 2010.

[20] I. Dobson, B. A. Carreras, and D. E. Newman, “A loading-dependent model of probabilistic cascading failure,” *Probability in the Engineering and Informational Sciences*, vol. 19, pp. 15–32 , 2005.

[21] I. Dobson, B. A. Carreras, and D. E. Newman, “A branching process approximation to cascading load-dependent system failure,” 37th Hawaii International Conference on System Sciences, Hawaii, January 2004.

[22] H. Ren, I. Dobson, “Using transmission line outage data to estimate cascading failure propagation in an electric power system,” *IEEE Trans. Circuits and Systems* Part II, 2008, vol. 55, no. 9, pp. 927-931.

[23] I. Dobson, J. Kim, K. R. Wierzbicki, “Testing branching process estimators of cascading failure with data from a simulation of transmission line outages,” *Risk Analysis*, vol. 30, no. 4, 2010, pp. 650 - 662.

[24] X. Yu and C. Singh, “A practical approach for integrated power system vulnerability analysis with protection failures,” *IEEE Trans. on Power Systems*, vol. 19, no. 4, pp. 1811-1820, 2004.

[25] X. Yu and C. Singh, “Power system reliability analysis considering protection failures,” IEEE PES Summer Meeting, vol. 2, pp. 963-968, 2002.

[26] M. A. Rios, D. S. Kirschen, D. Jawayeera, D. P. Nedic, and R. N. Allan, “Value of security: modeling time-dependent phenomena and weather conditions,” *IEEE Trans. on Power Systems*, vol. 17, pp. 543–548, 2002.

[27] J. Chen, J. S. Thorp, and I. Dobson, “Cascading dynamics and mitigation assessment in power system disturbances via a hidden failure model,” *Int. J. Electr. Power Energy Syst*. vol. 27, pp. 318–326, 2005.

[28] M. Anghel, K. A. Werley, and A. E. Motter, “Stochastic model for power grid dynamics,” 40th Hawaii International Conference on System Sciences, Hawaii, January 2007.

[29] D. J. Watts, Small worlds, *The dynamics of networks between order and randomness*, Princeton University Press, Princeton, NJ, USA 2003

[30] P. Hines, S. Blumsack, “A centrality measure for electrical networks,” 41st Hawaii International Conference on System Sciences, Hawaii, Jan. 2008.

[31] B. C. Lesieutre, S. Roy, V. Donde, A. Pinar, “Power system extreme event screening using graph partitioning,” 38th North American Power Symposium, Southern Illinois University Carbondale IL USA, Sept 2006.

[32] A. E. Motter and Y.-C. Lai, "Cascade-based attacks on complex networks," *Physical Review E,* vol. 66, pp. 065102, 2002.

[33] Q. Chen, K. Zhu, and J.D. McCalley, "Dynamic decision-event trees for rapid response to unfolding events in bulk transmission systems," in *IEEE 2001 Power Tech Proceedings*, vol. 2 , Porto, Portugal, Sept. 2001.

[34] J.C. Tan, P.A. Crossley, and P.G. McLaren, "Application of a wide area backup protection expert system to prevent cascading outages," *IEEE Transactions on Power Delivery*, vol. 17, no. 2, pp. 375 – 380, April 2002.

[35] C. C. Liu, Learning to recognize the vulnerable patterns of cascaded events, EPRI Technical Report, 2007.

[36] C. C. Liu, J. Jung, G. Heydt, V.Vittal, A. Phadke, “The strategic power infrastructure defense (SPID) - A conceptual design,” *IEEE Control System Magazine*, vol. 20, no. 4, pp. 40-52, Aug. 2000.

[37] H. Song, “The detection, prevention and mitigation of cascading outages in the power system,” Ph.D. dissertation, Dept. Electrical and Computer Engineering, Texas A&M University, College Station, 2006.

[38] D. Kirschen, R. Allon, and G. Strbac, "Contributions of individual generators to loads and flows," *Power Systems, IEEE Transactions on*, vol. 12, pp. 52-60, 1997.

[39] E.B. Makram, K.P. Thorton, and H.E. Brown, “Selection of lines to be switched to eliminate overloaded lines using a z-matrix method,” *IEEE Trans. Power Systems*, vol. 4, no. 2, pp. 653–661, May 1989.

[40] N. Muller and V. H. Quintana, “Line and shunt switching to alleviate overloads and voltage violations in power networks,” *Generation, Transmission and Distribution, IEE Proceedings C*, vol. 136, no. 4, pp. 246–253, July 1989.

[41] N.S. Rau, “Transmission loss and congestion cost allocation - an approach based on responsibility,” *IEEE Trans. Power Systems*, vol. 15, no. 4, pp. 1401–1409, Nov. 2000.

[42] T. Niimura and Y. Niu, “Transmission congestion relief by economic load management,” in Proc. of IEEE Power Engineering Society 2002 Summer Meeting, 2002, vol. 3, pp. 1645–1649.

[43] P. Kundur, *Power System Stability and Control*, McGraw Hill Inc., New York, 1994.

[44] H. Song and M. Kezunovic, “A new analysis method for early detection and prevention of cascading events,” *Electric Power Systems Research*, vol. 77, no. 8, pp. 1132-1142, June 2007.

[45] UCTE, “Final report system disturbance on 4 November 2006,” Union for the Co-ordination of Transmission of Electricity Technique Report, 2007, [Online]

Available:

http://www.eoliennes-refus.fr/FichiersREF/UCTE-FinalREPORT-4nov2007.pdf

[46] CNN, “Dam failure triggers huge blackout in Brazil,” 2009, [Online] Available: http://www.cnn.com

[47] Qiming Chen, “The probability, identification and prevention of rare events in power system,” PhD Dissertation, Dept. Electrical and Computer Engineering, Iowa State University, 2004.

[48] J. Zhu, *Power system applications of graph theory*, New York: Nova Science Publishers, Inc., 2009.

[49] D. Fay, H. Haddadi, A. Thomason, A. W. Moore, R. Mortier, A. Jamakovic, S. Uhlig, M. Rio, "Weighted spectral distribution for internet topology analysis: theory and applications," *Networking, IEEE/ACM Transactions on* , vol.18, no.1, pp.164-176, Feb. 2010.

[50] S. Pemmaraju, and S. Skiena, *Computational Discrete Mathematics: Combinatorics and Graph Theory with Mathematica*, New York: Cambridge Univ. Press, 2003.

[51] Xiao Long Huang, and Brahim Bensaou, “On max-min fairness and scheduling in wireless ad-hoc networks: analytical framework and implementation,” *In Proceedings of the 2nd ACM international symposium on Mobile ad hoc*

networking & computing (MobiHoc '01). ACM, New York, NY, USA, 221-231, 2001.

[52] J. R. Bettman, "A graph theory approach to comparing consumer information processing models," *Management Science*, vol. 18, pp. P114-P128, 1971.

[53] J. A. Barnes, “Graph theory and social networks: A technical comment on connectedeness and connectivity,” *Sociology*, vol. 3, no. 2, pp. 215-232, May 1969.

[54] S. M. Wagner, and N. Neshat, “Assessing the vulnerability of supply chains using graph theory,” *International Journal of Production Economics*, vol. 126, no. 1, pp. 121-129, July 2010.

[55] L.H. Hsu and C.K. Lin, *Graph Theory and Interconnection Networks*, CRC PR Inc, 2008.

[56] T.H. Lee, D.H. Thorne, and E. F. Hill, "A transportation method for economic dispatching - application and comparison," *Power Apparatus and Systems, IEEE Transactions on*, vol.PAS-99, no.6, pp.2373-2385, Nov. 1980.

[57] D. J. Watts, Small worlds, *The dynamics of networks between order and randomness*, Princeton: Princeton University Press, 2003.

[58] P. Hines and S. Blumsack, “A centrality measure for electrical networks,” 41st Hawaii International Conference on System Sciences, Hawaii, Jan. 2008.

[59] B. C. Lesieutre, S. Roy, V. Donde, and A. Pinar, “Power system extreme event screening using graph partitioning,” 38th North American Power Symposium, Southern Illinois University Carbondale IL USA, Sept. 2006.

[60] G. N. Korres, and P.J. Katsikas, "A hybrid method for observability analysis using a reduced network graph theory," *Power Systems, IEEE Transactions on,* vol.18, no.1, pp. 295- 304, Feb 2003.

[61] N. Liu, J. Zhang, H. Zhang, and W. Liu, "Security assessment for communication networks of power control systems using attack graph and MCDM," *Power Delivery, IEEE Transactions on*, vol.25, no.3, pp.1492-1500, July 2010.

[62] D. Dustegor, S. V. Poroseva, M. Y. Hussaini, and S. Woodruff, "Automated graph-based methodology for fault detection and location in power systems," *Power Delivery, IEEE Transactions on*, vol.25, no.2, pp.638-646, April 2010.

[63] D. P. Chassin and C. Posse, “Evaluating North American electric grid reliability using the Barabasi-Albert network model,” *Physica A: Statistical Mechanics and its Applications*, vol. 355, no. 2-4, pp. 667-677, September 2005.

[64] H. Song and M. Kezunovic, “Static analysis of vulnerability and security margin of the power system,” in Proc. IEEE PES Transmission & Distribution Conference & Exposition, Dallas, Texas, May. 2006.

[65] A. Bavelas, “A mathematical model for group structure,” *Human Organizations*, vol. 7, pp.16-30, 1948.

[66] G. Sabidussi, “The centrality index of a graph,” *Psychometrika*, vol. 31, no. 4, pp. 581-603, 1966.

[67] L. C. Freeman, “Centrality in social networks: Conceptual clarification,” *Social Networks*, vol. 1, pp. 215-239, 1979.

[68] L. C. Freeman, “A set of measures of centrality based on betweenness,” *Sociometry*, vol. 40, pp. 35-41, 1977.

[69] T. Athay, R. Podmore, and S. Virmani, “A practical method for the direct analysis of transient stability,” *IEEE Trans. on Power Apparatus and Systems*, vol. PAS-98, no. 2, pp. 573–584, March/April 1979.

[70] M. H. Haque and A. H. M. A. Rahim, “Determination of first swing stability limit of multimachine power systems through Taylor series expansions,” *Generation, Transmission and Distribution, IEE Proceedings C*, vol. 136, no. 6, pp. 373–379, Nov. 1989.

[71] R. D. Christie, “Power systems test case archive,” Website of EE Dept. of University of Washington, Aug. 1999, [Online] Available: http://www.ee.washington.edu/research/pstca/

[72] M. A. Pai, *Energy Function Analysis for Power System Stability*, Norwell: Kluwer Academic Publishers, 1989, pp.222-227

[73] NERC Disturbance Reports, North American Electric Reliability Council, New Jersey, 1996-2001.

[74] IEEE PSRC Report, Power swing and out-of-step considerations on transmission lines, IEEE PSRC WG D6 Workgroup, 2005.

[75] D. Tziouvaras and D. Hou, “Out-of-step protection fundamentals and advancements,” presented at the 30th Annual Western Protective Relay Conference, October 21-23, 2003, Spokane, Washington.

[76] L. Wang and A. Girgis, “A new method for power system transient instability detection,” *IEEE Trans. on Power Delivery*, vol. 12, no. 3, pp. 1082 – 1089, 1997.

[77] A. Mechraoui and D. W. P. Thomas, "A new blocking principle with phase and earth fault detection during fast power swings for distance protection," *IEEE Trans. on Power Delivery*, vol. 10, no.3, pp. 1242-1248, 1995.

[78] M. A. Redfern and M. J. Checksfield, "A study into new solution for the problems experienced with pole slipping protection," *IEEE Trans. on Power Delivery*, vo1.13, no.2, pp.394-404, 1998.

[79] Z. Xu, *New distance relay for transmission line*, Beijing: China water and hydroelectricity press, 2002.

[80] N. Zhang, H. Song, and M. Kezunovic, "Transient based relay testing: a new scope and methodology," presented at the 13th IEEE Mediterranean Electrotechnical Conference (MELECON'06), Torremolinos, Spain, May 2006.

[81] N. Zhang, and M. Kezunovic, "Verifying the protection system operation using an advanced fault analysis tool combined with the event tree analysis", in Proc. 2004 36th Annual North American Power Symposium (NAPS2004), pp. 133-139, Moscow, Idaho, Aug. 2004.

[82] NARI-Relays Co. Ltd, "Technical and application manual of RCS-901A/B EHV transmission line distance protection," NARI-Relays Co. Ltd. Feb. 2002.

[83] X. Lin, Y. Gao, P. Liu, "A novel scheme to identify symmetrical faults occurring during power swings," *IEEE Trans. on Power Delivery*, vol. 23, no. 1, pp. 73-78, Jan. 2008.

[84] G. Benmouyal, D. Hou, D. Tziouvaras, "Zero-setting power-swing blocking protection", presented at the 31st Annual Western Protective Relay Conference, Oct. 19-21, 2004, Spokane, Washington. Available: www.selinc.com/techpprs/6172_ZeroSetting_20050302.pdf

[85] B. Su, X. Dong, Y. Sun, B. R. J. Caunce, D. Tholomier, A. Apostolov, “Fast detctor of symmetrical fault during power swing for distance relay,” in Proc. 2005 IEEE Power eng. Soc. General Meeting, pp. 604-609.

[86] S. M. Brahma, “Distance relay with out-of-step blocking function using wavelet transform”, *IEEE Trans. on Power Delivery*, vol. 22, no. 3, pp. 1360-1366, July 2007.

[87] L. L. Grigsby, *Power System Stability and Control*, 2nd edition, CRC Press, 2007.

[88] F.Jiang, Z. Bo, and M.A. Redfern, “A new generator fault detection scheme using wavelet transform,” in Proc. 33rd Univ. Power Eng. Conf., Edinburgh, U.K., pp. 360-363, Sept. 1998.

[89] S. Huang, C. Hsieh, and C. Huang, “Application of Morlet wavelets to supervise power system disturbances,” *IEEE Trans. Power Delivery*, vol. 14, pp. 235-243, Jan.1999.

[90] J.L. Blackburn, *Protective Relaying Principles and Applications*, 2nd edition, New York: Marcel Dekker, 1998

[91] N. Zhang, “Advanced fault diagnosis techniques and their role in preventing cascading blackouts,” Ph.D. dissertation, Dept. Electrical and Computer Engineering, Texas A&M University, College Station, 2006.

[92] A. H. Osman and O. P.Malik, “Wavelet transform approach to distance protection of transmission lines,” in Proc. IEEE Power Eng. Soc. Summer Meeting, vol.1, 2001, pp.115-120.

[93] M. Chamia and S. Liberman, "Ultra high speed relay for EHV/UHV transmission lines-development, design and application," *IEEE Trans. Power App. Syst.*, Vol. 97, No.4, 1978, pp. 2104-2116.

[94] A. T. Johns, "New ultra-high-speed directional comparison technique for the protection of EHV transmission lines," in Proc. Inst. Elect. Eng. Conference, Vol. 127, No. 4, 1980, pp. 228-239.

[95] M. Vitins, "A fundamental concept for high speed relaying," *IEEE Trans. PowerApp. Syst.*, Vol. 100, No.1, 1981, pp. 163-168.

[96] A. T. Johns, R. K. Aggarwal, and Z. Q. Bo, "Non-unit protection technique for EHV transmission systems based on fault-generated noise, part 1: signal measurement," in *Proc. Inst. Elect. Eng.- Gen., Trans. Dist*., Vol. 141, No. 2, 1994, pp. 133-140.

[97] Q. H. Wu, J. F. Zhang, and D. J. Zhang, "Ultra high-speed directional protection of transmission lines using mathematical morphology," *IEEE Trans. Power Delivery*, Vol. 18, No.4, 2003, pp. 1127-1133.

[98] Wei Chen, O. P. Malik, Xianggen Yin, Deshu Chen, and Zhe Zhang, "Study of wavelet-based ultra high speed directional transmission line protection," *IEEE Trans. Power Delivery*, Vol. 18, No.4, 2003, pp. 1134-1139.

[99] J. Duan, B. Zhang, S. Luo, and Z. Yi, “Transient-based Ultra-high-speed Directional Protection using Wavelet Transforms for EHV Transmission Lines,” presented at the 2nd IEEE/PES Transmission and Distribution Conference, August 14-18, 2005.

[100] A. M. Gaouda, M. M. A. Salama, M. R. Sultan, and A. Y. Chikhani, “Power quality detection and classification using wavelet multi-resolution signal decomposition,” *IEEE Trans. Power Delivery*, vol. 14, no. 3, pp. 1469-1476, 1999.

[101] M. Sanaye-Pasand, and A.N. Jahromi, “Study, comparison and simulation of power system swing detection and prediction method,” in Proc. Power Engineering Society General Meeting, 2003, vol. 1, pp. 27 - 32, July 2003

[102] N. Zhang and M. Kezunovic, "A study of synchronized sampling based fault location algorithm performance under power swing and out-of-step conditions," in Proc. of PowerTech 2005, St. Petersburg, Russia, June 2005

[103] P. A. Crossley, P. G. McLaren, “Distance protection based on travelling waves”, *Power Apparatus and Systems, IEEE Transactions on* , vol.PAS-102, no. 9, pp. 2971-2982, September 1982.

[104] I. Daubechies, Ten Lectures on Wavelets, CBMS-NSF Regional Conference Series in Applied Mathematics, University of Lowell, Mass., June 1990

[105] C. S. Burrus, R. A. Gopinath, and H. Guo, Introduction to Wavelets and Wavelet Transforms: A Primer. Englewood Cliffs, NJ: Prentice-Hall, 1998.

[106] S. Mallat, “A theory for multiresolution signal decomposition: The wavelet representation,” *IEEE Trans. Pattern Anal. Mach. Intell.*, vol. 11, no. 7, pp. 674–693, Jul. 1989.

[107] D. B. Percival and A. T. Walden, *Wavelet Methods for Time Series Analysis*, New York: Cambridge Univ. Press, 2000.

[108] C. Kim and R. Aggarwal, “Wavelet transform in power system,” *Inst. Elect. Eng. Power Eng.*, vol.15, no. 4, pp. 193-202, Aug. 2001.

[109] J. Wu and C. Liu, “Investigation of engine fault diagnosis using discrete wavelet transform and neural network,” *Expert Systems with Applications*, vol. 35, no. 3, pp. 1200-1213, Oct. 2008.

[110] Power System Relaying Committee, “EMTP reference models for transmission line relay testing report, draft 10a,” Tech. Rep., 2004. [Online] Available: http://www.pserc.org/

[111] L. Priker and H.K. Hoidalen, ATPDraw Version 4.0 for Windows9X/NT/2000/XP, SINTEF Energy Research AS, Norway. [Online] Available: http://www.eeug.org/files/secret/atpdraw

APPENDIX A

Nomenclature

The nomenclature is used to provide the descriptions for the system data in following appendices.

Type: 1-PQ bus; 2-PV bus; 3-Swing bus.

P_L, Q_L: real and reactive parts of the load at buses, in MVA value.

B_s: shunt capacitor at buses, in MVA value.

V_m: bus voltage magnitudes, in p.u. value. PQ bus voltage magnitudes will be set as 0 for power flow flat start.

Area: control area.

P_g: real power output of generators, in MVA value.

Q_g: reactive power output of PV buses, in MVA value. Some PV buses are not generators.

$Q_{\max}$: Maximum reactive power output of PV buses, in MVA value.

$Q_{\min}$: Minimum reactive power output of PV buses, in MVA value.

V_{sp}: Scheduled PV bus voltage magnitudes, in p.u. value.

$P_{\max}$: Maximum real power output of generators, in MVA value.

fBus: from bus, the beginning bus of the line.

tBus: to bus, the ending bus of the line.

r : line resistance, in p.u. value.

x : line reactance, in p.u. value.

b : line charging capacitance, in p.u. value.

limit: transmission line limits, in MVA value.

tap-ratio: Non-nominal transformer ratios. 1 for lines and nominal transformers.

angle: phase-shifter angles.

H : generator inertial constant, in value of s at its own MVA rating.

D : damping, in value of s at its own MVA rating.

X_d : d-axis synchronous reactance, in value of p.u. at its own MVA rating.

$X_d^{'}$: d-axis transient reactance, in value of p.u. at its own MVA rating.

X_q : q-axis synchronous reactance, in value of p.u. at its own MVA rating.

$X_q^{'}$: q-axis transient reactance, in value of p.u. at its own MVA rating.

$\tau_{d0}^{'}$: d-axis open circuit transient time constant, in value of s.

$\tau_{q0}^{'}$: q-axis open circuit transient time constant, in value of s.

K_A : regulator gain.

K_E : exciter constant related to self-excited field.

K_F : regulator stabilizing circuit gain.

τ_A : regulator amplifier time constant.

τ_E : exciter time constant.

τ_F : regulator stabilizing circuit time constant.

K_{Se} : saturation parameter.

τ_{Se} : saturation parameter.

APPENDIX B

IEEE 118-bus Test System Data

Table 10 Bus Data of IEEE 118-bus System

BusNo	Type	P_L (MVA)	Q_L (MVA)	B_s (MVA)	V_m	Area
1	2	51.00	27.00	0.00	0.955	1
2	1	20.00	9.00	0.00	0.971	1
3	1	39.00	10.00	0.00	0.968	1
4	2	39.00	12.00	0.00	0.998	1
5	1	0.00	0.00	-40.0	1.002	1
6	2	52.00	22.00	0.00	0.990	1
7	1	19.00	2.00	0.00	0.989	1
8	2	28.00	0.00	0.00	1.015	1
9	1	0.00	0.00	0.00	1.043	1
10	2	0.00	0.00	0.00	1.050	1
11	1	70.00	23.00	0.00	0.985	1
12	2	47.00	10.00	0.00	0.990	1
13	1	34.00	16.00	0.00	0.968	1
14	1	14.00	1.00	0.00	0.984	1
15	2	90.00	30.00	0.00	0.970	1
16	1	25.00	10.00	0.00	0.984	1
17	1	11.00	3.00	0.00	0.995	1
18	2	60.00	34.00	0.00	0.973	1
19	2	45.00	25.00	0.00	0.963	1
20	1	18.00	3.00	0.00	0.958	1
21	1	14.00	8.00	0.00	0.959	1
22	1	10.00	5.00	0.00	0.970	1
23	1	7.00	3.00	0.00	1.000	1
24	2	13.00	0.00	0.00	0.992	2
25	2	0.00	0.00	0.00	1.050	1
26	2	0.00	0.00	0.00	1.015	1
27	2	71.00	13.00	0.00	0.968	1

28	1	17.00	7.00	0.00	0.962	1
29	1	24.00	4.00	0.00	0.963	1
30	1	0.00	0.00	0.00	0.968	1
31	2	43.00	27.00	0.00	0.967	1
32	2	59.00	23.00	0.00	0.964	1
33	1	23.00	9.00	0.00	0.972	2
34	2	59.00	26.00	14.00	0.986	2
35	1	33.00	9.00	0.00	0.981	2
36	2	31.00	17.00	0.00	0.980	2
37	1	0.00	0.00	-25.0	0.992	2
38	1	0.00	0.00	0.00	0.962	2
39	1	27.00	11.00	0.00	0.970	2
40	2	66.00	23.00	0.00	0.970	2
41	1	37.00	10.00	0.00	0.967	2
42	2	96.00	23.00	0.00	0.985	2
43	1	18.00	7.00	0.00	0.978	2
44	1	16.00	8.00	10.00	0.985	2
45	1	53.00	22.00	10.00	0.987	2
46	2	28.00	10.00	10.00	1.005	2
47	1	34.00	0.00	0.00	1.017	2
48	1	20.00	11.00	15.00	1.021	2
49	2	87.00	30.00	0.00	1.025	2
50	1	17.00	4.00	0.00	1.001	2
51	1	17.00	8.00	0.00	0.967	2
52	1	18.00	5.00	0.00	0.957	2
53	1	23.00	11.00	0.00	0.946	2
54	2	113.00	32.00	0.00	0.955	2
55	2	63.00	22.00	0.00	0.952	2
56	2	84.00	18.00	0.00	0.954	2
57	1	12.00	3.00	0.00	0.971	2
58	1	12.00	3.00	0.00	0.959	2
59	2	277.00	113.00	0.00	0.985	2
60	1	78.00	3.00	0.00	0.993	2
61	2	0.00	0.00	0.00	0.995	2
62	2	77.00	14.00	0.00	0.998	2
63	1	0.00	0.00	0.00	0.969	2
64	1	0.00	0.00	0.00	0.984	2

65	2	0.00	0.00	0.00	1.005	2
66	2	39.00	18.00	0.00	1.050	2
67	1	28.00	7.00	0.00	1.020	2
68	1	0.00	0.00	0.00	1.003	2
69	3	0.00	0.00	0.00	1.035	2
70	2	66.00	20.00	0.00	0.984	2
71	1	0.00	0.00	0.00	0.987	2
72	2	12.00	0.00	0.00	0.980	2
73	2	6.00	0.00	0.00	0.991	2
74	2	68.00	27.00	12.00	0.958	3
75	1	47.00	11.00	0.00	0.967	
76	2	68.00	36.00	0.00	0.943	3
77	2	61.00	28.00	0.00	1.006	3
78	1	71.00	26.00	0.00	1.003	3
79	1	39.00	32.00	20.00	1.009	3
80	2	130.00	26.00	0.00	1.040	3
81	1	0.00	0.00	0.00	0.997	3
82	1	54.00	27.00	20.00	0.989	3
83	1	20.00	10.00	10.00	0.985	3
84	1	11.00	7.00	0.00	0.980	3
85	2	24.00	15.00	0.00	0.985	3
86	1	21.00	10.00	0.00	0.987	3
87	2	0.00	0.00	0.00	1.015	3
88	1	48.00	10.00	0.00	0.987	3
89	2	0.00	0.00	0.00	1.005	3
90	2	163.00	42.00	0.00	0.985	3
91	2	10.00	0.00	0.00	0.980	3
92	2	65.00	10.00	0.00	0.993	3
93	1	12.00	7.00	0.00	0.987	3
94	1	30.00	16.00	0.00	0.991	3
95	1	42.00	31.00	0.00	0.981	3
96	1	38.00	15.00	0.00	0.993	3
97	1	15.00	9.00	0.00	1.011	3
98	1	34.00	8.00	0.00	1.024	3
99	2	42.00	0.00	0.00	1.010	3
100	2	37.00	18.00	0.00	1.017	3
101	1	22.00	15.00	0.00	0.993	3

102	1	5.00	3.00	0.00	0.991	3
103	2	23.00	16.00	0.00	1.001	3
104	2	38.00	25.00	0.00	0.971	3
105	2	31.00	26.00	20.00	0.965	3
106	1	43.00	16.00	0.00	0.962	3
107	2	50.00	12.00	6.00	0.952	3
108	1	2.00	1.00	0.00	0.967	3
109	1	8.00	3.00	0.00	0.967	3
110	2	39.00	30.00	6.00	0.973	3
111	2	0.00	0.00	0.00	0.980	3
112	2	68.00	13.00	0.00	0.975	3
113	2	6.00	0.00	0.00	0.993	1
114	1	8.00	3.00	0.00	0.960	1
115	1	22.00	7.00	0.00	0.960	1
116	2	184.00	0.00	0.00	1.005	2
117	1	20.00	8.00	0.00	0.974	1
118	1	33.00	15.00	0.00	0.949	3

Table 11 PV Bus Data of IEEE-118 System

BusNo	P_g (MVA)	Q_g (MVA)	Q_{max} (MVA)	Q_{min} (MVA)	V_{sp} (p.u.)	P_{max} (MVA)
1	0.00	0.00	15.00	-5.00	0.955	100.00
4	0.00	0.00	300.00	-300.00	0.998	100.00
6	0.00	0.00	50.00	-13.00	0.990	100.00
8	0.00	0.00	300.00	-300.00	1.015	100.00
10	450.00	0.00	250.00	-147.00	1.050	650.00
12	85.00	0.00	120.00	-35.00	0.990	185.00
15	0.00	0.00	30.00	-10.00	0.970	100.00
18	0.00	0.00	50.00	-16.00	0.973	100.00
19	0.00	0.00	24.00	-8.00	0.962	100.00
24	0.00	0.00	300.00	-300.00	0.992	100.00
25	220.00	0.00	140.00	-47.00	1.050	320.00
26	314.00	0.00	1000.00	-1000.00	1.015	414.00
27	0.00	0.00	300.00	-300.00	0.968	100.00
31	7.00	0.00	300.00	-300.00	0.967	107.00
32	0.00	0.00	42.00	-14.00	0.963	100.00
34	0.00	0.00	24.00	-8.00	0.984	100.00
36	0.00	0.00	24.00	-8.00	0.980	100.00
40	0.00	0.00	300.00	-300.00	0.970	100.00
42	0.00	0.00	300.00	-300.00	0.985	100.00
46	19.00	0.00	100.00	-100.00	1.005	119.00
49	204.00	0.00	210.00	-85.00	1.025	304.00
54	48.00	0.00	300.00	-300.00	0.955	148.00
55	0.00	0.00	23.00	-8.00	0.952	100.00
56	0.00	0.00	15.00	-8.00	0.954	100.00
59	155.00	0.00	180.00	-60.00	0.985	255.00
61	160.00	0.00	300.00	-100.00	0.995	260.00
62	0.00	0.00	20.00	-20.00	0.998	100.00
65	391.00	0.00	250.00	-67.00	1.005	591.00
66	392.00	0.00	250.00	-67.00	1.050	592.00
69	516.40	0.00	300.00	-300.00	1.035	805.20

70	0.00	0.00	32.00	-10.00	0.984	100.00
72	0.00	0.00	100.00	-100.00	0.980	100.00
73	0.00	0.00	100.00	-100.00	0.991	100.00
74	0.00	0.00	9.00	-6.00	0.958	100.00
76	0.00	0.00	23.00	-8.00	0.943	100.00
61	160.00	0.00	300.00	-100.00	0.995	260.00
77	0.00	0.00	70.00	-20.00	1.006	100.00
80	477.00	0.00	280.00	-165.00	1.040	677.00
85	0.00	0.00	23.00	-8.00	0.985	100.00
87	4.00	0.00	1000.00	-100.00	1.015	104.00
89	607.00	0.00	300.00	-210.00	1.005	807.00
90	0.00	0.00	300.00	-300.00	0.985	100.00
91	0.00	0.00	100.00	-100.00	0.980	100.00
92	0.00	0.00	9.00	-3.00	0.990	100.00
99	0.00	0.00	100.00	-100.00	1.010	100.00
100	252.00	0.00	155.00	-50.00	1.017	352.00
103	40.00	0.00	40.00	-15.00	1.010	140.00
104	0.00	0.00	23.00	-8.00	0.971	100.00
105	0.00	0.00	23.00	-8.00	0.965	100.00
107	0.00	0.00	250.00	-250.00	0.952	100.00
110	0.00	0.00	23.00	-8.00	0.973	100.00
111	36.00	0.00	1000.00	-100.00	0.980	136.00
112	0.01	0.00	1000.00	-100.00	0.975	100.00
113	0.00	0.00	250.00	-100.00	0.993	100.00
116	0.00	0.00	1000.00	-1000.00	1.005	100.00

Table 12 Line Data of IEEE-118 System

LineNo	fBus	tBus	r (p.u.)	x (p.u.)	b (p.u.)	limit(MVA)	tap-ratio	angle
1	1	2	0.03030	0.09990	0.02540	250	1.000	0.000
2	1	3	0.01290	0.04240	0.01082	250	1.000	0.000
3	4	5	0.00176	0.00798	0.00210	250	1.000	0.000
4	3	5	0.02410	0.10800	0.02840	250	1.000	0.000
5	5	6	0.01190	0.05400	0.01426	250	1.000	0.000
6	6	7	0.00459	0.02080	0.00550	250	1.000	0.000
7	8	9	0.00244	0.03050	1.16200	640	1.000	0.000
8	8	5	0.00000	0.02670	0.00000	510	0.985	0.000
9	9	10	0.00258	0.03220	1.23000	650	1.000	0.000
10	4	11	0.02090	0.06880	0.01748	250	1.000	0.000
11	5	11	0.02030	0.06820	0.01738	250	1.000	0.000
12	11	12	0.00595	0.01960	0.00502	250	1.000	0.000
13	2	12	0.01870	0.06160	0.01572	250	1.000	0.000
14	3	12	0.04840	0.16000	0.04060	250	1.000	0.000
15	7	12	0.00862	0.03400	0.00874	250	1.000	0.000
16	11	13	0.02225	0.07310	0.01876	250	1.000	0.000
17	12	14	0.02150	0.07070	0.01816	250	1.000	0.000
18	13	15	0.07440	0.24440	0.06268	250	1.000	0.000
19	14	15	0.05950	0.19500	0.05020	250	1.000	0.000
20	12	16	0.02120	0.08340	0.02140	250	1.000	0.000
21	15	17	0.01320	0.04370	0.04440	250	1.000	0.000
22	16	17	0.04540	0.18010	0.04660	250	1.000	0.000
23	17	18	0.01230	0.05050	0.01298	250	1.000	0.000
24	18	19	0.01119	0.04930	0.01142	250	1.000	0.000
25	19	20	0.02520	0.11700	0.02980	250	1.000	0.000
26	15	19	0.01200	0.03940	0.01010	250	1.000	0.000
27	20	21	0.01830	0.08490	0.02160	250	1.000	0.000
28	21	22	0.02090	0.09700	0.02460	250	1.000	0.000
29	22	23	0.03420	0.15900	0.04040	250	1.000	0.000
30	23	24	0.01350	0.04920	0.04980	250	1.000	0.000
31	23	25	0.01560	0.08000	0.08640	380	1.000	0.000
32	26	25	0.00000	0.03820	0.00000	380	0.960	0.000
33	25	27	0.03180	0.16300	0.17640	280	1.000	0.000

34	27	28	0.01913	0.08550	0.02160	250	1.000	0.000
35	28	29	0.02370	0.09430	0.02380	250	1.000	0.000
36	30	17	0.00000	0.03880	0.00000	520	0.960	0.000
37	8	30	0.00431	0.05040	0.51400	500	1.000	0.000
38	26	30	0.00799	0.08600	0.90800	380	1.000	0.000
39	17	31	0.04740	0.15630	0.03990	250	1.000	0.000
40	29	31	0.01080	0.03310	0.00830	250	1.000	0.000
41	23	32	0.03170	0.11530	0.11730	250	1.000	0.000
42	31	32	0.02980	0.09850	0.02510	250	1.000	0.000
43	27	32	0.02290	0.07550	0.01926	250	1.000	0.000
44	15	33	0.03800	0.12440	0.03194	250	1.000	0.000
45	19	34	0.07520	0.24700	0.06320	250	1.000	0.000
46	35	36	0.00224	0.01020	0.00268	250	1.000	0.000
47	35	37	0.01100	0.04970	0.01318	250	1.000	0.000
48	33	37	0.04150	0.14200	0.03660	250	1.000	0.000
49	34	36	0.00871	0.02680	0.00568	250	1.000	0.000
50	34	37	0.00256	0.00940	0.00984	250	1.000	0.000
51	38	37	0.00000	0.03750	0.00000	350	0.935	0.000
52	37	39	0.03210	0.10600	0.02700	250	1.000	0.000
53	37	40	0.05930	0.16800	0.04200	250	1.000	0.000
54	30	38	0.00464	0.05400	0.42200	250	1.000	0.000
55	39	40	0.01840	0.06050	0.01552	250	1.000	0.000
56	40	41	0.01450	0.04870	0.01222	250	1.000	0.000
57	40	42	0.05550	0.18300	0.04660	250	1.000	0.000
58	41	42	0.04100	0.13500	0.03440	250	1.000	0.000
59	43	44	0.06080	0.24540	0.06068	250	1.000	0.000
60	34	43	0.04130	0.16810	0.04226	250	1.000	0.000
61	44	45	0.02240	0.09010	0.02240	250	1.000	0.000
62	45	46	0.04000	0.13560	0.03320	250	1.000	0.000
63	46	47	0.03800	0.12700	0.03160	250	1.000	0.000
64	46	48	0.06010	0.18900	0.04720	250	1.000	0.000
65	47	49	0.01910	0.06250	0.01604	250	1.000	0.000
66	42	49	0.07150	0.32300	0.08600	250	1.000	0.000
67	42	49	0.07150	0.32300	0.08600	250	1.000	0.000
68	45	49	0.06840	0.18600	0.04440	250	1.000	0.000
69	48	49	0.01790	0.05050	0.01258	250	1.000	0.000
70	49	50	0.02670	0.07520	0.01874	250	1.000	0.000

71	49	51	0.04860	0.13700	0.03420	250	1.000	0.000
72	51	52	0.02030	0.05880	0.01396	250	1.000	0.000
73	52	53	0.04050	0.16350	0.04058	250	1.000	0.000
74	53	54	0.02630	0.12200	0.03100	250	1.000	0.000
75	49	54	0.07300	0.28900	0.07380	250	1.000	0.000
76	49	54	0.07300	0.28900	0.07380	250	1.000	0.000
77	54	55	0.01690	0.07070	0.02020	250	1.000	0.000
78	54	56	0.00275	0.00955	0.00732	250	1.000	0.000
79	55	56	0.00488	0.01510	0.00374	250	1.000	0.000
80	56	57	0.03430	0.09660	0.02420	250	1.000	0.000
81	50	57	0.04740	0.13400	0.03320	250	1.000	0.000
82	56	58	0.03430	0.09660	0.02420	250	1.000	0.000
83	51	58	0.02550	0.07190	0.01788	250	1.000	0.000
84	54	59	0.05030	0.22930	0.05980	250	1.000	0.000
85	56	59	0.08250	0.25100	0.05690	250	1.000	0.000
86	56	59	0.08250	0.25100	0.05690	250	1.000	0.000
87	55	59	0.04739	0.21580	0.05646	250	1.000	0.000
88	59	60	0.03170	0.14500	0.03760	250	1.000	0.000
89	59	61	0.03280	0.15000	0.03880	250	1.000	0.000
90	60	61	0.00264	0.01350	0.01456	250	1.000	0.000
91	60	62	0.01230	0.05610	0.01468	250	1.000	0.000
92	61	62	0.00824	0.03760	0.00980	250	1.000	0.000
93	63	59	0.00000	0.03860	0.00000	250	0.960	0.000
94	63	64	0.00172	0.02000	0.21600	250	1.000	0.000
95	64	61	0.00000	0.02680	0.00000	250	0.985	0.000
96	38	65	0.00901	0.09860	1.04600	250	1.000	0.000
97	64	65	0.00269	0.03020	0.38000	250	1.000	0.000
98	49	66	0.01800	0.09190	0.02480	250	1.000	0.000
99	49	66	0.01800	0.09190	0.02480	250	1.000	0.000
100	62	66	0.04820	0.21800	0.05780	250	1.000	0.000
101	62	67	0.02580	0.11700	0.03100	250	1.000	0.000
102	65	66	0.00000	0.03700	0.00000	250	0.935	0.000
103	66	67	0.02240	0.10150	0.02682	250	1.000	0.000
104	65	68	0.00138	0.01600	0.63800	480	1.000	0.000
105	47	69	0.08440	0.27780	0.07092	250	1.000	0.000
106	49	69	0.09850	0.32400	0.08280	250	1.000	0.000
107	68	69	0.00000	0.03700	0.00000	500	0.935	0.000

108	69	70	0.03000	0.12700	0.12200	300	1.000	0.000
109	24	70	0.00221	0.41150	0.10198	250	1.000	0.000
110	70	71	0.00882	0.03550	0.00878	250	1.000	0.000
111	24	72	0.04880	0.19600	0.04880	250	1.000	0.000
112	71	72	0.04460	0.18000	0.04444	250	1.000	0.000
113	71	73	0.00866	0.04540	0.01178	250	1.000	0.000
114	70	74	0.04010	0.13230	0.03368	250	1.000	0.000
115	70	75	0.04280	0.14100	0.03600	250	1.000	0.000
116	69	75	0.04050	0.12200	0.12400	280	1.000	0.000
117	74	75	0.01230	0.04060	0.01034	250	1.000	0.000
118	76	77	0.04440	0.14800	0.03680	250	1.000	0.000
119	69	77	0.03090	0.10100	0.10380	580	1.000	0.000
120	75	77	0.06010	0.19990	0.04978	250	1.000	0.000
121	77	78	0.00376	0.01240	0.01264	250	1.000	0.000
122	78	79	0.00546	0.02440	0.00648	250	1.000	0.000
123	77	80	0.01700	0.04850	0.04720	250	1.000	0.000
124	77	80	0.02940	0.10500	0.02280	250	1.000	0.000
125	79	80	0.01560	0.07040	0.01870	250	1.000	0.000
126	68	81	0.00175	0.02020	0.80800	560	1.000	0.000
127	81	80	0.00000	0.03700	0.00000	560	0.935	0.000
128	77	82	0.02980	0.08530	0.08174	250	1.000	0.000
129	82	83	0.01120	0.03665	0.03796	250	1.000	0.000
130	83	84	0.06250	0.13200	0.02580	250	1.000	0.000
131	83	85	0.04300	0.14800	0.03480	250	1.000	0.000
132	84	85	0.03020	0.06410	0.01234	250	1.000	0.000
133	85	86	0.03500	0.12300	0.02760	250	1.000	0.000
134	86	87	0.02828	0.20740	0.04450	250	1.000	0.000
135	85	88	0.02000	0.10200	0.02760	250	1.000	0.000
136	85	89	0.02390	0.17300	0.04700	250	1.000	0.000
137	88	89	0.01390	0.07120	0.01934	250	1.000	0.000
138	89	90	0.05180	0.18800	0.05280	250	1.000	0.000
139	89	90	0.02380	0.09970	0.10600	250	1.000	0.000
140	90	91	0.02540	0.08360	0.02140	250	1.000	0.000
141	89	92	0.00990	0.05050	0.05480	250	1.000	0.000
142	89	92	0.03930	0.15810	0.04140	250	1.000	0.000
143	91	92	0.03870	0.12720	0.03268	250	1.000	0.000
144	92	93	0.02580	0.08480	0.02180	250	1.000	0.000

145	92	94	0.04810	0.15800	0.04060	250	1.000	0.000
146	93	94	0.02230	0.07320	0.01876	250	1.000	0.000
147	94	95	0.01320	0.04340	0.01110	250	1.000	0.000
148	80	96	0.03560	0.18200	0.04940	250	1.000	0.000
149	82	96	0.01620	0.05300	0.05440	250	1.000	0.000
150	94	96	0.02690	0.08690	0.02300	250	1.000	0.000
151	80	97	0.01830	0.09340	0.02540	250	1.000	0.000
152	80	98	0.02380	0.10800	0.02860	250	1.000	0.000
153	80	99	0.04540	0.20600	0.05460	250	1.000	0.000
154	92	100	0.06480	0.29500	0.04720	250	1.000	0.000
155	94	100	0.01780	0.05800	0.06040	250	1.000	0.000
156	95	96	0.01710	0.05470	0.01474	250	1.000	0.000
157	96	97	0.01730	0.08850	0.02400	250	1.000	0.000
158	98	100	0.03970	0.17900	0.04760	250	1.000	0.000
159	99	100	0.01800	0.08130	0.02160	250	1.000	0.000
160	100	101	0.02770	0.12620	0.03280	250	1.000	0.000
161	92	102	0.01230	0.05590	0.01464	250	1.000	0.000
162	101	102	0.02460	0.11200	0.02940	250	1.000	0.000
163	100	103	0.01600	0.05250	0.05360	250	1.000	0.000
164	100	104	0.04510	0.20400	0.05410	250	1.000	0.000
165	103	104	0.04660	0.15840	0.04070	250	1.000	0.000
166	103	105	0.05350	0.16250	0.04080	250	1.000	0.000
167	100	106	0.06050	0.22900	0.06200	250	1.000	0.000
168	104	105	0.00994	0.03780	0.00986	250	1.000	0.000
169	105	106	0.01400	0.05470	0.01434	250	1.000	0.000
170	105	107	0.05300	0.18300	0.04720	250	1.000	0.000
171	105	108	0.02610	0.07030	0.01844	250	1.000	0.000
172	106	107	0.05300	0.18300	0.04720	250	1.000	0.000
173	108	109	0.01050	0.02880	0.00760	250	1.000	0.000
174	103	110	0.03906	0.18130	0.04610	250	1.000	0.000
175	109	110	0.02780	0.07620	0.02020	250	1.000	0.000
176	110	111	0.02200	0.07550	0.02000	250	1.000	0.000
177	110	112	0.02470	0.06400	0.06200	250	1.000	0.000
178	17	113	0.00913	0.03010	0.00768	250	1.000	0.000
179	32	113	0.06150	0.20300	0.05180	250	1.000	0.000
180	32	114	0.01350	0.06120	0.01628	250	1.000	0.000
181	27	115	0.01640	0.07410	0.01972	250	1.000	0.000

182	114	115	0.00230	0.01040	0.00276	250	1.000	0.000
183	68	116	0.00034	0.00405	0.16400	300	1.000	0.000
184	12	117	0.03290	0.14000	0.03580	250	1.000	0.000
185	75	118	0.01450	0.04810	0.01198	250	1.000	0.000
186	76	118	0.01640	0.05440	0.01356	250	1.000	0.000

Table 13 Generator Data of IEEE-118 System

GenNo	BusNo	MVA	H (s)	D (s)	X_d (p.u.)	$X_d^{'}$ (p.u.)	X_q (p.u.)	$X_q^{'}$ (p.u.)	$\tau_{d0}^{'}$ (p.u.)	$\tau_{q0}^{'}$ (p.u.)
1	10	800	8.00	0.00	0.0875	0.0875	0.0875	0.0875	7.40	0.000
2	12	800	22.00	0.00	0.0636	0.0636	0.0636	0.0636	6.10	0.300
3	25	800	8.00	0.00	0.1750	0.1750	0.1750	0.1750	6.10	0.300
4	26	800	14.00	0.00	0.1000	0.1000	0.1000	0.1000	4.75	1.500
5	31	800	26.00	0.00	0.0538	0.0538	0.0538	0.0538	4.75	1.500
6	46	800	8.00	0.00	0.0875	0.0875	0.0875	0.0875	7.40	0.000
7	49	800	8.00	0.00	0.0875	0.0875	0.0875	0.0875	6.10	0.300
8	54	800	8.00	0.00	0.0875	0.0875	0.0875	0.0875	6.10	0.300
9	59	800	8.00	0.00	0.0875	0.0875	0.0875	0.0875	4.75	1.500
10	61	800	12.00	0.00	0.1167	0.1167	0.1167	0.1167	4.75	1.500
11	65	800	10.00	0.00	0.1400	0.1400	0.1400	0.1400	7.40	0.000
12	66	800	12.00	0.00	0.1167	0.1167	0.1167	0.1167	6.10	0.300
13	69	800	20.00	0.00	0.0700	0.0700	0.0700	0.0700	6.10	0.300
14	80	800	20.00	0.00	0.0700	0.0700	0.0700	0.0700	4.75	1.500
15	87	800	30.00	0.00	0.0467	0.0467	0.0467	0.0467	4.75	1.500
16	89	800	38.148	0.00	0.0500	0.0500	0.0500	0.0500	7.40	0.000
17	100	800	32.00	0.00	0.0438	0.0438	0.0438	0.0438	6.10	0.300
18	103	800	8.00	0.00	0.0875	0.0875	0.0875	0.0875	6.10	0.300
19	111	800	16.00	0.00	0.0875	0.0875	0.0875	0.0875	4.75	1.500
20	112	800	15.00	0.00	0.0467	0.0467	0.0467	0.0467	4.75	1.500

Table 14 Exciter Data of IEEE-118 System

GenNo	BusNo	K_A	K_E	K_F	τ_A (s)	τ_E (s)	τ_F (s)	K_{Se} (s)	τ_{Se} (s)
1	10	20	1.00	0.0012	0.2500	0.000	1.00	0.0039	1.5550
2	12	20	1.00	0.0010	0.2500	0.314	1.00	0.0039	1.5550
3	25	20	1.00	0.0010	0.2500	0.314	1.00	0.0039	1.5550
4	26	20	1.00	0.0010	0.2500	0.314	1.00	0.0039	1.5550
5	31	20	1.00	0.0010	0.2500	0.314	1.00	0.0039	1.5550
6	46	20	1.00	0.0012	0.2500	0.000	1.00	0.0039	1.5550
7	49	20	1.00	0.0010	0.2500	0.314	1.00	0.0039	1.5550
8	54	20	1.00	0.0010	0.2500	0.314	1.00	0.0039	1.5550
9	59	20	1.00	0.0010	0.2500	0.314	1.00	0.0039	1.5550
10	61	20	1.00	0.0010	0.2500	0.314	1.00	0.0039	1.5550
11	65	20	1.00	0.0012	0.2500	0.000	1.00	0.0039	1.5550
12	66	20	1.00	0.0010	0.2500	0.314	1.00	0.0039	1.5550
13	69	20	1.00	0.0010	0.2500	0.314	1.00	0.0039	1.5550
14	80	20	1.00	0.0010	0.2500	0.314	1.00	0.0039	1.5550
15	87	20	1.00	0.0010	0.2500	0.314	1.00	0.0039	1.5550
16	89	20	1.00	0.0012	0.2500	0.000	1.00	0.0039	1.5550
17	100	20	1.00	0.0010	0.2500	0.314	1.00	0.0039	1.5550
18	103	20	1.00	0.0010	0.2500	0.314	1.00	0.0039	1.5550
19	111	20	1.00	0.0010	0.2500	0.314	1.00	0.0039	1.5550
20	112	20	1.00	0.0010	0.2500	0.314	1.00	0.0039	1.5550

APPENDIX C

IEEE 39-bus New England Test System Data

Table 15 Bus Data of IEEE 39-bus New England System

BusNo	Type	P_L (MVA)	Q_L (MVA)	B_s (MVA)	V_m	Area
1	1	0.00	0.00	0.00	1.047	1
2	1	0.00	0.00	0.00	1.049	1
3	1	322.00	2.40	0.00	1.030	1
4	1	500.00	184.00	0.00	1.003	1
5	1	0.00	0.00	0.00	1.005	1
6	1	0.00	0.00	0.00	1.007	1
7	1	233.80	84.00	0.00	0.996	1
8	1	522.00	176.00	0.00	0.995	1
9	1	0.00	0.00	0.00	1.028	1
10	1	0.00	0.00	0.00	1.017	1
11	1	0.00	0.00	0.00	1.012	1
12	1	8.50	88.00	0.00	1.000	1
13	1	0.00	0.00	0.00	1.014	1
14	1	0.00	0.00	0.00	1.011	1
15	1	320.00	153.00	0.00	1.015	1
16	1	329.00	32.30	0.00	1.032	1
17	1	0.00	0.00	0.00	1.034	1
18	1	158.00	30.00	0.00	1.031	1
19	1	0.00	0.00	0.00	1.050	1
20	1	680.00	103.00	0.00	0.991	1
21	1	274.00	115.00	0.00	1.032	1
22	1	0.00	0.00	0.00	1.050	1
23	1	247.50	84.60	0.00	1.045	1
24	1	308.60	-92.20	0.00	1.037	1
25	1	224.00	47.20	0.00	1.057	1
26	1	139.00	17.00	0.00	1.052	1

27	1	281.00	75.50	0.00	1.037	1
28	1	206.00	27.60	0.00	1.050	1
29	1	283.50	26.90	0.00	1.050	1
30	2	0.00	0.00	0.00	1.047	1
31	3	9.20	4.60	0.00	0.982	1
32	2	0.00	0.00	0.00	0.983	1
33	2	0.00	0.00	0.00	0.997	1
34	2	0.00	0.00	0.00	1.012	1
35	2	0.00	0.00	0.00	1.049	1
36	2	0.00	0.00	0.00	1.063	1
37	2	0.00	0.00	0.00	1.028	1
38	2	0.00	0.00	0.00	1.026	1
39	2	1104.00	250.00	0.00	1.030	1

Table 16 PV Bus Data of IEEE 39-bus New England System

BusNo	P_g (MVA)	Q_g (MVA)	$Q_{\max}$ (MVA)	$Q_{\min}$ (MVA)	V_{sp} (p.u.)	$P_{\max}$ (MVA)
30	250.00	144.92	99990	-99990	1.0475	350.00
31	572.83	207.04	99990	-99990	0.9820	1145.00
32	650.00	205.73	99990	-99990	0.9831	750.00
33	632.00	108.94	99990	-99990	0.9972	732.00
34	508.00	166.99	99990	-99990	1.0123	608.00
35	650.00	211.11	99990	-99990	1.0493	750.00
36	560.00	100.44	99990	-99990	1.0635	660.00
37	540.00	0.65	99990	-99990	1.0278	640.00
38	830.00	22.66	99990	-99990	1.0265	930.00
39	1000.00	87.88	99990	-99990	1.0300	1100.00

Table 17 Line Data of IEEE 39-bus New England System

LineNo	fBus	tBus	*r* (p.u.)	*x* (p.u.)	*b* (p.u.)	limit(MVA)	tap-ratio	angle
1	2	1	0.00350	0.04110	0.69870	1000	0.930	0.000
2	39	1	0.00100	0.02500	0.75000	1000	0.970	0.000
3	3	2	0.00130	0.01510	0.25720	1000	0.960	0.000
4	25	2	0.00700	0.00860	0.14600	1000	1.000	0.000
5	4	3	0.00130	0.02130	0.22140	1000	1.000	0.000
6	18	3	0.00110	0.01330	0.21380	1000	1.000	0.000
7	5	4	0.00080	0.01280	0.13420	1000	1.000	0.000
8	14	4	0.00080	0.01290	0.13820	1000	1.000	0.000
9	6	5	0.00020	0.00260	0.04340	1000	1.000	0.000
10	4	5	0.01335	0.04211	0.01280	1000	1.000	0.000
11	7	8	0.00000	0.17615	0.00000	1000	1.000	0.000
12	7	9	0.00000	0.11001	0.00000	1000	1.000	0.000
13	9	10	0.03181	0.08450	0.00000	1000	1.000	0.000
14	6	11	0.09498	0.19890	0.00000	1000	1.000	0.000
15	6	12	0.12291	0.25581	0.00000	1000	1.000	0.000
16	6	13	0.06615	0.13027	0.00000	1000	1.000	0.000
17	9	14	0.12711	0.27038	0.00000	1000	1.000	0.000
18	10	11	0.08205	0.19207	0.00000	1000	1.000	0.000
19	12	13	0.22092	0.19988	0.00000	1000	1.000	0.000
20	13	14	0.17093	0.34802	0.00000	1000	1.000	0.000
21	7	8	0.00000	0.17615	0.00000	1000	1.000	0.000
22	7	9	0.00000	0.11001	0.00000	1000	1.000	0.000
23	9	10	0.03181	0.08450	0.00000	1000	1.000	0.000
24	6	11	0.09498	0.19890	0.00000	1000	1.000	0.000
25	6	12	0.12291	0.25581	0.00000	1000	1.000	0.000
26	6	13	0.06615	0.13027	0.00000	1000	1.000	0.000
27	9	14	0.12711	0.27038	0.00000	1000	1.000	0.000
28	10	11	0.08205	0.19207	0.00000	1000	1.000	0.000
29	12	13	0.22092	0.19988	0.00000	1000	1.000	0.000
30	13	14	0.17093	0.34802	0.00000	1000	1.000	0.000
31	7	8	0.00000	0.17615	0.00000	1000	1.000	0.000
32	7	9	0.00000	0.11001	0.00000	1000	1.000	0.000
33	9	10	0.03181	0.08450	0.00000	1000	1.000	0.000

34	6	11	0.09498	0.19890	0.00000	1000	1.000	0.000
35	6	12	0.12291	0.25581	0.00000	1000	1.000	0.000
36	6	13	0.06615	0.13027	0.00000	1000	1.000	0.000
37	9	14	0.12711	0.27038	0.00000	1000	1.000	0.000
38	10	11	0.08205	0.19207	0.00000	1000	1.000	0.000
39	12	13	0.22092	0.19988	0.00000	1000	1.000	0.000
40	13	14	0.17093	0.34802	0.00000	1000	1.000	0.000
41	7	8	0.00000	0.17615	0.00000	1000	1.000	0.000
42	7	9	0.00000	0.11001	0.00000	1000	1.000	0.000
43	9	10	0.03181	0.08450	0.00000	1000	1.000	0.000
44	6	11	0.09498	0.19890	0.00000	1000	1.000	0.000
45	6	12	0.12291	0.25581	0.00000	1000	1.000	0.000
46	6	13	0.06615	0.13027	0.00000	1000	1.000	0.000

Table 18 Generator Data of IEEE 39-bus New England System

GenNo	BusNo	MVA	H (s)	D (s)	X_d (p.u.)	$X_d^{'}$ (p.u.)	X_q (p.u.)	$X_q^{'}$ (p.u.)	$\tau_{d0}^{'}$ (p.u.)	$\tau_{q0}^{'}$ (p.u.)
1	30	1000	3.50	0.00	0.310	0.310	0.310	0.310	8.96	0.310
2	31	1000	2.53	0.00	0.697	0.697	0.697	0.697	6.00	0.535
3	32	1000	2.98	0.00	0.531	0.531	0.531	0.531	5.89	0.600
4	33	1000	2.38	0.00	0.436	0.436	0.436	0.436	6.00	0.535
5	34	1000	2.17	0.00	1.320	1.320	1.320	1.320	6.00	0.535
6	35	1000	2.90	0.00	0.500	0.500	0.500	0.500	6.00	0.535
7	36	1000	2.20	0.00	0.490	0.490	0.490	0.490	6.00	0.535
8	37	1000	2.03	0.00	0.570	0.570	0.570	0.570	6.00	0.535
9	38	1000	2.88	0.00	0.570	0.570	0.570	0.570	6.00	0.535
10	39	1000	41.67	0.00	0.060	0.060	0.06	0.060	6.00	0.535

Table 19 Exciter Data of IEEE 39-bus New England System

GenNo	BusNo	K_A	K_E	K_F	τ_A (s)	τ_E (s)	τ_F (s)	K_{Se} (s)	τ_{Se} (s)
1	30	20	1.00	0.0630	0.2500	0.3140	0.3500	0.0039	1.5550
2	31	20	1.00	0.0630	0.2500	0.3140	0.3500	0.0039	1.5550
3	32	20	1.00	0.0630	0.2500	0.3140	0.3500	0.0039	1.5550
4	33	20	1.00	0.0630	0.2500	0.3140	0.3500	0.0039	1.5550
5	34	20	1.00	0.0630	0.2500	0.3140	0.3500	0.0039	1.5550
6	35	20	1.00	0.0630	0.2500	0.3140	0.3500	0.0039	1.5550
7	36	20	1.00	0.0630	0.2500	0.3140	0.3500	0.0039	1.5550
8	37	20	1.00	0.0630	0.2500	0.3140	0.3500	0.0039	1.5550
9	38	20	1.00	0.0630	0.2500	0.3140	0.3500	0.0039	1.5550
10	39	20	1.00	0.0630	0.2500	0.3140	0.3500	0.0039	1.5550

VITA

Chengzong Pang received his B.S. and M.S. degrees in electrical engineering from North China Electric Power University, Baoding, China, in 2000 and 2003 respectively. He received his Ph.D. degree from Texas A&M University, College Station, TX, USA, in Electrical Engineering in 2011. His research interests are power system analysis, simulation, stability, control, cascading events, protection, substation automation, intelligent system, and smart grid technologies.

Chengzong Pang may be reached at WERC 323, MS3128, Department of Electrical and Computer Engineering, College Station, TX 77843-3128. His email is pangchz@gmail.com.